An Implementation of the Finite Element Method for the Velocity-Current Magnetohydrodynamics Equations

by

K. Daniel Brauss

A dissertation submitted to the Graduate Faculty of
Auburn University
in partial fulfillment of the
requirements for the Degree of
Doctor of Philosophy

Auburn, Alabama
August 2, 2014

Keywords: magnetohydrodynamics, finite element method, numerical solution

Approved by

A. J. Meir, Chair, Professor of Mathematics and Statistics
Paul G. Schmidt, Professor of Mathematics and Statistics
Yanzhao Cao, Professor of Mathematics and Statistics
Dmitry Glotov, Professor of Mathematics and Statistics

Abstract

The aim of this research is to extend the numerical results in [78] of a velocity-current magnetohydrodynamics formulation proposed by A.J. Meir and Paul G. Schmidt in [74] for a stationary flow that models a conductive fluid in a bounded domain. A parallel finite element algorithm was successfully implemented on a high-performance computing, distributed-memory architecture at the Alabama Supercomputer Center (ASC) using the freely available, open-source academic and government libraries deal.ii, p4est and Trilinos. Extending the work of Elman, Silvester and Wathen [37] for the Navier-Stokes equations, a Schur complement preconditioner was developed for the current saddle-point problem to successfully utilize the iterative Krylov subspace solver GMRES (generalized minimal residual method) and solve large linear systems of equations arising from mesh refinement. To simplify and lower operation costs in forming the preconditioner, spectral equivalence was established between the Schur complement and a mass matrix. The resulting C++ code was tested succesfully on problems from [78] with similar results.

Acknowledgments

I have to thank God for the opportunity to continue my studies here at Auburn University. I have to thank my wife Minvera Rosario Brauss Blanco for her unwavering support. Without my wife, I would not have made it this far. Thank you Rose. I thank Eliana Catherine Brauss, my daughter, for being here and filling our lives. I thank all of my family for their support with all that we do. I thank all of my teachers for the passion that they have given to me. I thank Dr. A. J. Meir for his much appreciated support, patience and guidance as my Ph.D. advisor. Dr. Meir is a positive influence and a well-respected role model. I have learned a deeper independence from him that has helped me to grow. I thank Dr. Paul G. Schmidt for his support and his courses in functional analysis. Thanks to my other committee members Dr. Yanzhao Cao and Dr. Dmitry Glotov. Lastly, thanks to Dr. Narendra Govil and Dr. Geraldo DeSouza.

Table of Contents

List of Figures

List of Tables

Chapter 1

Introduction

1.1 Overview

Scientific theories often have a quantitative, mathematical nature to them, such as a well-founded set of governing equations developed through experimental tests and results. The equations ususally depict a variable, quantity or quantities that are of scientific interest and may be a direct measure of the success of a process or system (e.g., velocity in mass transfer) or an indirect measure of a system's state (e.g., pressure or concentration profiles indicating compression or swelling). Models whose governing equations involve complex multiphysics and systems of partial differential equations often arise in physics and engineering. Advances in scientific computing make it possible to numerically approximate solutions to the quantities of interest in such equations with increased accuracy and less simplifying assumptions. Numerically approximating and visualizing solutions to complex multiphysics models can then allow a scientist to investigate and analyze a process, assess its conditions, and address possible optimizations. With growth in computing, the area of computational science and applied mathematics has established itself as a the third pillar of scientific investigation [31]. By way of visualization, scientific computing can offer a deep understanding of phenomena being scientifically investigated as well as the limits of our theory and understanding of natural phenomena [23].

In this research, our interests are in the predictions of scientific quantities according to governing equations for electrically conducting fluid flow. We are interested in the dynamics of electrically conductive fluids in the presence of electromagnetic fields, placing our research

in the area of magnetohydrodynamics. We study viscous, incompressible, homogeneous, conductive fluids and therefore the governing incompressible Navier-Stokes equations [69]

$$\begin{aligned} \rho\frac{\partial \mathbf{v}}{\partial t} - \eta\Delta\mathbf{u} + \rho\left(\mathbf{u}\cdot\nabla\right)\mathbf{u} + \nabla p &= \mathbf{F} + \mathbf{J}\times\mathbf{B} \\ \nabla\cdot\mathbf{v} &= 0. \end{aligned}$$

We consider the Lorentz force $\mathbf{J}\times\mathbf{B}$ to act on the fluid by way of electrical and magnetic fields governed by the Maxwell equations [51, 38] and Ohm's Law

$$\begin{aligned} \nabla\cdot\mathbf{E} &= \frac{q}{\epsilon_0} \quad \text{(Gauss's Law for Electric Field)}, \\ \nabla\cdot\mathbf{B} &= 0 \quad \text{(Gauss's Law for Magnetic Field)}, \\ \nabla\times\mathbf{E} &= -\frac{\partial\mathbf{B}}{\partial t} \quad \text{(Faraday's law)}, \\ \nabla\times\mathbf{B} &= \mu_0\left(\mathbf{J} + \epsilon_0\frac{\partial\mathbf{E}}{\partial t}\right) \quad \text{(Ampere-Maxwell law)}, \end{aligned}$$

and

$$\mathbf{J} = \sigma\left(\mathbf{E} + \mathbf{u}\times\mathbf{B}\right) \quad \text{(Ohm's Law)}$$

The quantities of interest are the current $\mathbf{J}$, velocity $\mathbf{u}$, pressure p, electric potential ϕ, and magnetic field $\mathbf{B}$.

Magnetohydrodynamics (MHD) is the study of the dynamics of electrically conducting fluids under electromagnetic fields. Our focus is on the interaction of electrically conducting fluids with electromagnetic fields at the macroscopic level [29]. Applications modeled by such equations arise in liquid metal solidification processes [77, 83, 84, 41, 42, 70, 90, 49, 79, 32, 18] and silicon crystal growth processes used in the semiconductor and microelectronics

industry [50, 73, 56, 55] to hold, liquify and stir melts, control undesired convection, and filter out impurities. Other example applications are electromagnetic pumping, nuclear reactor cooling, plasmas in nuclear fusion and propulsion devices [66, 54, 76, 52, 62, 57, 3, 72, 71, 88]. We note that these studies address grand challenges seen in the National Academy of Engineering's (NAE) 21st Century's Grand Challenges for Engineering [82] and the 5 Grand Challenges from the Basic Energy Sciences Advisory Committee (BESAC) [39, 58] of the U.S. Department of Energy (DOE). One particular grand challenge from NAE is providing energy from thermonuclear fusion - the harnessing of the sun's energy. The above research also addresses the main theme of the BESAC grand challenges - designing and controlling material processes.

The velocity-current formulation of the MHD equations that we study was proposed by A.J. Meir and Paul G. Schmidt [74]. They have established existence and uniqueness of a solution to the equations as well as a convergent finite element iterative numerical approximation method [78]. The equations are a stationary (steady-state) form of the equations above and will be reviewed in chapter 2.

The main goal of this research was to extend the work conducted by A.J. Meir and Paul G. Schmidt in the numerical solution of the velocity-current MHD equations on three-dimensional domains by implementing a finite element method using parallel computing and a high-performance distributed memory cluster. To provide some motivation for this effort, we consider the flow of a fluid contained in a simple domain such as the unit cube. If we partition the unit cube in each coordinate direction into 101 segments to create a 100-by-100-by-100 domain mesh, and we perform the finite element method on this mesh, then the resulting linear system of equations will have unknowns that reach well into the millions. We have interest to apply our method to more complicated and larger domains as well as extend our work to include further multiphysics. This would mean that the number of unknowns could reach into the billions. We note that we are solving a nonlinear system of the partial differential equations using the finite element method and a picard iteration

scheme, and therefore solve this size of a system repeatedly to convergence. As might be expected, a large portion of computational time is spent solving the linear system and is common in scientific computing [99, 94].

1.2 Solver

We therefore wish to set up and efficiently solve a linear system $Ax = b$. Two general choices for solving a linear system are a direct solver or an iterative solver. A direct solver can be viewed as a form of Gaussian elimination performed on the system to decompose it into lower L and upper U triangular factors, $A = LU$. Many iterative solvers can be viewed as projection methods [85, 95] where the iterative solution to the system is obtained by projecting the exact solution to the system onto a particular subspace using a technique such as least squares. As our linear system is large, our interest is in the operations and memory required for such solvers. We summarize from a serial point of view.

The operation count for Gaussian elimination on a $n \times n$ matrix A, excluding row interchanges, is $O(n^3)$. Indeed, the pivot on the main diagonal element at the (1,1) position results in n multiplications across the first row. The elimination (zeroing) of the element below the pivot in the first column requires a multiplication on the first row (n flops) and a row addition (n flops). Performing elimination for each of the $n-1$ rows below the pivot results in a total of $n + (n+n)(n-1) = n + 2n(n-1)$ flops (floating point operations). The total number of operations across each column can be written as a series

$$\begin{aligned}\sum_{i=0}^{n-1}(n-i) + 2(n-i)(n-1-i) &= \sum_{i=1}^{n-1} i + 2(i)(i-1) = 2\sum_{i=1}^{n-1} i^2 - \sum_{i=1}^{n-1} i \\ &= \frac{(n-1)(n)(2n-1)}{3} - \frac{(n-1)(n)}{2} = O(n^3).\end{aligned}$$

To solve the system $Ax = b$, the same operations are applied to the system's right-hand side b creating a column vector we call c and requiring

$$n + \sum_{i=1}^{n-1} 2(i-1) = n(n-1) - n = O(n^2)$$

floating point operations. Upon completion, the system of equations has been transformed to $Ux = c$. To obtain the solution x, a backsolve is performed, starting from the lower row of U and working upward. The number of operations to solve the ith element of x is one multiplication and $i - 1$ additions. The complexity for solving all the elements of x, the entire backsolve, is

$$\sum_{i=1}^{n} 1 + \sum_{i=1}^{n} (i-1) = \sum_{i=1}^{n} i = \frac{n(n+1)}{2} = O(n^2).$$

The order of operations for the entire solution process is therefore $O(n^3)$. We note that bands in the system matrix are common for numerical approximation techniques to solutions of partial differential equations, such as the finite element method, and this matrix structure is taken advantage of by direct solvers. For a banded matrix with b nonzero diagonals below the main diagonal, the complexity when solving with Gaussian elimiation is less and dependent on the band size $O(nb^2)$ [44].

To compare the number of operations between a direct and iterative solver, we take as an example a second order PDE discretized using the finite element method over an irregular three-dimensional grid to obtain the system of equations $Ax = b$. A typical bandwith for this problem is $b = O(n^{2/3})$ [97]. The number of operations using the banded direct solver would therefore be $O(nb^2) = O(n^{7/3})$. For an iterative solver, the symmetry and positive definiteness of the system matrix makes the conjugate gradient (CG) method a natural choice. Per iteration the number of floating point operations is $O(n)$, see appendix C. To

estimate the number of operations for the complete iterative solve, we use an error bound after l iterations of the method given in the following theorem [44].

Theorem 1.1 *Suppose that $A \in \mathbb{R}^{n\times n}$ is symmetric positive definite and $b \in \mathbb{R}^n$. The error after l iterations of the CG algorithm in solving the system $Ax = b$ can be bounded as follows:*

$$\|x - x_l\|_A \leq 2\left(\frac{\sqrt{\kappa(A)}-1}{\sqrt{\kappa(A)}+1}\right)^l \|x - x_0\|_A ,$$

where $\kappa(A)$ is the condition number of A.

For discretized second order PDEs, it can be shown that $\kappa(A) = O(n^{2/3})$ [97]. Setting the iterative solver error tolerance to ϵ, we estimate the required number of iterations l to achieve the tolerance ϵ by using the error estimate from the theorem above. Here we have assumed that n is large and used $\kappa(A) = O(n^{2/3})$ to simplify.

$$\left(\frac{1-1/\sqrt{\kappa(A)}}{1+1/\sqrt{\kappa(A)}}\right)^l < \left(1-\frac{2}{\sqrt{\kappa(A)}}\right)^l < e^{\frac{-2l}{\sqrt{\kappa(A)}}} < \epsilon$$

Solving for l, we have the number of conjugate gradient iterations bounded $l < -\frac{\ln(\epsilon)\sqrt{\kappa(A)}}{2} = O(n^{1/3})$. With this estimate, the number of floating point operations for the method would be $O(n^{4/3})$. For large matrix sizes n, this example indicates the conjugate gradient method would require less floating point operations. It would make sense to choose the CG solver using this measurement.

Another important aspect of the solver is memory requirements. As can be seen with the conjugate gradient method, iterative solvers can require only the memory to store the sparse matrix A. If A has m nonzero entries per row and $m << n$, then the memory requirement would be $O(n)$. In comparison, the factorization that occurs during a direct solve often creates fill-in and increases memory consumption. Memory requirements for Krylov iterative solvers such as the conjugate gradient method can also be reduced by the use of matrix-free

methods. Matrix-free methods do not store the matrix A itself, but only the action of A on a vector.

It must be noted that iterative solvers are not as robust as direct solvers in terms of dealing with arbitrary and ill-conditioned matrices. Slow convergence can be a likely scenario for fluid dynamics and electronic device simulations [85]. Further, modern sparse direct solvers can tackle problems with several million unknowns [101]. These solvers efficiently handle and minimize the fill-in that may occur in the factors L and U. To achieve such efficiency, two steps are commonly employed before factorization by such solvers: (i) an ordering of rows and columns that can minimize fill and (ii) a symbolic analysis of the matrix structure to determine a good pivot sequence that can reduce memory requirements and floating-point operations [45].

To solve our system we have considered Krylov subspace iterative solvers that project the solution of the system $Ax = b$ into the Krylov space, span $(b, Ab, A^2b, ...)$. Two examples of commonly-used Krylov iterative solver methods are the conjugate gradient (CG) method and the generalized minimal residual (GMRES) method, see appendix C. The CG method is both an iterative and direct solver, designed to solve symmetric, positive definite systems in a finite number of steps - at most the size of the matrix. GMRES is an iterative least squares solver developed for nonsymmetric indefinite systems. As our system is nonsymmetric indefinite, we have decided to use GMRES. [97].

For system matrices having sizes numbering into the millions and larger, the benefits mentioned for a Krylov iterative solver, like GMRES, over a direct solver can be significant. There is one stipulation to success with a solver like GMRES. A critical component of such a method must be obtained - a preconditioner. [15, 95]. Indeed, without a preconditioner we have seen GMRES fail to converge for our system.

1.3 Preconditioner

Having chosen the iterative solver GMRES, the main focus of our research was finding and implementing a good preconditioner. In the development of the theory of the solvability of our magnetohydrodynamic equations and MHD equations in general [77, 2] work is often extended from the analysis of the Navier-Stokes equations. With no known preconditioners available for our system, it seems natural to start our search for an effective preconditioner in work done for numerically solving the Navier-Stokes equations. Two common methods, to solve these equations are ILU (incomplete LU factorization method) and block preconditioning using the Schur complement [98, 40]. ILU is a general preconditioning method for linear systems, where Schur complement methods are applicable to saddle-point problems. Preconditioners for the Stokes and Navier-Stokes problems based on the Schur complement have been shown to be effective and independent of mesh size where the ILU method may not [91, 37, 36, 34, 35, 33]. In chapter 3 we review and extend the work of Elman, Silvester and Wathen and exploit similarities of our matrix system, developing a preconditioner for our system of equations. In this direction we note the works on general and particular saddlepoint problems related to maxwell and navier-stokes equations [102, 48, 16]. In chapter 4 we show results from implementation of the preconditioner on examples from [77] for two different domains.

1.4 Implementation

One research goal was to implement our method using current computing capabilities. This included using high performance computing, a distributed memory architecture, object-oriented programming, and freely available open-source software libraries. We have in mind ease in extension of the research to more complex physics and problem types. A necessary choice to start the implementation was the operating platform. A commonly-used operating system platform for HPC (High Performance Computing) systems is linux.

Motivation to use the linux operating system becomes evident when viewing the top 500 fastest HPC systems in the world at `http://www.top500.org`. Running approximately one million cores at ten petaFLOPs per second, the five fasted distributed-memory high performance supercomputers, as of November 2013, use the linux operating system `http://en.wikipedia.org/wiki/TOP500`.

Several advantages of freely available open source libraries are (i) code that constitutes building blocks for a certain types of solution methods (e.g., finite element method) and eliminates the necessity to reinvent efficient components, (ii) code that has been tested, revised and written to exploit high performance computing architectures, (iii) a generalized tool for later use to develop code for other types of applied problems, (iv) exposure to software engineering standards through open-source files, (v) contributions to software development with advanced programming techniques, (vi) development of networks with peers and discussions of options for such solution methods.

Object oriented programming allows for modularization and implementation of design patterns for effective use of code, particularly important for large codes and libraries. Library development can be hidden from the interface between the user and the library, allowing users to operate from a high level without an in-depth understanding of the complete workings that make up each component of the library. Without object-oriented programming, the user may have to understand the underpinnings of a large portion (hundreds of thousands of lines of code) of the library code to realize the purpose of a specific part. The library can advance in the development of its objects (e.g., revised data structures) while letting the user implement these advances in a familiar setting. Combining this technique with version control, such as the subversion version control system (SVN) [25, 80], teams of programmers, developers and software engineers can tackle various parts of the library separately and at the same time - having interfaces well defined. Open-source software libraries that are object-oriented and well-documented allow the user the opportunity to modify the library's code to fit user needs. Object-oriented, open-source programming can further the

development of the library through implementation of user modifications that may benefit the library community.

In searching for such a library, we found deal.ii. deal.ii (Differential Equations Analysis Library) is a software library having these qualities and geared toward the finite element method. The library is actively developed. Initially developed at the University of Heidelberg in Heidelberg, Germany [10, 8, 11, 9, 12], deal.ii became the main support library for code development in this research. deal.ii interfaces to several libraries. For parallel iterative and direct solutions of systems of equations, deal.ii interfaces to the libraries Trilinos and PETSc from the Sandia National Laboratory and the Argonne National Laboratory [60, 59, 86, 7], respectively. deal.ii also interfaces to the library p4est, developed at the University of Texas at Austin, for domain decomposition [20, 65] over the distributed memory architecture. We mention these three libraries in particular, since they were the main support libraries used in parallel development. At the time of this research project, Trilinos and p4est were being incorporated and tested on thousands of cores by the deal.ii developers. PETSc was also capable of utilization for parallel solution methods with domain decomposition using the library METIS. However, this technique required each cluster's node to keep the domain's entire mesh in memory. In comparison, p4est decomposes the domain mesh and distributes pieces to each node. As our code developed, we switched from PETSc and METIS to Trilinos and p4est due to this efficiency in use of memory.

Two important components for successful use of a software library are active development and quality documentation. The quality of the deal.ii documentation made for effective use of the library. The tutorials were particularly helpful. In particular, the tutorial step-32 [68] became a skeleton (with the multi-threading removed) for the current code with respect to the use of p4est and trilinos. Another contribution to the successful use of deal.ii was its active mailing list. The developers and community of users were very helpful in answering questions concerning the library and troubleshooting the installation of software.

Chapter 2

The Problem

2.1 Problem Formulation

The velocity-current formulation developed by Meir and Schmidt assumes the fluid to be incompressible and finitely conducting. The fluid is contained in a bounded domain, and is allowed to interact with magnetic fields both within and outside of the domain. The boundaries of the fluid domain are assumed to be nonideal. Ideal boundaries refer to perfectly conducting walls [89]. In the presence of perfectly conducting walls, one can restrict attention to only the domain containing the body of conducting fluid and neglect the fluid's electromagnetic interaction with the rest of Euclidean space. The model problem that we study is the steady flow of a conducting fluid in a bounded three-dimensional domain. The flow is driven by currents entering and exiting the domain at the boundary as well as induced magnetic fields in the domain and known magnetic fields external to the domain.

The stationary (steady-state) flow of a viscous electrically-conducting incompressible fluid in a bounded domain was modelled by the Navier-Stokes equations

$$-\eta\Delta\mathbf{u} + \rho\left(\mathbf{u}\cdot\nabla\right)\mathbf{u} + \nabla p - \mathbf{J}\times\mathbf{B} = \mathbf{F}, \tag{2.1}$$

where the parameters are the viscosity η and the density ρ, and the variables are the velocity $\mathbf{u}$, the pressure p, the current density $\mathbf{J}$, the magnetic field $\mathbf{B}$ and the given body forces $\mathbf{F}$. The flow was allowed to interact with electric currents and magnetic fields through the

coupling of the Navier-Stokes equations and Ohm's Law

$$\sigma^{-1}\mathbf{J} + \nabla\phi - \mathbf{u} \times \mathbf{B} = \mathbf{E}, \tag{2.2}$$

via the Lorentz force $\mathbf{J} \times \mathbf{B}$ and the magnetic induction $\mathbf{u} \times \mathbf{B}$. The new quantities introduced in Ohm's law are a parameter, the conductivity σ, a variable, the electric potential ϕ, and the externally generated electric field $\mathbf{E}$.

Incompressibility, conservation of mass and conservation of charge were accounted for by the continuity equations

$$\nabla \cdot \mathbf{u} = 0 \qquad \text{and} \qquad \nabla \cdot \mathbf{J} = 0. \tag{2.3}$$

To eliminate the magnetic field as an unknown, superposition was used

$$\mathbf{B} = \mathbf{B}_0 + \mathcal{B}(\mathbf{J}), \tag{2.4}$$

where $\mathbf{B}_0$ is the sum of the fields due to external sources and $\mathcal{B}(\mathbf{J})$ is the field generated by the fluid through induction. The field $\mathcal{B}(\mathbf{J})$ was obtained from the Biot-Savart law

$$\mathcal{B}(\mathbf{J})(\mathbf{x}) = -\frac{\mu}{4\pi} \int_\Omega \frac{\mathbf{x} - \mathbf{y}}{|\mathbf{x} - \mathbf{y}|^3} \times \mathbf{J}(\mathbf{y})\, d\mathbf{y} \tag{2.5}$$

where $\mathbf{x} \in \mathbb{R}^3$ and μ is the magnetic permeability. The fields due to external sources were decomposed into their components as well

$$\mathbf{B}_0(\mathbf{x}) = \mathbf{B}_{\text{ext}}(\mathbf{x}) - \frac{\mu}{4\pi} \int_{\mathbb{R}^3 \setminus \overline{\Omega}} \frac{\mathbf{x} - \mathbf{y}}{|\mathbf{x} - \mathbf{y}|^3} \times \mathbf{J}_{\text{ext}}(\mathbf{y})\, d\mathbf{y} \tag{2.6}$$

for $\mathbf{x} \in \mathbb{R}^3$. $\mathbf{B}_{\text{ext}}$ consisted of external magnetic fields other than the one induced by known current(s) $\mathbf{J}_{\text{ext}}$ outside the domain. Further constraints were conservation of charge $\nabla \cdot \mathbf{J}_{\text{ext}} = 0$ for the external current(s) and $\nabla \cdot \mathbf{B}_{\text{ext}} = 0$ in $\mathbb{R}^3$ and $\nabla \times \mathbf{B}_{\text{ext}} = 0$ in Ω.

For the system 2.1 - 2.3 to be well-posed, boundary conditions for $\mathbf{u}$ and $\mathbf{J}$ on the boundary Γ are necessary. The conditions

$$\mathbf{u} = \mathbf{g} \qquad \text{on } \Gamma \tag{2.7}$$

and

$$\mathbf{J} \cdot \mathbf{n} = \mathbf{J}_{\text{ext}} \cdot \mathbf{n} \qquad \text{on } \Gamma \tag{2.8}$$

were imposed.

We let L^2 and H^1 denote the usual Lebesgue and Sobolev spaces of square-integrable functions and square-integrable functions with a generalized square-integrable derivative, on the implied domains (i.e., Ω, $\mathbb{R} \setminus \overline{\Omega}$, or $\mathbb{R}^3$). Let $H^{1/2}(\Gamma)$ denote the trace space of $H^1(\Omega)$. Let H_0^1 denote the subspace of functions from $H^1(\Omega)$ that vanish on the boundary Γ (in the sense of traces) and let $H^{-1}(\Omega)$ denote its dual. Finally we let boldface type denote spaces consisting of $\mathbb{R}^3$ vector-valued functions. For example, $\mathbf{L}^2(\Omega) = (L^2(\Omega))^3$. Let $\mathbf{W}^1(\mathbb{R}^3)$ be the Beppo-Levi space whose inner product is given by $\langle \mathbf{f}, \mathbf{g} \rangle_{\mathbf{W}^1(\mathbb{R}^3)} = \int_{\mathbb{R}^3} \nabla \mathbf{f} \cdot \nabla \mathbf{g}$.

With the given spaces, we state a problem formulation such that the equations and the singular integrals in the decomposition of $\mathbf{B}$ are well-defined in the weak formulation that will follow.

Problem P_0**:** Given parameters $\eta, \rho, \sigma, \mu > 0$ and data

$$\begin{aligned}
&\mathbf{F} \in \mathbf{H}^{-1}(\Omega), \mathbf{E} \in \mathbf{L}^2(\Omega), \\
&\mathbf{g} \in \mathbf{H}^{1/2}(\Gamma) \text{ with } \int_\Gamma \mathbf{g} \cdot \mathbf{n} = 0, \\
&\mathbf{J}_{\text{ext}} \in \mathbf{L}^2\left(\mathbb{R}^3 \setminus \overline{\Omega}\right) \text{ with } \nabla \cdot \mathbf{J}_{\text{ext}} = 0 \text{ in } \mathbb{R}^3 \setminus \overline{\Omega} \text{ and } \int_\Gamma \mathbf{J}_{\text{ext}} \cdot \mathbf{n} = 0,
\end{aligned}$$

and

$$\mathbf{B}_{\text{ext}} \in \mathbf{W}^1\left(\mathbb{R}^3\right) \text{ with } \nabla \cdot \mathbf{B}_{\text{ext}} = 0 \text{ in } \mathbb{R}^3 \text{ and } \nabla \times \mathbf{B}_{\text{ext}} = 0 \text{ in } \Omega,$$

find functions $\mathbf{u} \in \mathbf{H}^1(\Omega), \mathbf{J} \in \mathbf{L}^2(\Omega), p \in L^2(\Omega/\mathbb{R}),$ and $\phi \in H^1(\Omega/\mathbb{R})$, such that

$$\begin{aligned} -\eta\Delta\mathbf{u} + \rho(\mathbf{u}\cdot\nabla)\mathbf{u} + \nabla p - \mathbf{J}\times\mathbf{B} &= \mathbf{F} \quad \text{in } \Omega, \\ \sigma^{-1}\mathbf{J} + \nabla\phi - \mathbf{u}\times\mathbf{B} &= \mathbf{E} \quad \text{in } \Omega, \\ \nabla\cdot\mathbf{u} = 0 \quad \text{and} \quad \nabla\cdot\mathbf{J} &= 0 \quad \text{in } \Omega, \\ \mathbf{u} = \mathbf{g} \quad \text{and} \quad \mathbf{J}\cdot\mathbf{n} &= \mathbf{J}_{\text{ext}}\cdot\mathbf{n} \quad \text{on } \Gamma, \end{aligned}$$

and

$$\begin{aligned} \mathbf{B} &= \mathbf{B}_0 + \mathcal{B}(\mathbf{J}), \\ \mathcal{B}(\mathbf{J})(\mathbf{x}) &= -\frac{\mu}{4\pi}\int_\Omega \frac{\mathbf{x}-\mathbf{y}}{|\mathbf{x}-\mathbf{y}|^3}\times\mathbf{J}(\mathbf{y})\,d\mathbf{y}, \\ \mathbf{B}_0(\mathbf{x}) &= \mathbf{B}_{\text{ext}}(\mathbf{x}) - \frac{\mu}{4\pi}\int_{\mathbb{R}^3\setminus\overline{\Omega}} \frac{\mathbf{x}-\mathbf{y}}{|\mathbf{x}-\mathbf{y}|^3}\times\mathbf{J}_{\text{ext}}(\mathbf{y})\,d\mathbf{y}. \end{aligned}$$

are satisfied. □

Letting $\tilde{\mathbf{J}} \in \mathbf{L}^2(\mathbb{R}^3)$ be defined as $\mathbf{J}$ in Ω and $\mathbf{J}_{\text{ext}}$ in $\mathbb{R}^3 \setminus \overline{\Omega}$ then $\nabla\cdot\tilde{\mathbf{J}} = 0$ (in the sense of distributions on $\mathbb{R}^3$) and $\mathbf{B} = \mathbf{B}_{\text{ext}} + \tilde{\mathbf{B}}$ with $\tilde{\mathbf{B}}$ given by

$$\tilde{\mathbf{B}}(x) = -\frac{\mu}{4\pi}\int_{\mathbb{R}^3} \frac{\mathbf{x}-\mathbf{y}}{|\mathbf{x}-\mathbf{y}|^3}\times\tilde{\mathbf{J}}(\mathbf{y})\,d\mathbf{y}$$

for $\mathbf{x} \in \mathbb{R}^3$. $\tilde{\mathbf{B}} \in \mathbf{W}^1(\mathbb{R}^3)$ is the unique solution of Maxwell's equations

$$\nabla\cdot\tilde{\mathbf{B}} = 0 \text{ and } \nabla\times\tilde{\mathbf{B}} = \mu\tilde{\mathbf{J}} \tag{2.9}$$

in $\mathbf{W}^1(\mathbb{R}^3)$. We require $\mathbf{B}_{\text{ext}}$ to belong to $\mathbf{W}^1(\mathbb{R}^3)$ as well [78].

2.2 Weak Formulation

A mixed weak formulation of the original problem is obtained by multiplying the system equations (2.1) - (2.3) by test functions $\mathbf{v} \in \mathbf{H}_0^1(\Omega)$, $\mathbf{K} \in \mathbf{L}^2(\Omega)$, $q \in L^2(\Omega)/\mathbb{R}$, and $\psi \in H^1(\Omega)/\mathbb{R}$, respectively and integrating over the domain Ω.

$$\begin{aligned} -\eta \int_\Omega \Delta \mathbf{u} \cdot \mathbf{v} + \rho \int_\Omega ((\mathbf{u} \cdot \nabla)\mathbf{u}) \cdot \mathbf{v} + \int_\Omega \nabla p \cdot \mathbf{v} - \int_\Omega (\mathbf{J} \times \mathbf{B}) \cdot \mathbf{v} &= \int_\Omega \mathbf{F} \cdot \mathbf{v} \\ \sigma^{-1} \int_\Omega \mathbf{J} \cdot \mathbf{K} + \int_\Omega \nabla \phi \cdot \mathbf{K} - \int_\Omega (\mathbf{u} \times \mathbf{B}) \cdot \mathbf{K} &= \int_\Omega \mathbf{E} \cdot \mathbf{K} \\ \int_\Omega (\nabla \cdot \mathbf{u}) q = 0 \quad \text{and} \quad \int_\Omega (\nabla \cdot \mathbf{J}) \psi &= 0 \end{aligned}$$

We add the first two equations and the third and fourth. Using integration by parts, the divergence theorem and some identities (see Appendix A) we obtain

$$\begin{aligned} \eta \int_\Omega \nabla \mathbf{u} \colon \nabla \mathbf{v} + \frac{\rho}{2} \left(\int_\Omega ((\mathbf{u} \cdot \nabla)\mathbf{u}) \cdot \mathbf{v} - \int_\Omega ((\mathbf{u} \cdot \nabla)\mathbf{v}) \cdot \mathbf{u} \right) - \int_\Omega p \nabla \cdot \mathbf{v} - \int_\Omega (\mathbf{J} \times \mathbf{B}) \cdot \mathbf{v} \\ + \sigma^{-1} \int_\Omega \mathbf{J} \cdot \mathbf{K} + \int_\Omega \nabla \phi \cdot \mathbf{K} + \int_\Omega (\mathbf{K} \times \mathbf{B}) \cdot \mathbf{u} = \int_\Omega \mathbf{F} \cdot \mathbf{v} + \int_\Omega \mathbf{E} \cdot \mathbf{K} \\ \int_\Omega (\nabla \cdot \mathbf{u}) q + \int_\Omega \mathbf{J} \cdot \nabla \psi = \int_\Gamma \mathbf{J} \cdot \mathbf{n} \end{aligned}$$

Combining together Navier-Stokes and Ohm's Law and then the continuity equations, we have the system in terms of the multilinear forms

$$\begin{aligned} a_0((\mathbf{u}, \mathbf{J}), (\mathbf{v}, \mathbf{K})) + a_1((\mathbf{u}, \mathbf{J}), (\mathbf{u}, \mathbf{J}), (\mathbf{v}, \mathbf{K})) + b((\mathbf{v}, \mathbf{K}), (p, \phi)) &= \int_\Omega \mathbf{F} \cdot \mathbf{v} + \int_\Omega \mathbf{E} \cdot \mathbf{K}, \\ b((\mathbf{u}, \mathbf{J}), (q, \psi)) &= \int_\Gamma \mathbf{J}_{\text{ext}} \cdot \mathbf{n}, \end{aligned}$$

where $a_0 \colon (\mathbf{H}^1(\Omega) \times \mathbf{L}^2(\Omega)) \times (\mathbf{H}^1(\Omega) \times \mathbf{L}^2(\Omega)) \to \mathbb{R}$ is defined as

$$a_0((\mathbf{u}, \mathbf{J}), (\mathbf{v}, \mathbf{K})) = \eta \int_\Omega (\nabla \mathbf{u}) : (\nabla \mathbf{v}) + \sigma^{-1} \int_\Omega \mathbf{J} \cdot \mathbf{K} + \int_\Omega ((\mathbf{K} \times \mathbf{B}_0) \cdot \mathbf{u} - (\mathbf{J} \times \mathbf{B}_0) \cdot \mathbf{v}),$$

$a_1 \colon \left(\mathbf{H}^1(\Omega) \times \mathbf{L}^2(\Omega)\right) \times \left(\mathbf{H}^1(\Omega) \times \mathbf{L}^2(\Omega)\right) \times \left(\mathbf{H}^1(\Omega) \times \mathbf{L}^2(\Omega)\right) \to \mathbb{R}$ as

$$\begin{aligned} a_1\left((\mathbf{u},\mathbf{J}),(\mathbf{u},\mathbf{J}),(\mathbf{v},\mathbf{K})\right) &= \frac{\rho}{2}\int_\Omega \left(\left(\left(\mathbf{u}\cdot\nabla\right)\mathbf{u}\right)\cdot\mathbf{v} - \left(\left(\mathbf{u}\cdot\nabla\right)\mathbf{v}\right)\cdot\mathbf{u}\right) \\ &\qquad + \int_\Omega \left(\left(\mathbf{K}\times\mathcal{B}\left(\mathbf{J}\right)\right)\cdot\mathbf{u} - \left(\mathbf{J}\times\mathcal{B}\left(\mathbf{J}\right)\right)\cdot\mathbf{v}\right), \end{aligned}$$

and $b \colon \left(\mathbf{H}^1(\Omega) \times \mathbf{L}^2(\Omega)\right) \times \left(L^2(\Omega)/\mathbb{R} \times H^1(\Omega)/\mathbb{R}\right) \to \mathbb{R}$ as

$$b\left((\mathbf{v},\mathbf{K}),(p,\phi)\right) = -\int_\Omega \left(\nabla\cdot\mathbf{v}\right)\mathcal{P}\left(p\right) + \int_\Omega \mathbf{K}\cdot\left(\nabla\phi\right)$$

The pressure solution p to the system is only unique up to a constant, and therefore the L^2 orthogonal projection $\mathcal{P}$ has been introduced for uniqueness and is given by

$$\mathcal{P}\left(f\right) := f - \frac{1}{|\Omega|}\int_\Omega f.$$

Hence,

$$\begin{aligned} \mathcal{P}\left(p+c\right) &= \left(p+c\right) - \frac{1}{|\Omega|}\int_\Omega p + c \\ &= p + c - \frac{1}{|\Omega|}\int_\Omega p - \frac{1}{|\Omega|}\int_\Omega c = p - \frac{1}{|\Omega|}\int_\Omega p \\ &= \mathcal{P}\left(p\right) \end{aligned}$$

To shorten the notation above, define $\mathbf{Y} := \mathbf{H}^1(\Omega) \times \mathbf{L}^2(\Omega)$, $M := L^2(\Omega)/\mathbb{R} \times H^1(\Omega)/\mathbb{R}$, and $\mathbf{X} := \mathbf{H}^1_0(\Omega) \times \mathbf{L}^2(\Omega)$.

To help establish existence and uniqueness, the interial term of the Navier-Stokes equations has been "skew-symmetrized", making the bilinear form $a_1\left((\mathbf{v}_0,\mathbf{K}_0),(\cdot,\cdot),(\cdot,\cdot)\right)$ skew-symmetric on $\mathbf{Y}\times\mathbf{Y}$.

$$\frac{1}{2}\int_\Omega \left(\left(\left(\mathbf{v}_1\cdot\nabla\right)\mathbf{v}_2\right)\cdot\mathbf{v}_3 - \left(\left(\mathbf{v}_1\cdot\nabla\right)\mathbf{v}_3\right)\cdot\mathbf{v}_2\right) = \int_\Omega \left(\left(\mathbf{v}_1\cdot\nabla\right)\mathbf{v}_2\right)\cdot\mathbf{v}_3$$

whenever $\nabla \cdot \mathbf{v}_1 = 0$ and $\mathbf{v}_3\big|_\Gamma = 0$. Given below is a second version of our problem.

Problem P_1**:** Given parameters $\eta, \rho, \sigma, \mu > 0$ and data

$$\begin{aligned}
&\mathbf{F} \in \mathbf{H}^{-1}(\Omega), \mathbf{E} \in \mathbf{L}^2(\Omega), \\
&\mathbf{g} \in \mathbf{H}^{1/2}(\Gamma) \text{ with } \int_\Gamma \mathbf{g} \cdot \mathbf{n} = 0 \\
&\mathbf{J}_{\text{ext}} \in \mathbf{L}^2\left(\mathbb{R}^3 \setminus \overline{\Omega}\right) \text{ with } \nabla \cdot \mathbf{J}_{\text{ext}} = 0 \text{ in } \mathbb{R}^3 \setminus \overline{\Omega} \text{ and } \int_\Gamma \mathbf{J}_{\text{ext}} \cdot \mathbf{n} = 0, \quad \text{and} \\
&\mathbf{B}_{\text{ext}} \in \mathbf{W}^1\left(\mathbb{R}^3\right) \text{ with } \nabla \cdot \mathbf{B}_{\text{ext}} = 0 \text{ in } \mathbb{R}^3 \text{ and } \nabla \times \mathbf{B}_{\text{ext}} = 0 \text{ in } \Omega,
\end{aligned}$$

find functions $(\mathbf{u}, \mathbf{J}) \in \mathbf{Y}$ with $\mathbf{u}\big|_\Gamma = \mathbf{g}$ and $(p, \phi) \in M$, such that

$$\begin{aligned}
a_0((\mathbf{u}, \mathbf{J}), (\mathbf{v}, \mathbf{K})) + a_1((\mathbf{u}, \mathbf{J}), (\mathbf{u}, \mathbf{J}), (\mathbf{v}, \mathbf{K})) + b((\mathbf{v}, \mathbf{K}), (p, \phi)) &= \int_\Omega \mathbf{F} \cdot \mathbf{v} + \int_\Omega \mathbf{E} \cdot \mathbf{K}, \\
b((\mathbf{u}, \mathbf{J}), (q, \psi)) &= \int_\Gamma \mathbf{J}_{\text{ext}} \cdot \mathbf{n}
\end{aligned}$$

for all $(q, \psi) \in M$ and $(\mathbf{v}, \mathbf{K}) \in \mathbf{X}$. $\mathcal{B}\colon \mathbf{L}^2(\Omega) \to \mathbf{W}^1(\mathbb{R}^3)$ defined by

$$\mathcal{B}(\mathbf{f})(x) := -\frac{\mu}{4\pi} \int_\Omega \frac{x - y}{|x - y|^3} \times \mathbf{f}(y)\, dy \qquad \forall x \in \mathbb{R}^3$$

is a bounded linear operator from $\mathbf{L}^2(\Omega)$ to $\mathbf{W}^1(\mathbb{R}^3)$ [75] and $\mathbf{B}_0$ is the component of the magnetic field that is generated by outside sources, previously defined. □

The properties of a_0, a_1 and b needed to establish existence and uniqueness are collected in the lemma below.

Lemma 1

1. *The forms a_0, a_1 and b are bounded on on $\mathbf{Y} \times \mathbf{Y}$, $\mathbf{Y} \times \mathbf{Y} \times \mathbf{Y}$, and $\mathbf{Y} \times M$, respectively, with norms*

$$\|a_0\| \leq c \max\left\{1, \eta, \sigma^{-1}, \mu\right\} \left(1 + \|J_{ext}\|_{\mathbf{L}^2\left(\mathbb{R}^3 \setminus \overline{\Omega}\right)} + \left\|\mathbf{B}_{ext}\big|_\Omega\right\|_{\mathbb{L}^3(\Omega)}\right)$$

$$\|a_1\| \;\leq\; c\max\{\rho,\mu\}, \qquad \textit{and } \|b\| \leq \sqrt{3},$$

where c depends only on Ω ($c = c(\Omega)$).

2. *The form a_0 is positive definite on $\mathbf{X}\times\mathbf{X}$ with a number $\alpha \geq c^{-1}\min\{\eta,\sigma^{-1}\}$ such that*

$$a_0((\mathbf{v},\mathbf{K}),(\mathbf{v},\mathbf{K})) \geq \alpha\|(\mathbf{v},\mathbf{K})\|^2_{\mathbf{Y}} \qquad \forall\,(\mathbf{v},\mathbf{K})\in\mathbf{X}$$

(where $c = c(\Omega)$).

3. *The form b satisfies the Ladyzhenskaya-Babuska-Brezzi condition (LBB-condition) on $\mathbf{X}\times M$ with a number $\beta(\Omega) > 0$ such that*

$$\inf_{(q,\psi)\in M}\sup_{(\mathbf{v},\mathbf{K})\in\mathbf{X}}\frac{b((\mathbf{v},\mathbf{K}),(q,\psi))}{\|(\mathbf{v},\mathbf{K})\|_{\mathbf{Y}}\|(q,\psi)\|_M} \geq \beta.$$

We note that the two conditions

$$\inf_{q\in L^2(\Omega)/\mathbb{R}}\sup_{\mathbf{v}\in\mathbf{H}^1(\Omega)}\frac{\int_\Omega(\nabla\cdot\mathbf{v})\,q}{\|\mathbf{v}\|_{\mathbf{H}^1(\Omega)}\|q\|_{L^2(\Omega)/\mathbb{R}}} \geq \beta_1 \quad \text{and}$$
$$\inf_{\psi\in H^1(\Omega)/\mathbb{R}}\sup_{\mathbf{K}\in\mathbf{L}^2(\Omega)}\frac{\int_\Omega\mathbf{K}\cdot(\nabla\psi)}{\|\mathbf{K}\|_{\mathbf{L}^2(\Omega)}\|\psi\|_{H^1(\Omega)/\mathbb{R}}} \geq \beta_2$$

are sufficient to establish the last part of the lemma [21].

Thanks to the LBB-condition, there exist $\mathbf{u}_0\in\mathbf{H}^1(\Omega)$ and $\mathbf{J}_0\in\mathbf{L}^2(\Omega)$ [78] such that

$$\nabla\cdot\mathbf{u}_0 = 0 \text{ in } \Omega, \quad \mathbf{u}_0 = \mathbf{j} \text{ on } \Gamma \quad \text{and} \quad \nabla\cdot\mathbf{J}_0 = 0 \text{ in } \Omega, \quad \mathbf{J}_0\cdot\mathbf{n} = j \text{ on } \Gamma.$$

Therefore, the problem can be reduced by writing

$$\mathbf{u} = \mathbf{u}_0 + \tilde{\mathbf{u}} \quad \text{and} \quad \mathbf{J} = \mathbf{J}_0 + \tilde{\mathbf{J}}$$

and defining the forms $a\colon \mathbf{X}\times\mathbf{X}\times\mathbf{X}\to\mathbb{R}$ and $l\in\mathbf{X}^*$ by

$$\begin{aligned}
&a\left(\left(\mathbf{v}_1,\mathbf{K}_1\right),\left(\mathbf{v}_2,\mathbf{K}_2\right),\left(\mathbf{v}_3,\mathbf{K}_3\right)\right)\\
&\quad:=a_0\left(\left(\mathbf{v}_2,\mathbf{K}_2\right),\left(\mathbf{v}_3,\mathbf{K}_3\right)\right)+a_1\left(\left(\mathbf{v}_1,\mathbf{K}_2\right),\left(\mathbf{v}_2,\mathbf{K}_2\right),\left(\mathbf{v}_3,\mathbf{K}_3\right)\right)\\
&\qquad+a_1\left(\left(\mathbf{v}_2,\mathbf{K}_2\right),\left(\mathbf{u}_0,\mathbf{J}_0\right),\left(\mathbf{v}_3,\mathbf{K}_3\right)\right)+a_1\left(\left(\mathbf{u}_0,\mathbf{J}_0\right),\left(\mathbf{v}_2,\mathbf{K}_2\right),\left(\mathbf{v}_3,\mathbf{K}_3\right)\right)
\end{aligned}$$

and

$$\begin{aligned}
l\left(\mathbf{v},\mathbf{K}\right) \;:=\; &\int_\Omega \mathbf{F}\cdot\mathbf{v}+\int_\Omega \mathbf{E}\cdot\mathbf{K}\\
&-a_0\left(\left(\mathbf{u}_0,\mathbf{J}_0\right),\left(\mathbf{v},\mathbf{K}\right)\right)-a_1\left(\left(\mathbf{u}_0,\mathbf{J}_0\right),\left(\mathbf{u}_0,\mathbf{J}_0\right),\left(\mathbf{v},\mathbf{K}\right)\right).
\end{aligned}$$

With the space $\mathbf{V}:=\left\{(\mathbf{v},\mathbf{K})\in\mathbf{X}\colon b\left((\mathbf{v},\mathbf{K}),(q,\psi)\right)=0\quad\forall\,(q,\psi)\in M\right\}$, we have a final problem version.

Problem P_2: Find $\left(\tilde{\mathbf{u}},\tilde{\mathbf{J}}\right)\in\mathbf{V}$ such that $a\left(\left(\tilde{\mathbf{u}},\tilde{\mathbf{J}}\right),\left(\tilde{\mathbf{u}},\tilde{\mathbf{J}}\right),(\mathbf{v},\mathbf{K})\right)=l\left(\mathbf{v},\mathbf{K}\right)$ for all $(\mathbf{v},\mathbf{K})\in\mathbf{V}$. □

We refer to [78] for the equivalence of problem versions. To establish existence and uniqueness we have the lemma and theorem below.

Lemma 2

1. *The mapping* $(\mathbf{v},\mathbf{K})\to a\left((\mathbf{v},\mathbf{K}),(\mathbf{v},\mathbf{K}),(\mathbf{v}_0,\mathbf{K}_0)\right)$*, for any* $(\mathbf{v}_0,\mathbf{K}_0)\in\mathbf{V}$*, is weakly sequentially continuous on* $\mathbf{V}$*.*

2. *For every* $(\mathbf{v}_0,\mathbf{K}_0)\in\mathbf{V}$ *and all* $(\mathbf{v},\mathbf{K})\in\mathbf{V}$*, we have*

$$a\left(\left(\mathbf{v}_0,\mathbf{K}_0\right),\left(\mathbf{v},\mathbf{K}\right),\left(\mathbf{v},\mathbf{K}\right)\right)\geq\left(\alpha-\lambda\left\|a_1\right\|\left\|(\mathbf{g},j)\right\|\right)\left\|(\mathbf{v},\mathbf{K})\right\|_{\mathbf{Y}}^2$$

where α *and* λ *are constants established in [78] and* $\|(\mathbf{g},j)\|$ *denotes the norm of* $(\mathbf{g},j)\in\mathbf{H}^{1/2}(\Gamma)\times H^{-1/2}(\Gamma)$*.*

3. *The mapping* $(\mathbf{v}_0, \mathbf{K}_0) \rightarrow a\left((\mathbf{v}_0, \mathbf{K}_0), (\cdot,\cdot), (\cdot,\cdot)\right)$ *is uniformly Lipschitz continuous, with Lipschitz constant* $\|a_1\|$ *from* $\mathbf{V}$ *into the space* $\mathcal{L}(\mathbf{V}, \mathbf{V}^*)$ *of bounded linear operators from* $\mathbf{V}$ *into* $\mathbf{V}^*$.

Theorem 2.1 *Let* $N = N(\mathbf{F}, \mathbf{E}, \mathbf{g}, \mathbf{J}_{ext}, \mathbf{B}_{ext})$ *denote the norm of the functional* $l\big|_{\mathbf{V}}$. *Let* $\|(\mathbf{g}, j)\|$ *denote the norm of* $(\mathbf{g}, j)$ *in* $\mathbf{H}^{1/2}(\Gamma) \times H^{-1/2}(\Gamma)$, *where* $j = \mathbf{J}_{ext} \cdot \mathbf{n}$, *and choose constants* α *and* λ *(mentioned above). For Problem P (Version 3) we have the following*

1. *If* $\|(\mathbf{g}, j)\| < \frac{\alpha}{\lambda \|a_1\|}$, *then there exists at least one solution* $\left(\tilde{\mathbf{u}}, \tilde{\mathbf{J}}\right)$ *that satisfies*

$$\left\| \left(\tilde{\mathbf{u}}, \tilde{\mathbf{J}}\right) \right\|_{\mathbf{Y}} \leq \frac{N}{\alpha - \lambda \|a_1\| \|(\mathbf{g}, j)\|}.$$

2. *If* $\|(\mathbf{g}, j)\| < \frac{\alpha}{\lambda \|a_1\|}$, *then the solution is unique.*

The theorem asserts the existence of a solution for all versions of the problem if the boundary data $\mathbf{g}$ and $j = \mathbf{J}_{ext} \cdot \mathbf{n}$ are sufficiently small, and uniqueness is guaranteed if all the data $\mathbf{F}, \mathbf{E}, \mathbf{g}, \mathbf{J}_{ext}$, and $\mathbf{B}_{ext}$ are sufficiently small with the constants α, λ, and $\|a_1\|$ independent of the data [78].

In steps similar to the infinite-dimensional problem, existence and uniqueness was established for a finite-dimensional approximation to the problem [78]. In that direction, we introduce the notation B for a Banach space and $\left(B^h\right)_{h \in I}$ for a family of finite-dimensional subspaces of B. I is a subset of the interval $(0, 1)$ such that 0 is its only limit point. $\left(B^h\right)_{h \in I}$ is said to be a finite-dimensional approximation of B if $\forall f \in B$, we have $\inf_{f^h \in B^h} \left\| f - f^h \right\|_B \rightarrow 0$ as $h \rightarrow 0$.

To continue, we assume that $\left(\mathbf{Y}_1^h\right)_{h \in I}$, $\left(\mathbf{Y}_1^h\right)_{h \in I}$, $\left(M_1^h\right)_{h \in I}$, and $\left(M_2^h\right)_{h \in I}$ are finite-dimensional approximations of $\mathbf{Y}_1 = \mathbf{H}^1(\Omega)$, $\mathbf{Y}_2 = \mathbf{L}^2(\Omega)$, $M_1 = L^2(\Omega) \setminus \mathbb{R}$, and $M_2 = H^1(\Omega) \setminus \mathbb{R}$, respectively. Therefore, $\mathbf{Y}^h := \mathbf{Y}_1^h \times \mathbf{Y}_2^h$ and $M^h := M_1^h \times M_2^h$ approximate $\mathbf{Y}$ and M, respectively. With $\mathbf{X}_1 := \mathbf{H}_0^1(\Omega)$, $\mathbf{X}_2 := \mathbf{Y}_2$ and $\mathbf{X} := \mathbf{X}_1 \times \mathbf{X}_2$ we define $\mathbf{X}_1^h := \mathbf{Y}_1^h \bigcap \mathbf{X}_1^h$,

$\mathbf{X}_2^h := \mathbf{Y}_2^h$, $\mathbf{X}^h := \mathbf{X}_1^h \times \mathbf{X}_2^h$, and let $\mathbf{Y}_{1,\Gamma}^h$ denote the trace space of $\mathbf{Y}_1^h$

$$\mathbf{Y}_{1,\Gamma}^h = \left\{ \mathbf{v}^h \big|_\Gamma : \mathbf{v}^h \in \mathbf{Y}_1^h \right\}$$

of $\mathbf{Y}_{1,\Gamma} := \mathbf{H}^{1/2}(\Gamma)$. For further details, please see [78].

With the set of parameters η, ρ, σ, μ and data $\mathbf{F}, \mathbf{E}, \mathbf{g}, \mathbf{J}_{ext}$, and $\mathbf{B}_{ext}$ given and $j := \mathbf{J}_{ext} \cdot \mathbf{n}$, we choose a family $\left(\mathbf{g}^h\right)_{h \in I}$ of approximate boundary values $\mathbf{g}^h \in \mathbf{Y}_{1,\Gamma}^h$ such that $\mathbf{g}^h \to \mathbf{g}$ in $\mathbf{Y}_{1,\Gamma}$ as $h \to 0$. Finally, we consider a family P_1^h $(h \in I)$ of finite-dimensional approximations to Problem P_1, as follows

Problem P_1^h: Find $\left(\mathbf{u}^h, \mathbf{J}^h\right) \in \mathbf{Y}^h$ with $\mathbf{u}^h \big|_\Gamma = \mathbf{g}^h$ and $\left(p^h, \phi^h\right) \in M^h$ such that

$$\begin{aligned} a_0\left(\left(\mathbf{u}^h, \mathbf{J}^h\right), \left(\mathbf{v}^h, \mathbf{K}^h\right)\right) + a_1\left(\left(\mathbf{u}^h, \mathbf{J}^h\right), \left(\mathbf{u}^h, \mathbf{J}^h\right), \left(\mathbf{v}^h, \mathbf{K}^h\right)\right) \\ + b\left(\left(\mathbf{v}^h, \mathbf{K}^h\right), \left(p^h, \phi^h\right)\right) = \int_\Omega \mathbf{F} \cdot \mathbf{v} + \int_\Omega \mathbf{E} \cdot \mathbf{K} \end{aligned}$$

and

$$b\left(\left(\mathbf{u}^h, \mathbf{J}^h\right), \left(q^h, \psi^h\right)\right) = \int_\Gamma \left(\mathbf{J}_{\text{ext}} \cdot \mathbf{n}\right) \psi^h,$$

for all $\left(q^h, \psi^h\right) \in M^h$ and $\left(\mathbf{v}^h, \mathbf{K}^h\right) \in \mathbf{X}^h$. With existence and uniqueness established for the finite-dimensional problem, we consider a convergent finite element iteration scheme [78] to numerically approximate the infinite-dimensional solution to the problem.

2.3 Linearization

We use Newton's method

$$\mathbf{X}^{(k+1)} = \mathbf{X}^{(k)} - \frac{\mathbf{H}\left(\mathbf{X}^{(k)}\right)}{\mathbf{H}'\left(\mathbf{X}^{(k)}\right)} \tag{2.10}$$

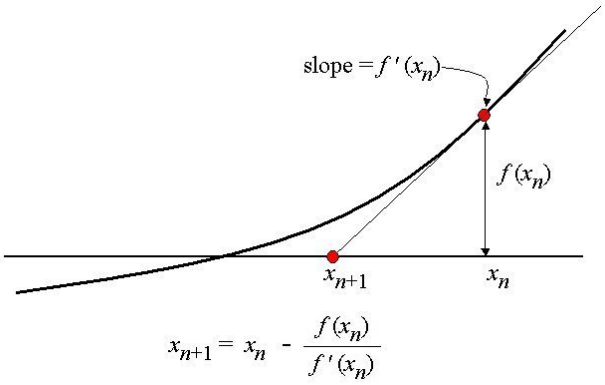

Figure 2.1: Newton's Method.

as a heuristic tool to develop the convergent iterative scheme introduced in [78], where the vector function $\mathbf{H}(\mathbf{X})$

$$\mathbf{H}(\mathbf{X}) = \begin{bmatrix} \eta\Delta\mathbf{u}_1 + \rho(\mathbf{u}\cdot\nabla)\mathbf{u}_1 + \frac{\partial p}{\partial x} - (\mathbf{J}_2\mathbf{B}_3 - \mathbf{J}_3\mathbf{B}_2) - \mathbf{F}_1 \\ \eta\Delta\mathbf{u}_2 + \rho(\mathbf{u}\cdot\nabla)\mathbf{u}_2 + \frac{\partial p}{\partial y} + (\mathbf{J}_1\mathbf{B}_3 - \mathbf{J}_3\mathbf{B}_1) - \mathbf{F}_2 \\ \eta\Delta\mathbf{u}_3 + \rho(\mathbf{u}\cdot\nabla)\mathbf{u}_3 + \frac{\partial p}{\partial z} - (\mathbf{J}_1\mathbf{B}_2 - \mathbf{J}_2\mathbf{B}_1) - \mathbf{F}_3 \\ \sigma^{-1}\mathbf{J}_1 + \frac{\partial \phi}{\partial x} - (\mathbf{u}_2\mathbf{B}_3 - \mathbf{u}_3\mathbf{B}_2) - \mathbf{E}_1 \\ \sigma^{-1}\mathbf{J}_2 + \frac{\partial \phi}{\partial y} - (\mathbf{u}_1\mathbf{B}_3 - \mathbf{u}_3\mathbf{B}_1) - \mathbf{E}_2 \\ \sigma^{-1}\mathbf{J}_3 + \frac{\partial \phi}{\partial z} - (\mathbf{u}_1\mathbf{B}_2 - \mathbf{u}_2\mathbf{B}_1) - \mathbf{E}_3 \\ \frac{\partial \mathbf{u}_1}{\partial x} + \frac{\partial \mathbf{u}_2}{\partial y} + \frac{\partial \mathbf{u}_3}{\partial z} \\ \frac{\partial \mathbf{J}_1}{\partial x} + \frac{\partial \mathbf{J}_2}{\partial y} + \frac{\partial \mathbf{J}_3}{\partial z} \end{bmatrix}$$

and the variable $\mathbf{X} = (\mathbf{u}_1, \mathbf{u}_2, \mathbf{u}_3, p, \mathbf{J}_1, \mathbf{J}_2, \mathbf{J}_3, \phi)$ were obtained from the equations

$$\begin{aligned} -\eta\Delta\mathbf{u} + \rho(\mathbf{u}\cdot\nabla)\mathbf{u} + \nabla p - \mathbf{J}\times\mathbf{B} &= \mathbf{F} \\ \sigma^{-1}\mathbf{J} + \nabla\phi - \mathbf{u}\times\mathbf{B} &= \mathbf{E}, \\ \nabla\cdot\mathbf{u} = 0 \qquad \text{and} \qquad \nabla\cdot\mathbf{J} &= 0. \end{aligned}$$

Since

$$\mathbf{B} = \mathbf{B}_0 + \mathcal{B}(\mathbf{J})$$

$$= \mathbf{B}_0 - \frac{\mu}{4\pi}\int_\Omega \frac{\mathbf{x}-\mathbf{y}}{|\mathbf{x}-\mathbf{y}|^3}\times \mathbf{J}(\mathbf{y})\,d\mathbf{y} = \begin{bmatrix} (\mathbf{B}_0)_1 - \frac{\mu}{4\pi}\int_\Omega \frac{(\mathbf{x}_2-\mathbf{y}_2)\mathbf{J}_3(\mathbf{y})-(\mathbf{x}_3-\mathbf{y}_3)\mathbf{J}_2(\mathbf{y})}{|\mathbf{x}-\mathbf{y}|^3}d\mathbf{y} \\ (\mathbf{B}_0)_2 - \frac{\mu}{4\pi}\int_\Omega \frac{(\mathbf{x}_1-\mathbf{y}_1)\mathbf{J}_3(\mathbf{y})-(\mathbf{x}_3-\mathbf{y}_3)\mathbf{J}_1(\mathbf{y})}{|\mathbf{x}-\mathbf{y}|^3}d\mathbf{y} \\ (\mathbf{B}_0)_3 - \frac{\mu}{4\pi}\int_\Omega \frac{(\mathbf{x}_1-\mathbf{y}_1)\mathbf{J}_2(\mathbf{y})-(\mathbf{x}_2-\mathbf{y}_2)\mathbf{J}_1(\mathbf{y})}{|\mathbf{x}-\mathbf{y}|^3}d\mathbf{y} \end{bmatrix}$$

we have

$$\mathbf{H}(\mathbf{X}) = \begin{bmatrix} \eta\Delta\mathbf{u}_1 + \rho(\mathbf{u}\cdot\nabla)\mathbf{u}_1 + \frac{\partial p}{\partial x} - \mathbf{J}_2\left((\mathbf{B}_0)_3 - \frac{\mu}{4\pi}\int_\Omega \frac{(\mathbf{x}_1-\mathbf{y}_1)\mathbf{J}_2-(\mathbf{x}_2-\mathbf{y}_2)\mathbf{J}_1}{|\mathbf{x}-\mathbf{y}|^3}d\mathbf{y}\right) \\ \qquad +\mathbf{J}_3\left((\mathbf{B}_0)_2 - \frac{\mu}{4\pi}\int_\Omega \frac{(\mathbf{x}_1-\mathbf{y}_1)\mathbf{J}_3-(\mathbf{x}_3-\mathbf{y}_3)\mathbf{J}_1}{|\mathbf{x}-\mathbf{y}|^3}d\mathbf{y}\right) - \mathbf{F}_1 \\ \\ \eta\Delta\mathbf{u}_2 + \rho(\mathbf{u}\cdot\nabla)\mathbf{u}_2 + \frac{\partial p}{\partial y} + \mathbf{J}_1\left((\mathbf{B}_0)_3 - \frac{\mu}{4\pi}\int_\Omega \frac{(\mathbf{x}_1-\mathbf{y}_1)\mathbf{J}_2-(\mathbf{x}_2-\mathbf{y}_2)\mathbf{J}_1}{|\mathbf{x}-\mathbf{y}|^3}d\mathbf{y}\right) \\ \qquad -\mathbf{J}_3\left((\mathbf{B}_0)_1 - \frac{\mu}{4\pi}\int_\Omega \frac{(\mathbf{x}_2-\mathbf{y}_2)\mathbf{J}_3-(\mathbf{x}_3-\mathbf{y}_3)\mathbf{J}_2}{|\mathbf{x}-\mathbf{y}|^3}d\mathbf{y}\right) - \mathbf{F}_2 \\ \\ \eta\Delta\mathbf{u}_3 + \rho(\mathbf{u}\cdot\nabla)\mathbf{u}_3 + \frac{\partial p}{\partial z} - \mathbf{J}_1\left((\mathbf{B}_0)_2 - \frac{\mu}{4\pi}\int_\Omega \frac{(\mathbf{x}_1-\mathbf{y}_1)\mathbf{J}_3-(\mathbf{x}_3-\mathbf{y}_3)\mathbf{J}_1}{|\mathbf{x}-\mathbf{y}|^3}d\mathbf{y}\right) \\ \qquad +\mathbf{J}_2\left((\mathbf{B}_0)_1 - \frac{\mu}{4\pi}\int_\Omega \frac{(\mathbf{x}_2-\mathbf{y}_2)\mathbf{J}_3-(\mathbf{x}_3-\mathbf{y}_3)\mathbf{J}_2}{|\mathbf{x}-\mathbf{y}|^3}d\mathbf{y}\right) - \mathbf{F}_3 \\ \\ \sigma^{-1}\mathbf{J}_1 + \frac{\partial\phi}{\partial x} - \mathbf{u}_2\left((\mathbf{B}_0)_3 - \frac{\mu}{4\pi}\int_\Omega \frac{(\mathbf{x}_1-\mathbf{y}_1)\mathbf{J}_2-(\mathbf{x}_2-\mathbf{y}_2)\mathbf{J}_1}{|\mathbf{x}-\mathbf{y}|^3}d\mathbf{y}\right) \\ \qquad +\mathbf{u}_3\left((\mathbf{B}_0)_2 - \frac{\mu}{4\pi}\int_\Omega \frac{(\mathbf{x}_1-\mathbf{y}_1)\mathbf{J}_3-(\mathbf{x}_3-\mathbf{y}_3)\mathbf{J}_1}{|\mathbf{x}-\mathbf{y}|^3}d\mathbf{y}\right) - \mathbf{E}_1 \\ \\ \sigma^{-1}\mathbf{J}_2 + \frac{\partial\phi}{\partial y} + \mathbf{u}_1\left((\mathbf{B}_0)_3 - \frac{\mu}{4\pi}\int_\Omega \frac{(\mathbf{x}_1-\mathbf{y}_1)\mathbf{J}_2-(\mathbf{x}_2-\mathbf{y}_2)\mathbf{J}_1}{|\mathbf{x}-\mathbf{y}|^3}d\mathbf{y}\right) \\ \qquad -\mathbf{u}_3\left((\mathbf{B}_0)_1 - \frac{\mu}{4\pi}\int_\Omega \frac{(\mathbf{x}_2-\mathbf{y}_2)\mathbf{J}_3-(\mathbf{x}_3-\mathbf{y}_3)\mathbf{J}_2}{|\mathbf{x}-\mathbf{y}|^3}d\mathbf{y}\right) - \mathbf{E}_2 \\ \\ \sigma^{-1}\mathbf{J}_3 + \frac{\partial\phi}{\partial z} - \mathbf{u}_1\left((\mathbf{B}_0)_2 - \frac{\mu}{4\pi}\int_\Omega \frac{(\mathbf{x}_1-\mathbf{y}_1)\mathbf{J}_3-(\mathbf{x}_3-\mathbf{y}_3)\mathbf{J}_1}{|\mathbf{x}-\mathbf{y}|^3}d\mathbf{y}\right) \\ \qquad +\mathbf{u}_2\left((\mathbf{B}_0)_1 - \frac{\mu}{4\pi}\int_\Omega \frac{(\mathbf{x}_2-\mathbf{y}_2)\mathbf{J}_3-(\mathbf{x}_3-\mathbf{y}_3)\mathbf{J}_2}{|\mathbf{x}-\mathbf{y}|^3}d\mathbf{y}\right) - \mathbf{E}_3 \\ \\ \frac{\partial\mathbf{u}_1}{\partial x} + \frac{\partial\mathbf{u}_2}{\partial y} + \frac{\partial\mathbf{u}_3}{\partial z} \\ \\ \frac{\partial\mathbf{J}_1}{\partial x} + \frac{\partial\mathbf{J}_2}{\partial y} + \frac{\partial\mathbf{J}_3}{\partial z} \end{bmatrix}$$

Differentiating $\mathbf{H}(\mathbf{X})$ using the Gateaux deritave

$$H'_G\left(\mathbf{X}^{(k)}\right)(\Delta\mathbf{X}) = \lim_{\epsilon\to 0}\frac{\mathbf{H}\left(\mathbf{X}^{(k)}+\epsilon\Delta\mathbf{X}\right)-\mathbf{H}\left(\mathbf{X}^{(k)}\right)}{\epsilon}, \tag{2.11}$$

where $\Delta\mathbf{X} = \mathbf{X}^{(k+1)} - \mathbf{X}^{(k)}$ and $\epsilon\Delta\mathbf{X} = \epsilon\left(\Delta\mathbf{u}_1, \Delta\mathbf{u}_2, \Delta\mathbf{u}_3, \Delta p, \Delta\mathbf{J}_1, \Delta\mathbf{J}_2, \Delta\mathbf{J}_3\right)$, we obtain (see Appendix B) the Newton iteration

$$\begin{bmatrix} -\eta\nabla\cdot\nabla\mathbf{u}^{(k+1)} + \rho\left(\mathbf{u}^{(k+1)}\cdot\nabla\right)\mathbf{u}^{(k)} - \rho\left(\mathbf{u}^{(k)}\cdot\nabla\right)\mathbf{u}^{(k)} + \rho\left(\mathbf{u}^{(k)}\cdot\nabla\right)\mathbf{u}^{(k+1)} \\ +\nabla p^{(k+1)} - \mathbf{J}^{(k)}\times\mathcal{B}\left(\mathbf{J}^{(k+1)}\right) + \mathbf{J}^{(k)}\times\mathcal{B}\left(\mathbf{J}^{(k)}\right) - \mathbf{J}^{(k+1)}\times\mathbf{B}\left(\mathbf{J}^{(k)}\right) \\ \sigma^{-1}\mathbf{J}^{(k+1)} + \nabla\phi^{(k+1)} - \mathbf{u}^{(k)}\times\mathcal{B}\left(\mathbf{J}^{(k+1)}\right) + \mathbf{u}^{(k)}\times\mathcal{B}\left(\mathbf{J}^{(k)}\right) - \mathbf{u}^{(k+1)}\times\mathbf{B}\left(\mathbf{J}^{(k)}\right) \\ \nabla\cdot\mathbf{u}^{(k+1)} \\ \nabla\cdot\mathbf{J}^{(k+1)} \end{bmatrix} = \begin{bmatrix} \mathbf{F} \\ \mathbf{E} \\ 0 \\ 0 \end{bmatrix}. \quad (2.12)$$

Dropping off the first two terms from the linearization of each of the three nonlinear terms of the equations, we have a Picard iteration [53]

$$\begin{bmatrix} -\eta\nabla\cdot\nabla\mathbf{u}^{(k+1)} + \rho\left(\mathbf{u}^{(k)}\cdot\nabla\right)\mathbf{u}^{(k+1)} + \nabla p^{(k+1)} - \mathbf{J}^{(k+1)}\times\mathbf{B}\left(\mathbf{J}^{(k)}\right) \\ \sigma^{-1}\mathbf{J}^{(k+1)} + \nabla\phi^{(k+1)} - \mathbf{u}^{(k+1)}\times\mathbf{B}\left(\mathbf{J}^{(k)}\right) \\ \nabla\cdot\mathbf{u}^{(k+1)} \\ \nabla\cdot\mathbf{J}^{(k+1)} \end{bmatrix} = \begin{bmatrix} \mathbf{F} \\ \mathbf{E} \\ 0 \\ 0 \end{bmatrix}.$$

We can see that these are the original equations with a component of each nonlinear term being lagged to create the linearization. The corresponding weak formulation would then be

$$\begin{aligned} \eta\int_\Omega\left(\nabla\mathbf{u}_{(k+1)}\right):\left(\nabla\mathbf{v}\right) + \rho + \int_\Omega\left(\left(\mathbf{u}_{(k)}\cdot\nabla\right)\mathbf{u}_{(k+1)}\right)\cdot\mathbf{v} - \int_\Omega p_{(k+1)}\left(\nabla\cdot\mathbf{v}\right) - \int_\Omega\left(\mathbf{J}_{(k+1)}\times\mathcal{B}\left(\mathbf{J}_{(k)}\right)\right)\cdot\mathbf{v} \\ - \int_\Omega\left(\mathbf{J}_{(k+1)}\times\mathbf{B}_0\right)\cdot\mathbf{v} + \sigma^{-1}\int_\Omega\mathbf{J}_{(k+1)}\cdot\mathbf{K} + \int_\Omega\nabla\phi_{(k+1)}\cdot\mathbf{K} - \int_\Omega\left(\mathbf{u}_{(k+1)}\times\mathcal{B}\left(\mathbf{J}_{(k)}\right)\right)\cdot\mathbf{K} \\ - \int_\Omega\left(\mathbf{u}_{(k+1)}\times\mathbf{B}_0\right)\cdot\mathbf{K} = \int_\Omega\mathbf{F}\cdot\mathbf{v} + \int_\Omega\mathbf{E}\cdot\mathbf{K} \\ \int_\Omega\left(\nabla\cdot\mathbf{u}_{(k+1)}\right)q + \int_\Omega\mathbf{J}_{(k+1)}\cdot\nabla\psi = \int_\Gamma\left(\mathbf{J}_{ext}\cdot\mathbf{n}\right)\psi \end{aligned}$$

Recalling the forms

$$a_0\left(\left(\mathbf{v}_1,\mathbf{K}_1\right),\left(\mathbf{v}_2,\mathbf{K}_2\right)\right):=\eta\int_\Omega\left(\nabla\mathbf{v}_1\right):\ \left(\nabla\mathbf{v}_2\right)+\sigma^{-1}\int_\Omega\mathbf{K}_1\cdot\mathbf{K}_2 \\ +\int_\Omega\left(\left(\mathbf{K}_2\times\mathbf{B}_0\right)\cdot\mathbf{v}_1-\left(\mathbf{K}_1\times\mathbf{B}_0\right)\cdot\mathbf{v}_2\right), \quad (2.13)$$

$$a_1\left(\left(\mathbf{v}_1,\mathbf{K}_1\right),\left(\mathbf{v}_2,\mathbf{K}_2\right),\left(\mathbf{v}_3,\mathbf{K}_3\right)\right):=\frac{\rho}{2}\int_\Omega\left(\left(\left(\mathbf{v}_1\cdot\nabla\right)\mathbf{v}_2\right)\cdot\mathbf{v}_3-\left(\left(\mathbf{v}_1\cdot\nabla\right)\mathbf{v}_3\right)\cdot\mathbf{v}_2\right) \\ +\int_\Omega\left(\left(\mathbf{K}_3\times\mathcal{B}\left(\mathbf{K}_1\right)\right)\cdot\mathbf{v}_2-\left(\mathbf{K}_2\times\mathcal{B}\left(\mathbf{K}_1\right)\right)\cdot\mathbf{v}_3\right), \quad (2.14)$$

and

$$b\left(\left(\mathbf{v},\mathbf{K}\right),\left(q,\psi\right)\right):=-\int_\Omega\left(\nabla\cdot\mathbf{v}\right)\mathcal{P}\left(q\right)+\int_\Omega\mathbf{K}\cdot\left(\nabla\psi\right), \quad (2.15)$$

we are now ready to state the convergent Picard iteration scheme proposed by Meir and Schmidt for the numerical solution of Problem P_1^h.

Iteration Scheme. Given $\left(\mathbf{u}_0^h,\mathbf{J}_0^h\right)\in\mathbf{Y}^h$ with $\mathbf{u}_0^h\big|_\Gamma=\mathbf{g}^h$, for $n\in\mathbb{N}$, find $\left(\mathbf{u}_n^h,\mathbf{J}_n^h\right)\in\mathbf{Y}^h$ with $\mathbf{u}_n^h\big|_\Gamma=\mathbf{g}^h$ and $\left(p_n^h,\phi_n^h\right)\in M^h$ such that

$$a_0\left(\left(\mathbf{u}_{(k+1)}^h,\mathbf{J}_{(k+1)}^h\right),\left(\mathbf{v}^h,\mathbf{K}^h\right)\right)+a_1\left(\left(\mathbf{u}_{(k)}^h,\mathbf{J}_{(k)}^h\right),\left(\mathbf{u}_{(k+1)}^h,\mathbf{J}_{(k+1)}^h\right),\left(\mathbf{v}^h,\mathbf{K}^h\right)\right) \\ +b\left(\left(\mathbf{v}^h,\mathbf{K}^h\right),\left(p_{(k+1)}^h,\phi_{(k+1)}^h\right)\right)=\int_\Omega\mathbf{F}\cdot\mathbf{v}^h+\int_\Omega\mathbf{E}\cdot\mathbf{K}^h$$

and

$$b\left(\left(\mathbf{u}_{(k+1)}^h,\mathbf{J}_{(k+1)}^h\right),\left(q^h,\psi^h\right)\right)=\int_\Gamma\left(\mathbf{J}_{ext}\cdot\mathbf{n}\right)\psi^h$$

for all $\left(\mathbf{v}^h,\mathbf{K}^h\right)\in\mathbf{X}^h$ and $\left(q^h,\psi^h\right)\in M^h$. For further details, we refer to [78].

Chapter 3

Matrix System and Preconditioner

3.1 Matrix Formulation

Restating the convergent Picard iteration scheme with n in place of $k+1$,

$$a_0\left(\left(\mathbf{u}^h_{(n)},\mathbf{J}^h_{(n)}\right),\left(\mathbf{v}^h,\mathbf{K}^h\right)\right)+a_1\left(\left(\mathbf{u}^h_{(n-1)},\mathbf{J}^h_{(n-1)}\right),\left(\mathbf{u}^h_{(n)},\mathbf{J}^h_{(n)}\right),\left(\mathbf{v}^h,\mathbf{K}^h\right)\right)$$
$$+b\left(\left(\mathbf{v}^h,\mathbf{K}^h\right),\left(p^h_{(n)},\phi^h_{(n)}\right)\right)=\int_\Omega \mathbf{F}\cdot\mathbf{v}^h+\int_\Omega \mathbf{E}\cdot\mathbf{K}^h$$

and

$$b\left(\left(\mathbf{u}^h_{(n)},\mathbf{J}^h_{(n)}\right),\left(q^h,\psi^h\right)\right)=\int_\Gamma\left(\mathbf{J}_{ext}\cdot\mathbf{n}\right)\psi^h$$

for all $\left(\mathbf{v}^h,\mathbf{K}^h\right)\in\mathbf{X}^h$ and $\left(q^h,\psi^h\right)\in M^h$. The scheme is expanded using the definition of a_0, a_1, and b

$$\begin{aligned}
&\eta\int_\Omega \nabla\mathbf{u}^h_{(n)}\colon\nabla\mathbf{v}^h+\sigma^{-1}\int_\Omega \mathbf{J}^h_{(n)}\cdot\mathbf{K}^h+\int_\Omega\left(\mathbf{K}^h\times\mathbf{B_0}\right)\cdot\mathbf{u}^h_{(n)}-\int_\Omega\left(\mathbf{J}^h_{(n)}\times\mathbf{B_0}\right)\cdot\mathbf{v}^h\\
&\quad+\rho\int_\Omega\left(\left(\mathbf{u}^h_{(n-1)}\cdot\nabla\right)\mathbf{u}^h_{(n)}\right)\cdot\mathbf{v}^h+\int_\Omega\left(\mathbf{K}^h\times\mathcal{B}\left(\mathbf{J}^h_{(n-1)}\right)\right)\cdot\mathbf{u}^h_{(n)}-\int_\Omega\left(\mathbf{J}^h_{(n)}\times\mathcal{B}\left(\mathbf{J}^h_{(n-1)}\right)\right)\cdot\mathbf{v}^h\\
&\quad-\int_\Omega p^h_{(n)}\nabla\cdot\mathbf{v}^h+\int_\Omega\nabla\phi^h_{(n)}\cdot\mathbf{K}^h=\int_\Omega\mathbf{F}\cdot\mathbf{v}^h+\int_\Omega\mathbf{E}\cdot\mathbf{K}^h\\
&-\int_\Omega\nabla\cdot\mathbf{u}^h_{(n)}q+\int_\Omega\mathbf{J}^h_{(n)}\nabla\psi^h=\int_\Gamma(\mathbf{J}_{ext}\cdot\mathbf{n})\psi
\end{aligned}$$

Choosing a basis for each of the finite-dimensional subspaces $\left\{\vec{\phi}^u_k\right\}_{k=1}^{n^h_u}\subset\mathbf{Y}^h_1$, $\left\{\vec{\phi}^J_k\right\}_{k=1}^{n^h_J}\subset\mathbf{Y}^h_2$, $\{\phi^p_k\}_{k=1}^{n^h_p}\subset M^h_1$, and $\left\{\phi^\phi_k\right\}_{k=1}^{n^h_\phi}\subset M^h_2$, we can write the unknowns of problem P^h_1 as a linear

combination of the respective basis

$$
\begin{aligned}
p^h_{(n)} &= \sum_{k=1}^{n_p^h} c_k^{(p,n)} \varphi_k^{(p)} \\
\mathbf{u}^h_{(n)} &= \sum_{k=1}^{n_u^h} c_k^{(u,n)} \vec{\varphi}_k^{(u)} \\
\phi^h_{(n)} &= \sum_{k=1}^{n_\phi^h} c_k^{(\phi,n)} \varphi_k^{(\phi)} \\
\mathbf{J}^h_{(n)} &= \sum_{k=1}^{n_J^h} c_k^{(J,n)} \vec{\varphi}_k^{(J)}
\end{aligned}
$$

Substituting this representation into the iteration scheme and and using distributive properties of the gradient, divergence, cross product and dot product we have

$$
\begin{aligned}
&\sum_{i=1}^{n_u^h} c_i^{(u,n)} \eta \int_\Omega \nabla \vec{\varphi}_i^{(u)} : \nabla \vec{\varphi}_j^{(u)} + \sum_{i=1}^{n_J^h} c_i^{(J,n)} \sigma^{-1} \int_\Omega \vec{\varphi}_i^{(J)} \cdot \vec{\varphi}_k^{(J)} \\
&\quad + \sum_{i=1}^{n_u^h} c_i^{(u,n)} \int_\Omega \left(\vec{\varphi}_k^{(J)} \times \vec{B}_0 \right) \cdot \vec{\varphi}_i^{(u)} - \sum_{i=1}^{n_J^h} c_i^{(J,n)} \int_\Omega \left(\vec{\varphi}_i^{(J)} \times \vec{B}_0 \right) \cdot \vec{\varphi}_j^{(u)} \\
&\quad + \sum_{i=1}^{n_u^h} c_i^{(u,n)} \rho \int_\Omega \left(\left(\vec{u}^h_{(n-1)} \cdot \nabla \right) \vec{\varphi}_i^{(u)} \right) \cdot \vec{\varphi}_j^{(u)} + \sum_{i=1}^{n_u^h} c_i^{(u,n)} \int_\Omega \left(\vec{\varphi}_k^{(J)} \times \vec{\mathcal{B}} \left(\vec{J}^h_{(n-1)} \right) \right) \cdot \vec{\varphi}_i^{(u)} \\
&\quad - \sum_{i=1}^{n_J^h} c_i^{(J,n)} \int_\Omega \left(\vec{\varphi}_i^{(J)} \times \vec{\mathcal{B}} \left(\vec{J}^h_{(n-1)} \right) \right) \cdot \vec{\varphi}_j^{(u)} - \sum_{i=1}^{n_p^h} c_i^{(p,n)} \int_\Omega \varphi_i^{(p)} \nabla \cdot \vec{\varphi}_j^{(u)} \\
&\quad + \sum_{i=1}^{n_\phi^h} c_i^{(\phi,n)} \int_\Omega \nabla \varphi_i^{(\phi)} \cdot \vec{\varphi}_k^{(J)} = \int_\Omega \mathbf{F} \cdot \vec{\varphi}_j^{(u)} + \int_\Omega \mathbf{E} \cdot \vec{\varphi}_k^{(J)}
\end{aligned}
$$

and

$$
- \sum_{i=1}^{n_u^h} c_i^{(u,n)} \int_\Omega \nabla \cdot \vec{\varphi}_i^{(u)} \varphi_l^{(p)} + \sum_{i=1}^{n_J^h} c_i^{(J,n)} \int_\Omega \vec{\varphi}_i^{(J)} \cdot \nabla \varphi_m^{(\phi)} = \int_\Gamma (\vec{J}_{ext} \cdot \vec{n}) \varphi_l^{(\phi)}.
$$

Letting

$$
\begin{aligned}
A_{(u)} &= \left[a^{(u)}_{(i,j)}\right] := \left[\eta \int_\Omega \nabla\vec{\varphi}^{(u)}_i : \nabla\vec{\varphi}^{(u)}_j\right] \quad 1 \le i \le n_u, 1 \le j \le n_u,\\
A_{(J)} &= \left[a^{(J)}_{(i,k)}\right] := \left[\sigma^{-1} \int_\Omega \vec{\varphi}^{(J)}_i \cdot \vec{\varphi}^{(J)}_k\right] \quad 1 \le i \le n_J, 1 \le k \le n_J,\\
B_{(p)} &= \left[b^{(p)}_{(i,l)}\right] := \left[\int_\Omega \varphi^{(p)}_l \nabla \cdot \vec{\varphi}^{(u)}_i\right] \quad 1 \le i \le n_u, 1 \le l \le n_p,\\
B_{(\phi)} &= \left[b^{(\phi)}_{(i,m)}\right] := \left[\int_\Omega \vec{\varphi}^{(J)}_i \cdot \nabla\varphi^{(\phi)}_m\right] \quad 1 \le i \le n_J, 1 \le m \le n_\phi,\\
C &= \left[c_{(i,k)}\right] := \left[\int_\Omega \left(\vec{\varphi}^{(J)}_k \times \vec{B}_0\right) \cdot \vec{\varphi}^{(u)}_i\right] \quad 1 \le i \le n_u, 1 \le k \le n_J,\\
N_{(u)} &= \left[n^{(u)}_{(i,j)}\right] := \left[\rho \int_\Omega \left(\left(\vec{u}^h_{(n-1)} \cdot \nabla\right) \vec{\varphi}^{(u)}_i\right) \cdot \vec{\varphi}^{(u)}_j\right] \quad 1 \le i \le n_u, 1 \le j \le n_u,
\end{aligned}
$$

and

$$
N_{(J)} = \left[n^{(J)}_{(i,k)}\right] := \left[\int_\Omega \left(\vec{\varphi}^{(J)}_k \times \vec{\mathcal{B}}\left(\vec{J}^h_{(n-1)}\right)\right) \cdot \vec{\varphi}^{(u)}_i\right] \quad 1 \le i \le n_u, 1 \le k \le n_J
$$

denote the matrices formed by the respective terms of the iteration scheme, given on the right-hand side of each definition. We group the coordinates from each linear combination of the uknowns of problem P_1^h into a vector. We do that same for the respective right-hand sides of each equation of the iteration scheme, and for the sake of simplicity reuse the notations $\mathbf{F}$ and $\mathbf{E}$.

$$
\begin{aligned}
\mathbf{c}^{(u,n)} &:= \left[c^{(u,n)}_1 \dots c^{(u,n)}_i \dots c^{(u,n)}_{n_u}\right]^t,\\
\mathbf{c}^{(p,n)} &:= \left[c^{(p,n)}_1 \dots c^{(p,n)}_i \dots c^{(p,n)}_{n_p}\right]^t,\\
\mathbf{c}^{(J,n)} &:= \left[c^{(J,n)}_1 \dots c^{(J,n)}_i \dots c^{(J,n)}_{n_J}\right]^t,\\
\mathbf{c}^{(\phi,n)} &:= \left[c^{(\phi,n)}_1 \dots c^{(\phi,n)}_i \dots c^{(\phi,n)}_{n_\phi}\right]^t,\\
\mathbf{F} &= \left[\int_\Omega \mathbf{F} \cdot \phi^{(u)}_1 \dots \int_\Omega \mathbf{F} \cdot \phi^{(u)}_j \dots \int_\Omega \mathbf{F} \cdot \phi^{(u)}_{n_u}\right]^t,\\
\mathbf{E} &= \left[\int_\Omega \mathbf{E} \cdot \phi^{(J)}_1 \dots \int_\Omega \mathbf{E} \cdot \phi^{(J)}_k \dots \int_\Omega \mathbf{E} \cdot \phi^{(J)}_{n_J}\right]^t,
\end{aligned}
$$

and

$$\mathbf{G} \;=\; \left[\int_\Gamma \vec{J}_{ext}\varphi_1^{(\phi)} \ldots \int_\Gamma \vec{J}_{ext}\varphi_l^{(\phi)} \ldots \int_\Gamma \vec{J}_{ext}\varphi_{n_\phi}^{(\phi)}\right]^t.$$

With these definitions we can write the iterative scheme in a matrix form

$$\begin{bmatrix} A_{(u)}+N_{(u)} & B_{(p)}^t & -\left(N_{(J)}+C\right)^t & 0 \\ B_{(p)} & 0 & 0 & 0 \\ N_{(J)}+C & 0 & A_{(J)} & B_{(\phi)}^t \\ 0 & 0 & B_{(\phi)} & 0 \end{bmatrix} \begin{bmatrix} \mathbf{c}^{(u,n)} \\ \mathbf{c}^{(p,n)} \\ \mathbf{c}^{(J,n)} \\ \mathbf{c}^{(\phi,n)} \end{bmatrix} = \begin{bmatrix} \mathbf{F} \\ \mathbf{0} \\ \mathbf{E} \\ \mathbf{G} \end{bmatrix}.$$

3.2 Finite Element Spaces

We choose finite element spaces for our finite-dimensional spaces. Recalling from [78] that the spaces must satisfying the LBB-conditions

$$\inf_{q^h \in M_1^h} \sup_{\mathbf{v}^h \in \mathbf{Y}_1^h} \frac{\int_\Omega \left(\nabla \cdot \mathbf{v}^h\right) q^h}{\|\mathbf{v}^h\|_{\mathbf{Y}_1^h} \|q^h\|_{M_1^h}} \geq \beta_1 > 0$$

and

$$\inf_{\psi^h \in M_2^h} \sup_{\mathbf{K}^h \in \mathbf{Y}_2^h} \frac{\int_\Omega \mathbf{K}^h \cdot \left(\nabla \psi^h\right)}{\|\mathbf{K}^h\|_{\mathbf{Y}_2^h} \|\psi^h\|_{M_2^h}} \geq \beta_2 > 0,$$

we determine velocity-pressure pairs $\left(\mathbf{X}_1^h, M_1^h\right)$ and the current-potential pairs $\left(\mathbf{X}_2^h, M_2^h\right)$. The LBB condition for the velocity-pressure pair appears in the theory on the Stokes and Navier-Stokes equations. Taylor-Hood elements are examples of velocity-pressure finite-element pairs that satisfy the condition. For Taylor-Hood elements we choose triquadratics for the velocity and trilinears for the pressure.

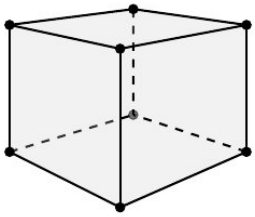

(a) Q1 Trilinear Nodes.

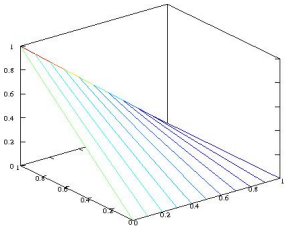

(b) Q1 Basis Function.

Figure 3.1: 2-D Example of Q1 Basis Function for Pressure

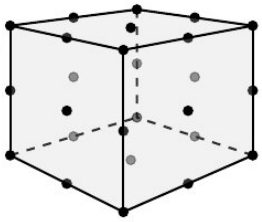

(a) Q2 Triquadratic Nodes.

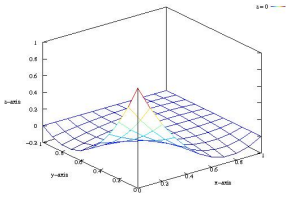

(b) 2D Q2 Basis Function.

Figure 3.2: 2-D Example of Q2 Basis Function for Velocity

For each component k of the velocity vector basis function $\vec{\varphi}_i^{(u)}$ we use triquadratic elements of the form

$$\left(\varphi_i^{(\phi)}(x)\right)_k = \sum_{\substack{i1,\,i2,\,i3 \geq 0 \\ i_1+i_2+i_3 \leq 2}} \alpha_{i_1,i_2,i_3} x_1^{i_1} x_2^{i_2} x_3^{i_3} \in \left\{\Pi_{1\leq i\leq 3}\left(\alpha_{i0}+\alpha_{i1}x_i+\alpha_{i2}x_i^2\right) : \alpha_{ij} \in \mathbb{R}\right\}.$$

For the pressure basis functions $\varphi_i^{(p)}$, we use trilinears

$$\varphi_i^{(p)}(x) = \sum_{\substack{i1,\,i2,\,i3 \geq 0 \\ i_1+i_2+i_3 \leq 1}} \alpha_{i_1,i_2,i_3} x_1^{i_1} x_2^{i_2} x_3^{i_3} \in \left\{\Pi_{1\leq i\leq 3}\left(\alpha_{i0}+\alpha_{i1}x_i\right) : \alpha_{ij} \in \mathbb{R}\right\}.$$

To satisfy the LBB condition for the current density and electric potential pairs, we chose triquadratic elements for the electric potential and Nedelec elements of the first kind and

second degree for the current density [81, 92, 17],

$$\vec{\varphi}_i^{(J)}(x)\mathcal{P}^k = \left\{ \mathbf{u} = \begin{pmatrix} u_1 \\ u_2 \\ u_3 \end{pmatrix} : u_1 \in \mathcal{Q}_{k-1,k,k}, u_2 \in \mathcal{Q}_{k,k-1,k}, u_3 \in \mathcal{Q}_{k,k,k-1} \right\}.$$

where $k = 2$. For example, with $k = 2$ the first component u_1 is located in the tensor product of a linear in x, quadratic in y, and quadratic in z. u_1 will be linear and discontinuous in x and quadratic and continuous in y and z. These properties of the Nedelec element are due to the degrees of freedom having the form [17]

$$\int_e \mathbf{u} \cdot \boldsymbol{\tau} q ds \qquad \forall q \in \mathbb{P}_{k-1}(e),$$
$$\frac{1}{|f|} \int_f (\mathbf{u} \times \mathbf{n}) \cdot \mathbf{q} dA, \qquad \forall \mathbf{q} \in (\mathbb{P}_{k-2}(f))^3,$$

and

$$\int_K \mathbf{u} \cdot \mathbf{q} dV, \qquad \forall \mathbf{q} \in (\mathbb{P}_{k-3}(K))^3,$$

where K is a reference element, e is an edge of K, f is a face of K, $\boldsymbol{\tau}$ is the unit vector along the edge e, and $\mathbb{P}_k$ is the linear space of polynomials of degree $\leq k$. Note $p \in \mathbb{P}_k$ if and only if

$$p(x) = \sum_{\substack{i_1, i_2, i_3 \geq 0 \\ i_1 + i_2 + i_3 \leq k}} \alpha_{i_1,i_2,i_2} x_1^{i_1} x_2^{i_2} x_3^{i_3}$$

3.3 Preconditioner

We are now in a position to numerically solve the linear system. Having chosen GMRES to solve the system, we consider the preconditioner. To solve the system efficiently, we wish to minimize the number of iterations to convergence of the iterative solver. Hence we consider

bounds on the size of the residual $r_n = b - Ax_n$, since the tolerance on this value indicates when the solver has converged. In particular, we have the theorem [95]

Theorem 3.1 *At step n of the GMRES iteration for the system $Ax = b$, the residual $r_n = b - Ax_n$ satisfies*

$$\|r_n\| = \|p_n(A)b\| \leq \inf_{p_n \in P_n} \|p_n(A)\| \, \|b\| \leq \kappa(V) \inf_{p_n \in P_n} \|p_n\|_{\Lambda(A)} \, \|b\|$$

where $\Lambda(A)$ is the set of eigenvalues of A, V is a nonsingular matrix of eigenvectors (assuming A is diagonalizable), $P_n = \{p \text{ a polynomial} : \text{degree}(p) \leq n, p(0) = 1\}$ and $\|p_n\|_{\Lambda(A)}$ is defined by

$$\|p_n\|_{\Lambda(A)} = \sup_{z \in \Lambda(A)} \{p_n(z) : z \in \Lambda(A) \subset \mathbb{R}, p_n \in P_n\}$$

From the theorem, we conclude that if the system matrix A is normal, then a small condition number for the matrix of eigenvectors V will decrease the estimate on $\|r_n\|$ and help to reduce the number of iterations to reach convergence. Perhaps more importantly, polynomials in P_n existing such that their values when applied to A have a small norm will also decrease the bound on the residual. More can be said if the matrix A is normal. The norm on the polynomials is considered over the spectrum of A ($\Lambda(A)$). If n is small then the zeros of the polynomial would also be small. For this to occur, the number of eigenvalues of A would have to be small or grouped together in a small number of clusters m. With this in mind, we consider our matrix system

$$\begin{bmatrix} A_{(u)} + N_{(u)} & B_{(p)}^t & -\left(N_{(J)} + C\right)^t & 0 \\ B_{(p)} & 0 & 0 & 0 \\ N_{(J)} + C & 0 & A_{(J)} & B_{(\phi)}^t \\ 0 & 0 & B_{(\phi)} & 0 \end{bmatrix} \begin{bmatrix} \mathbf{c}^{(u,n)} \\ \mathbf{c}^{(p,n)} \\ \mathbf{c}^{(J,n)} \\ \mathbf{c}^{(\phi,n)} \end{bmatrix} = \begin{bmatrix} \mathbf{F} \\ \mathbf{0} \\ \mathbf{E} \\ \mathbf{G} \end{bmatrix}.$$

To construct a preconditioner, we start by considering the work done for the Stokes and Navier-Stokes equations. These equations correspond to the upper left 2-by-2 block of our system matrix. Successful constructions of preconditioners for this system have been carried out by Elman, Silvester and Wathen [37]. The lower-right two-by-two block of our system is similar in form to the Navier-Stokes system. We therefore plan to extend the work of Elman, Silvester and Wathen to this portion of our system. To the best of our knowledge, this extension to our system can not be found in the literature. As a first preconditioner we construct one that is block-diagonal, and based on the system after removal of the terms due to the nonlinearities $\mathbf{u} \times \mathbf{B}$ (magnetic induction), $\mathbf{J} \times \mathbf{B}$ (the Lorentz force), and $\mathbf{u} \cdot \nabla \mathbf{u}$ (the interial term). We therefore plan to construct a preconditioner for the system

$$\begin{bmatrix} A_{(u)} & B_{(p)}^t & 0 & 0 \\ B_{(p)} & 0 & 0 & 0 \\ 0 & 0 & A_{(J)} & B_{(\phi)}^t \\ 0 & 0 & B_{(\phi)} & 0 \end{bmatrix} \text{ and } \begin{bmatrix} \mathbf{A} & \mathbf{B}^t \\ \mathbf{B} & \mathbf{0} \end{bmatrix} = \left[\begin{array}{cc:cc} A_{(u)} & & \vdots & B_{(p)}^t & 0 \\ 0 & A_{(J)} & \vdots & 0 & B_{(\phi)}^t \\ \hdots & \hdots & & \hdots & \hdots \\ B_{(p)} & 0 & \vdots & 0 & 0 \\ 0 & B_{(\phi)} & \vdots & 0 & 0 \end{array}\right].$$

For the Stokes equations, Elman, Silvester and Wathen developed a block-diagonal preconditioner using the pressure Schur complement $S_{(p)} = B_p A_u^{-1} B_p^t$. Their preconditioner was

$$P_1 = \begin{bmatrix} A_u^{-1} & 0 \\ 0 & B_p A_u^{-1} B_p^t \end{bmatrix}$$

To extend their work, we consider the potential Schur complement $S_{(\phi)} = B_{(\phi)} A_{(J)}^{-1} B_{(\phi)}^t$ and make plans to use it to precondition the lower-right 2-by-2 block of our system in a similar manner. Following their work, we recall the definition of the pressure mass matrix $Q_{(p)} = \left[q_{ij}^{(p)}\right] = \left[\int_\Omega \varphi_i^{(p)} \varphi_j^{(p)}\right]$ along with the following theorem about its spectral equivalence with the pressure Schur complement matrix $S_{(p)}$ [37].

Theorem 3.2 *For any flow problem with a Dirichlet boundary condition and discretized using a uniformly stable mixed approximation on a shape regular, quasi-uniform subdivision of* $\mathbb{R}^3$*, the pressure Schur complement matrix* $B_{(p)}A_{(u)}^{-1}B_{(p)}^t$ *is spectrally equivalent to the pressure mass matrix* $Q_{(p)}$*:*

$$\beta_1^2 \leq \frac{\left\langle B_{(p)}A_{(u)}^{-1}B_{(p)}^t\mathbf{q},\mathbf{q}\right\rangle}{\left\langle Q_{(p)}\mathbf{q},\mathbf{q}\right\rangle} \leq 1 \qquad \forall \mathbf{q} \in \mathbb{R}^{n_p} \text{ such that } \mathbf{q} \neq \mathbf{1}$$

and further

$$\beta_1^2 \leq \frac{\left\langle B_{(p)}^t Q_{(p)}^{-1}B_{(p)}\mathbf{v},\mathbf{v}\right\rangle}{\left\langle A_{(u)}\mathbf{v},\mathbf{v}\right\rangle} \leq 1 \quad \text{for all } \mathbf{v} \in \mathbb{R}^{n_u} \quad \text{with } \mathbf{v} \notin \text{null}\left(B_{(p)}\right).$$

A definition for spectral equivalence is given below [96].

Definition 1 *Consider two sequences of Hermitian positive definite matrices* A_h *and* C_h *and assume that all the eigenvalues* λ *of* $C_h^{-1}A_h$ *satisfy* $c_1 < \lambda < c_2$ *with positive* c_1 *and* c_2 *independent of* h*. Then* A_h *and* C_h *are said to be* ***spectrally equivalent****.*

From the definition, we can see that C_h is a good preconditioner for the system matrix A_h in terms of GMRES, since the preconditioned system's eigenvalues cluster between c_1 and c_2. The definition holds for $Q_{(p)}$ and $B_{(p)}A_{(u)}^{-1}B_{(p)}^t$ upon considering the eigenvalue problem $Q_{(p)}^{-1}B_{(p)}A_{(u)}^{-1}B_{(p)}^t\mathbf{x} = \lambda\mathbf{x}$. and the resultant inner product $\left\langle B_{(p)}A_{(u)}^{-1}B_{(p)}^t\mathbf{x},\mathbf{x}\right\rangle = \lambda\left\langle Q_{(p)}^{-1}\mathbf{x},\mathbf{x}\right\rangle$. The bounds from the theorem give the desired result. Hence, pressure mass matrix $Q_{(p)}$ is a good preconditioner for pressure Schur complement $B_{(p)}A_{(u)}^{-1}B_{(p)}^t$.

To construct, a preconditioner for the lower right 2-by-2 block, we define the laplace potential mass matrix $Q_{(\nabla\phi)} = \left[q_{ij}^{(\nabla\phi)}\right] = \left[\int_\Omega \nabla\varphi_i^{(\phi)} \cdot \nabla\varphi_j^{(\phi)}\right]$ and state and prove a corresponding theorem.

Theorem 3.3 *For any uniformly stable mixed approximation for the electric potential and current-density on a shape regular, quasi-uniform subdivision of* $\mathbb{R}^3$*, the potential Schur complement matrix* $S_{(\phi)} = B_{(\phi)}A_{(J)}^{-1}B_{(\phi)}^t$ *is spectrally equivalent to the laplace potential mass matrix* $Q_{(\nabla\phi)}$*:*

$$\beta_2^2 \leq \frac{\left\langle B_{(\phi)}A_{(J)}^{-1}B_{(\phi)}^t\mathbf{q},\mathbf{q}\right\rangle}{\left\langle Q_{(\nabla\phi)}\mathbf{q},\mathbf{q}\right\rangle} \leq 1 \qquad \forall \mathbf{q} \in \mathbb{R}^{n_\phi} \text{ such that } \mathbf{q} \neq \mathbf{1}.$$

The condition number of the potential Schur complement satisfies

$$\kappa\left(S_{(\phi)}\right) = \frac{\lambda_{max}\left(S_\phi\right)}{\lambda_{min}\left(S_\phi\right)} < \frac{C}{\beta_2^2 c}.$$

To make clear some of the statements in the theorem, we give definitions for shape regular and quasi-uniform [37] and prove a lemma. Let $\mathcal{T}_h$ be a decomposition of a convex polyhedral domain of interest into hexahedral "brick" elements Δ_k, and let $h_x^{(k)}$, $h_y^{(k)}$, and $h_z^{(k)}$ be the lengths of the brick element Δ_k in the x, y, and z directions, respectively. We call a sequence of hexahedral meshes $\{\mathcal{T}_h\}$ **shape regular** [37] if there exists a maximum brick edge ratio γ_* such that every brick element $\Delta_k \in \mathcal{T}_h$ satisfies $1 \leq \gamma_{\Delta_k} \leq \gamma_*$, where

$$\gamma_{\Delta_k} = \max\left(\left\{\frac{h_x^{(k)}}{h_y^{(k)}}, \frac{h_x^{(k)}}{h_z^{(k)}}, \frac{h_y^{(k)}}{h_x^{(k)}}, \frac{h_y^{(k)}}{h_z^{(k)}}, \frac{h_z^{(k)}}{h_x^{(k)}}, \frac{h_z^{(k)}}{h_y^{(k)}}\right\}\right).$$

From this definition, we see that the ratio of the longest edge to the shortest edge of each element Δ_k is bounded from above and below, and the uniform boundedness guarantees that the elements do not degenerate with refinement. Letting h_k denote the length of the longest edge of Δ_k, we call the sequence of meshes $\{\mathcal{T}_h\}$ **quasi-uniform** [37] if there exists a constant $\rho > 0$ such that

$$\min_{\Delta_k \in \mathcal{T}_h} h_k \geq \rho \max_{\Delta_k \in \mathcal{T}_h} h_k \quad \left(\text{ with } \max_{\Delta_k \in \mathcal{T}_h} h_k \geq \min_{\Delta_k \in \mathcal{T}_h} h_k\right).$$

for every mesh in the sequence. The definition implies that the local mesh size h_k is about constant for each mesh, with the ratio of the largest local mesh size to the smallest local mesh size bounded between $\frac{1}{\rho}$ and 1, and these bounds carry over with each refinement.

Lemma 3 *Using a* $\mathbf{Q}_2$ *triquadratic element approximation of the electric potential on a shape-regular subdivision in* $\mathbb{R}^3$ *for which a shape regular condition holds, the laplace potential mass matrix* $Q_{(\nabla\phi)}$ *approximates the scaled identity matrix in the sense that*

$$ch^3 \leq \frac{\langle Q_{(\nabla\phi)}\mathbf{q}, \mathbf{q}\rangle}{\langle \mathbf{q}, \mathbf{q}\rangle} \leq Ch^3 \qquad \forall \mathbf{q} \in \mathbb{R}^{n_\phi},$$

where $h = \max_{\Delta_k \in \mathcal{T}_h} h_k$ *and the constants* c *and* C *are independent of* h.

Proof:

First, note that $Q_{(\nabla\phi)} = \left[\int_\Omega \nabla\varphi_i^{(\phi)} \cdot \nabla\varphi_j^{(\phi)}\right]$ is symmetric and positive definite. In particular,

$$\begin{aligned}
0 \;\leq\; & \left\|\nabla\phi^h\right\|^2_{L^2(\Omega)} = \int_\Omega \nabla\phi^h \cdot \nabla\phi^h = \int_\Omega \nabla\phi^h \cdot \nabla \sum_{i=1}^{n_\phi} \mathbf{c}_i^{(\phi)}\varphi_i^{(\phi)} = \sum_{i=1}^{n_\phi} \mathbf{c}_i^{(\phi)} \int_\Omega \nabla\phi^h \cdot \nabla\varphi_i^{(\phi)} \\
= \; & \begin{bmatrix} \int_\Omega \nabla\phi^h \cdot \nabla\varphi_1^{(\phi)} & \dots & \int_\Omega \nabla\phi^h \cdot \nabla\varphi_{n_\phi}^{(\phi)} \end{bmatrix} \begin{bmatrix} \mathbf{c}_1^{(\phi)} \\ \vdots \\ \mathbf{c}_{n_\phi}^{(\phi)} \end{bmatrix} \\
= \; & \begin{bmatrix} \sum_{j=1}^{n_\phi} \mathbf{c}_j^{(\phi)} \int_\Omega \nabla\varphi_j^{(\phi)} \cdot \nabla\varphi_1^{(\phi)} & \dots & \sum_{j=1}^{n_\phi} \mathbf{c}_j^{(\phi)} \int_\Omega \nabla\varphi_j^{(\phi)} \cdot \nabla\varphi_{n_\phi}^{(\phi)} \end{bmatrix} \begin{bmatrix} \mathbf{c}_1^{(\phi)} \\ \vdots \\ \mathbf{c}_{n_\phi}^{(\phi)} \end{bmatrix} \\
= \; & \begin{bmatrix} \mathbf{c}_1^{(\phi)} & \dots & \mathbf{c}_{n_\phi}^{(\phi)} \end{bmatrix} \begin{bmatrix} \int_\Omega \nabla\varphi_1^{(\phi)} \cdot \nabla\varphi_1^{(\phi)} & \dots & \int_\Omega \nabla\varphi_1^{(\phi)} \cdot \nabla\varphi_{n_\phi}^{(\phi)} \\ \vdots & \ddots & \vdots \\ \int_\Omega \nabla\varphi_{n_\phi}^{(\phi)} \cdot \nabla\varphi_1^{(\phi)} & \dots & \int_\Omega \nabla\varphi_{n_\phi}^{(\phi)} \cdot \nabla\varphi_{n_\phi}^{(\phi)} \end{bmatrix} \begin{bmatrix} \mathbf{c}_1^{(\phi)} \\ \vdots \\ \mathbf{c}_{n_\phi}^{(\phi)} \end{bmatrix} = \left\langle Q_{(\nabla\phi)}\mathbf{c}^{(\phi)}, \mathbf{c}^{(\phi)} \right\rangle.
\end{aligned}$$

We can therefore form a basis for $\mathbb{R}^{n_\phi}$ out of the eigenvectors of $Q_{(\nabla\phi)}$ and denote the minimum and maximum eigenvalues as λ_{min} and λ_{max} respectively, with

$$\lambda_{min} \langle \mathbf{q}, \mathbf{q} \rangle \leq \left\langle Q_{(\nabla\phi)} \mathbf{q}, \mathbf{q} \right\rangle \leq \lambda_{max} \langle \mathbf{q}, \mathbf{q} \rangle \qquad \forall \mathbf{q} \in \mathbb{R}^{n_\phi}.$$

Consider an arbitrary element Δ_k of the grid $\mathcal{T}_h$. Letting $Q^{(k)}_{(\nabla\phi)} = \left[\int_{\Delta_k} \nabla\varphi_i^{(\phi)} \cdot \nabla\varphi_j^{(\phi)} \right]$, we have $Q_{(\nabla\phi)} = \sum_{k \in \mathcal{T}_h} Q^{(k)}_{(\nabla\phi)}$ and

$$0 \leq \left\| \phi^h \right\|^2_{L^2(\Delta_k)} = \left\langle Q^{(k)}_{(\nabla\phi)} \mathbf{c}^{(\phi)}, \mathbf{c}^{(\phi)} \right\rangle.$$

With $Q^{(k)}_{(\nabla\phi)}$ symmetric and positive definite, the same is true for $\frac{1}{h_x^{(k)} h_y^{(k)} h_z^{(k)}} Q^{(k)}_{(\nabla\phi)}$. Similar to $Q_{(\nabla\phi)}$, we have

$$\lambda^{(k)}_{min} \langle \mathbf{q}, \mathbf{q} \rangle \leq \left\langle \frac{1}{h_x^{(k)} h_y^{(k)} h_z^{(k)}} Q^{(k)}_{(\nabla\phi)} \mathbf{q}, \mathbf{q} \right\rangle \leq \lambda^{(k)}_{max} \langle \mathbf{q}, \mathbf{q} \rangle \qquad \forall \mathbf{q} \in \mathbb{R}^{n_\phi}.$$

Shape regularity of the triangulations $\{\mathcal{T}_h\}$ implies that there exists a maximum brick edge ratio γ_* such that every element $\Delta_k \in \mathcal{T}_h$ satisfies $1 \leq \gamma_{\Delta_k} \leq \gamma_*$. Without loss of generality, let $h_x^{(k)} \leq h_y^{(k)} \leq h_z^{(k)} = h_k$. Then $\frac{h_x^{(k)}}{h_z^{(k)}} < \frac{h_y^{(k)}}{h_z^{(k)}} < 1$ and $\gamma_{\Delta_k} = \frac{h_z^{(k)}}{h_x^{(k)}} > \frac{h_y^{(k)}}{h_x^{(k)}} > 1$. With

$$h_x^{(k)} h_y^{(k)} h_z^{(k)} = \frac{h_x^{(k)}}{h_z^{(k)}} \frac{h_y^{(k)}}{h_z^{(k)}} \left(h_z^{(k)} \right)^3 = \frac{1}{\gamma_{\Delta_k}} \frac{h_y^{(k)}}{h_z^{(k)}} h_k^3 \geq \frac{1}{\gamma_{\Delta_k}} \frac{h_x^{(k)}}{h_z^{(k)}} h_k^3 \geq \frac{1}{\gamma^2_{\Delta_k}} h_k^3 \geq \frac{1}{\gamma_*} h_k^3$$

and

$$h_x^{(k)} h_y^{(k)} h_z^{(k)} = \frac{h_y^{(k)}}{h_x^{(k)}} \frac{h_z^{(k)}}{h_x^{(k)}} \left(h_x^{(k)} \right)^3 \leq \frac{h_y^{(k)}}{h_x^{(k)}} \frac{h_z^{(k)}}{h_x^{(k)}} h_k^3 \leq \frac{h_z^{(k)}}{h_x^{(k)}} \frac{h_z^{(k)}}{h_x^{(k)}} h_k^3 = \gamma^2_{\Delta_k} h_k^3 \leq \gamma_*^2 h_k^3,$$

we have

$$\begin{aligned} h_k^3 \frac{1}{\gamma_*^2} \lambda^{(k)}_{min} \langle \mathbf{q}, \mathbf{q} \rangle &\leq h_x^{(k)} h_y^{(k)} h_z^{(k)} \lambda^{(k)}_{min} \langle \mathbf{q}, \mathbf{q} \rangle \leq \left\langle Q^{(k)}_{(\nabla\phi)} \mathbf{q}, \mathbf{q} \right\rangle \\ &\leq h_x^{(k)} h_y^{(k)} h_z^{(k)} \lambda^{(k)}_{max} \langle \mathbf{q}, \mathbf{q} \rangle \leq h_k^3 \gamma_*^2 \lambda^{(k)}_{max} \langle \mathbf{q}, \mathbf{q} \rangle. \end{aligned}$$

The sequence of triangulations $\{\mathcal{T}_h\}$ are quasi-uniform and there exists a constant $\rho > 0$ such that $\min_{\Delta_k \in \mathcal{T}_h} h_k \geq \rho \max_{\Delta_k \in \mathcal{T}_h} h_k$. With $h = \max_{\Delta_k \in \mathcal{T}_h} h_k$ we have

$$\rho^3 h^3 \frac{1}{\gamma_*^2} \lambda_{min}^{(k)} \langle \mathbf{q}, \mathbf{q} \rangle \leq \left\langle Q_{(\nabla\phi)}^{(k)} \mathbf{q}, \mathbf{q} \right\rangle \leq h^3 \gamma_*^2 \lambda_{max}^{(k)} \langle \mathbf{q}, \mathbf{q} \rangle$$

and since $\left\langle Q_{(\nabla\phi)} \mathbf{q}, \mathbf{q} \right\rangle = \sum_{\Delta_k \in \mathcal{T}_h} \left\langle Q^{(k)} \mathbf{q}, \mathbf{q} \right\rangle$ we have

$$\rho^3 h^3 \frac{1}{\gamma_*^2} \langle \mathbf{q}, \mathbf{q} \rangle \sum_{k=1}^{n_{\Delta_k}} \lambda_{min}^{(k)} \leq \left\langle Q_{(\nabla\phi)} \mathbf{q}, \mathbf{q} \right\rangle \leq h^3 \gamma_*^2 \langle \mathbf{q}, \mathbf{q} \rangle \sum_{k=1}^{n_{\Delta_k}} \lambda_{max}^{(k)}.$$

Letting $c = \frac{\rho^3}{\gamma_*^2} \sum_{k=1}^{n_\Delta} \lambda_{min}^{(k)}$ and $C = \gamma_*^2 \sum_{k=1}^{n_{\Delta_k}} \lambda_{max}^{(k)}$, gives

$$ch^3 \leq \frac{\left\langle Q_{(\nabla\phi)} \mathbf{q}, \mathbf{q} \right\rangle}{\langle \mathbf{q}, \mathbf{q} \rangle} \leq Ch^3 \qquad \mathbf{q} \in \mathbb{R}^{n_\phi}. \qquad \square$$

We now prove Theorem 3.3.

Proof:

The lower bound of the inequality that we wish to establish is a consequence of the LBB condition

$$\beta_2 \leq \min_{\psi^h \neq \text{constant}} \max_{\vec{K}^h \neq \vec{0}} \frac{\left| \left(\mathbf{K}^h, \nabla \psi^h \right) \right|}{\|\psi^h\|_{1,\Omega} \|\mathbf{K}^h\|_{0,\Omega}}.$$

We start first with the upper bound. Writing the components from the numerator of the LBB condition as linear combinations of basis functions

$$\mathbf{K}^h = \sum_{i=1}^{n_J} \mathbf{k}_i \vec{\varphi}_i^{(J)} = \boldsymbol{\varphi}_{(J)}^t \mathbf{k} \quad \text{and} \quad \psi^h = \sum_{i=1}^{n_\phi} \mathbf{q}_i \varphi_i^{(\phi)} = \boldsymbol{\varphi}_{(\phi)}^t \mathbf{q},$$

the integral in the numerator of the LBB condition can then be written as

$$\int_\Omega \mathbf{K}^h \cdot \nabla \psi^h \;=\; \sum_{i=1}^{n_J} \mathbf{k}_i \sum_{j=1}^{n_\phi} \mathbf{q}_j \int_\Omega \vec{\varphi}_i^{(J)} \cdot \nabla \psi_j^h = \left\langle \mathbf{k}, B_{(\phi)}^t \mathbf{q} \right\rangle .$$

For the denominator we have

$$\left\| \vec{K}^h \right\|_{L_2(\Omega)}^2 = \int_\Omega \vec{K}^h \cdot \vec{K}^h = \sum_{i=1}^{n_J} \mathbf{k}_i \sum_{j=1}^{n_J} \mathbf{k}_j \int_\Omega \vec{\varphi}_i^{(J)} \cdot \vec{\varphi}_j^{(J)} = \left\langle A_{(J)} \mathbf{k}, \mathbf{k} \right\rangle$$

and

$$\begin{aligned}
\left\| \psi^h \right\|_{L_2(\Omega)}^2 &= \int_\Omega \psi^h \psi^h + \nabla \psi^h \cdot \nabla \psi^h \\
&= \sum_{i=1}^{n_\phi} \mathbf{q}_i \sum_{j=1}^{n_\phi} \mathbf{q}_j \int_\Omega \varphi_i^{(\phi)} \varphi_j^{(\phi)} + \sum_{i=1}^{n_\phi} \mathbf{q}_i \sum_{j=1}^{n_\phi} \mathbf{q}_j \int_\Omega \nabla \varphi_i^{(\phi)} \cdot \nabla \varphi_j^{(\phi)} \\
&= \left\langle \mathbf{q}, Q_{(\phi)} \mathbf{q} \right\rangle + \left\langle \mathbf{q}, Q_{(\nabla\phi)} \mathbf{q} \right\rangle = \left\langle \mathbf{q}, \left(Q_{(\phi)} + Q_{(\nabla\phi)} \right) \mathbf{q} \right\rangle \leq \left\langle \mathbf{q}, Q_{(\nabla\phi)} \mathbf{q} \right\rangle ,
\end{aligned}$$

since $Q_{(\phi)}$ and $Q_{(\nabla\phi)}$ are symmetric positive definite. With $A_{(J)}$ symmetric positive definite we can diagonalize it with a matrix P and define its root

$$A_{(J)} = PDP^{-1} \quad \text{and} \quad A_{(J)}^{1/2} = PD^{1/2}P^{-1}.$$

Thus,

$$\left| \left\langle \mathbf{k}, B_{(\phi)}^t \mathbf{q} \right\rangle \right| = \left| \left(\vec{K}^h, \nabla \psi^h \right) \right| \leq \left\| K^h \right\|_{(L_2(\Omega))^3} \left\| \nabla \psi^h \right\|_{L_2(\Omega)} = \sqrt{\left\langle \mathbf{k}, A_{(J)} \mathbf{k} \right\rangle} \sqrt{\left\langle \mathbf{q}, Q_{\nabla\phi} \mathbf{q} \right\rangle}$$

and we obtain the upper bound

$$\frac{\left| \left\langle \mathbf{k}, B_{(\phi)}^t \mathbf{q} \right\rangle \right|}{\sqrt{\left\langle \mathbf{k}, A_{(J)} \mathbf{k} \right\rangle} \sqrt{\left\langle \mathbf{q}, Q_{\nabla+\phi} \mathbf{q} \right\rangle}} \leq 1 \qquad \forall \mathbf{k} \in \mathbb{R}^{n_J} \quad \forall \mathbf{q} \in \mathbb{R}^{n_\phi}.$$

In particular, for $\mathbf{k} = A_{(J)}^{-1} B_{(\phi)}^t \mathbf{q}$ we have

$$\frac{\sqrt{\left\langle B_{(\phi)} A_{(J)}^{-1} B_{(\phi)}^t \mathbf{q}, \mathbf{q} \right\rangle}}{\sqrt{\left\langle \mathbf{q}, Q_{(\nabla\phi)} \mathbf{q} \right\rangle}} \leq 1 \qquad \forall \mathbf{q} \in \mathbb{R}^{n_\phi}.$$

For the lower bound, we start with the LBB condition

$$\begin{aligned}
\beta_2 &\leq \min_{\psi^h \neq \text{const}} \max_{\vec{K}^h \neq \vec{0}} \frac{\left| \int_\Omega \vec{K}^h \cdot (\nabla \psi^h) \right|}{\left\| \vec{K}^h \right\|_{(L_2(\Omega))^3} \left\| \psi^h \right\|_{H_1(\Omega)}} = \min_{\mathbf{q} \neq \mathbf{1}} \max_{\mathbf{k} \neq \mathbf{0}} \frac{\left| \left\langle \mathbf{k}, B_{(\phi)}^t \mathbf{q} \right\rangle \right|}{\sqrt{\left\langle \mathbf{k}, A_{(J)} \mathbf{k} \right\rangle} \sqrt{\left\langle \mathbf{q}, \left(Q_{(\phi)} + Q_{(\nabla\phi)} \right) \mathbf{q} \right\rangle}} \\
&\leq \min_{\mathbf{q} \neq \mathbf{1}} \max_{\mathbf{k} \neq \mathbf{0}} \frac{\left| \left\langle \mathbf{k}, B_{(\phi)}^t \mathbf{q} \right\rangle \right|}{\sqrt{\left\langle \mathbf{k}, A_{(J)} \mathbf{k} \right\rangle} \sqrt{\left\langle \mathbf{q}, Q_{(\nabla\phi)} \mathbf{q} \right\rangle}} = \min_{\mathbf{q} \neq \mathbf{1}} \frac{1}{\sqrt{\left\langle \mathbf{q}, Q_{(\nabla\phi)} \mathbf{q} \right\rangle}} \max_{\mathbf{k} \neq \mathbf{0}} \frac{\left| \left\langle \mathbf{k}, B_{(\phi)}^t \mathbf{q} \right\rangle \right|}{\sqrt{\left\langle \mathbf{k}, A_{(J)} \mathbf{k} \right\rangle}} \\
&= \min_{\mathbf{q} \neq \mathbf{1}} \frac{1}{\sqrt{\left\langle \mathbf{q}, Q_{(\nabla\phi)} \mathbf{q} \right\rangle}} \max_{\mathbf{w} \neq \mathbf{0}} \frac{\left| \left\langle A_{(J)}^{-1/2} \mathbf{w}, B_{(\phi)}^t \mathbf{q} \right\rangle \right|}{\sqrt{\left\langle A_{(J)}^{1/2} \mathbf{k}, A_{(J)}^{1/2} \mathbf{k} \right\rangle}} = \min_{\mathbf{q} \neq \mathbf{1}} \frac{1}{\sqrt{\left\langle \mathbf{q}, Q_{(\nabla\phi)} \mathbf{q} \right\rangle}} \max_{\mathbf{w} \neq \mathbf{0}} \frac{\left| \left\langle \mathbf{w}, A_{(J)}^{-1/2} B_{(\phi)}^t \mathbf{q} \right\rangle \right|}{\sqrt{\langle \mathbf{w}, \mathbf{w} \rangle}} \\
&= \min_{\mathbf{q} \neq \mathbf{1}} \frac{1}{\sqrt{\left\langle \mathbf{q}, Q_{(\nabla\phi)} \mathbf{q} \right\rangle}} \frac{\left\langle A_{(J)}^{-1/2} B_{(\phi)}^t \mathbf{q}, A_{(J)}^{-1/2} B_{(\phi)}^t \mathbf{q} \right\rangle}{\sqrt{\left\langle A_{(J)}^{-1/2} B_{(\phi)}^t \mathbf{q}, A_{(J)}^{-1/2} B_{(\phi)}^t \mathbf{q} \right\rangle}} = \min_{\mathbf{q} \neq \mathbf{1}} \frac{\sqrt{\left\langle B_{(\phi)} A_{(J)}^{-1} B_{(\phi)}^t \mathbf{q}, \mathbf{q} \right\rangle}}{\sqrt{\left\langle \mathbf{q}, Q_{(\nabla\phi)} \mathbf{q} \right\rangle}}.
\end{aligned}$$

The maximum is attained when $w = \pm A_{(J)}^{-1/2} B_{(\phi)}^t \mathbf{q}$. This can be seen by incorporating the norm of $\mathbf{w}$ in the denominator into the first term of inner product in the numerator and recalling the scalar product formula $|\mathbf{a}| \, |\mathbf{b}| \cos(\theta) = \langle \mathbf{a}, \mathbf{b} \rangle$. The largest absolute value will occur when the unit vector $\frac{\mathbf{w}}{\sqrt{\langle \mathbf{w}, \mathbf{w} \rangle}}$ is in the same direction or opposite direction of the other vector. The two inequalities yield the result

$$\beta_2^2 \leq \frac{\left\langle B_{(\phi)} A_{(J)}^{-1} B_{(\phi)}^t \mathbf{q}, \mathbf{q} \right\rangle}{\left\langle Q_{(\nabla\phi)} \mathbf{q}, \mathbf{q} \right\rangle} \leq 1 \qquad \forall \mathbf{q} \in \mathbb{R}^{n_\phi} \text{ such that } \mathbf{q} \neq \mathbf{1}$$

Using the previous lemma, we have the bounds

$$\begin{aligned}
\beta_2^2 c h^3 &< \lambda_{min} \left(B_{(\phi)} A_{(J)}^{-1} B_{(\phi)}^t \right) \langle \mathbf{q}, \mathbf{q} \rangle \leq \left\langle B_{(\phi)} A_{(J)}^{-1} B_{(\phi)}^t \mathbf{q}, \mathbf{q} \right\rangle \\
&\leq \lambda_{max} \left(B_{(\phi)} A_{(J)}^{-1} B_{(\phi)}^t \right) < C h^3 \qquad \forall \mathbf{q} \in \mathbb{R}^{n_\phi} \text{ with } \mathbf{q} \neq \mathbf{1}
\end{aligned}$$

and the condition number of the potential Schur complement satisfies

$$\kappa\left(B_{(\phi)}A_{(J)}^{-1}B_{(\phi)}^{t}\right)=\frac{\lambda_{max}\left(B_{(\phi)}A_{(J)}^{-1}B_{(\phi)}^{t}\right)}{\lambda_{min}\left(B_{(\phi)}A_{(J)}^{-1}B_{(\phi)}^{t}\right)}<\frac{C}{\beta_2^2 c}\qquad\square$$

Corollary 1 *From the eigenvalues σ of*

$$\begin{bmatrix}A_{(J)}^{-1} & 0\\ 0 & Q^{-1}\end{bmatrix}\begin{bmatrix}0 & B_{(\phi)}^{t}\\ B_{(\phi)} & 0\end{bmatrix}\begin{bmatrix}\mathbf{k}\\ \boldsymbol{\psi}\end{bmatrix}=\sigma\begin{bmatrix}\mathbf{k}\\ \boldsymbol{\psi}\end{bmatrix}$$

we have that

$$\beta_2^2\leq\frac{\left\langle B_{(\phi)}^{t}Q_{(\nabla\phi)}^{-1}B_{(\phi)}\mathbf{k},\mathbf{k}\right\rangle}{\left\langle A_{(J)}\mathbf{k},\mathbf{k}\right\rangle}\leq 1\quad\forall\mathbf{k}\in\mathbb{R}^{n_J}\ \textit{such that}\ \mathbf{k}\notin\textit{null}\left(B_{(\phi)}\right)$$

Proof: We consider two cases $\sigma=0$ and $\sigma\neq 0$. For the case $\sigma=0$ with $\begin{bmatrix}\mathbf{k}^t & \boldsymbol{\psi}^t\end{bmatrix}^t\neq\mathbf{0}$ (eigenvalue problem), the preconditioning matrix on the left is nonsingular and therefore implies that $B_{(\phi)}^{t}\boldsymbol{\psi}=\mathbf{0}$ and $B_{(\phi)}\mathbf{k}=\mathbf{0}$. Conversely, if $\mathbf{k}\neq\mathbf{0}$ and $\boldsymbol{\psi}\neq\mathbf{0}$ with $B_{(\phi)}^{t}\boldsymbol{\psi}=\mathbf{0}$ and $B_{(\phi)}\mathbf{k}=\mathbf{0}$, then $\sigma=0$. Looking at the individual rows we have

$$B_{(\phi)}^{t}\boldsymbol{\psi}=\sigma A_{(J)}\mathbf{k}\quad\text{ and }\quad B_{(\phi)}\mathbf{k}=\sigma Q\boldsymbol{\psi}.$$

Therefore

$$\left\langle\mathbf{k},B_{(\phi)}^{t}\boldsymbol{\psi}\right\rangle=\sigma\left\langle A_{(J)}\mathbf{k},\mathbf{k}\right\rangle\quad\text{ and }\quad\left\langle\boldsymbol{\psi},B_{(\phi)}\mathbf{k}\right\rangle=\sigma\left\langle Q\boldsymbol{\psi},\boldsymbol{\psi}\right\rangle.$$

Further, $\left\langle A_{(J)}\mathbf{k},\mathbf{k}\right\rangle=\left\langle Q\boldsymbol{\psi},\boldsymbol{\psi}\right\rangle$, if $\sigma\neq 0$. From this equality and the positive definiteness of $A_{(J)}$ and $Q_{(\nabla\psi)}$, $\sigma\neq 0$ implies $\mathbf{k}\neq\mathbf{0}$ and $\boldsymbol{\psi}\neq\mathbf{0}$. Our interest is thus in the case $\sigma\neq 0$.

Multiplying the system by the diagonal matrix shown below

$$\begin{bmatrix} B_{(\phi)} & 0 \\ 0 & B_{(\phi)}^t \end{bmatrix} \begin{bmatrix} A_{(J)}^{-1} & 0 \\ 0 & Q^{-1} \end{bmatrix} \begin{bmatrix} 0 & B_{(\phi)}^t \\ B_{(\phi)} & 0 \end{bmatrix} \begin{bmatrix} \mathbf{k} \\ \boldsymbol{\psi} \end{bmatrix} = \sigma \begin{bmatrix} B_{(\phi)} & 0 \\ 0 & B_{(\phi)}^t \end{bmatrix} \begin{bmatrix} \mathbf{k} \\ \boldsymbol{\psi} \end{bmatrix}$$

we can write each row in terms of a single component of the eigenvector

$$B_{(\phi)} A_{(J)}^{-1} B_{(\phi)}^t \boldsymbol{\psi} = \sigma B_{(\phi)} \mathbf{k} = \sigma^2 Q \boldsymbol{\psi} \quad \text{and} \quad B_{(\phi)}^t Q_{(\phi)}^{-1} B_{(\phi)} \mathbf{k} = \sigma B_{(\phi)}^t \boldsymbol{\psi} = \sigma^2 A_{(J)} \mathbf{k}.$$

Hence, we obtain two related eigenvalue problems

$$Q^{-1} B_{(\phi)} A_{(J)}^{-1} B_{(\phi)}^t \boldsymbol{\psi} = \sigma^2 \boldsymbol{\psi} \quad \text{and} \quad A_{(J)}^{-1} B_{(\phi)}^t Q_{(\phi)}^{-1} B_{(\phi)} \mathbf{k} = \sigma^2 \mathbf{k}.$$

Further,

$$\frac{\left\langle B_{(\phi)} A_{(J)}^{-1} B_{(\phi)}^t \boldsymbol{\psi}, \boldsymbol{\psi} \right\rangle}{\langle Q \boldsymbol{\psi}, \boldsymbol{\psi} \rangle} = \sigma^2 = \frac{\left\langle B_{(\phi)}^t Q_{(\nabla \phi)}^{-1} B_{(\phi)} \mathbf{k}, \mathbf{k} \right\rangle}{\left\langle A_{(J)} \mathbf{k}, \mathbf{k} \right\rangle}.$$

The positive definiteness of $Q_{(\nabla \phi)}$ and that of the potential Schur complement from the previous theorem, we have n_ϕ positive eigenvalues σ^2. By this relation and the previous theorem, we obtain

$$\beta_2^2 \leq \frac{\left\langle B_{(\phi)}^t Q_{(\nabla \phi)}^{-1} B_{(\phi)} \mathbf{k}, \mathbf{k} \right\rangle}{\left\langle A_{(J)} \mathbf{k}, \mathbf{k} \right\rangle} \leq 1$$

as desired. □

Following similar arguments as in [37] we formulate the block-diagonal preconditioner that we will use for our problem. In the following theorem we look at its effects on the eigenvalues of the simplified system.

Theorem 3.4 *If* $\mathbf{u}^h$*,* p^h *and* $\mathbf{J}^h$*,*ϕ^h *have uniformly stable mixed approximations such that spectral equivalence of the Schur complements with the mass matrices hold, then for the*

system

$$\begin{bmatrix} A_{(u)}^{-1} & 0 & 0 & 0 \\ 0 & A_{(J)}^{-1} & 0 & 0 \\ 0 & 0 & Q_{(p)}^{-1} & 0 \\ 0 & 0 & 0 & Q_{(\nabla\phi)}^{-1} \end{bmatrix} \begin{bmatrix} A_{(u)} & 0 & B_{(p)}^{t} & 0 \\ 0 & A_{(J)} & 0 & B_{(\phi)}^{t} \\ B_{(p)} & 0 & 0 & 0 \\ 0 & B_{(\phi)} & 0 & 0 \end{bmatrix} \begin{bmatrix} \mathbf{u} \\ \mathbf{J} \\ \mathbf{p} \\ \boldsymbol{\phi} \end{bmatrix} = \lambda \begin{bmatrix} \mathbf{u} \\ \mathbf{J} \\ \mathbf{p} \\ \boldsymbol{\phi} \end{bmatrix}$$

all negative eigenvalues satisfy

$$-1 \leq \lambda \leq \frac{1}{2} - \frac{\sqrt{1 + 4\min(\beta_1, \beta_2)}}{2},$$

and all positive eigenvalues satisfy

$$1 \leq \lambda \leq \frac{1}{2} + \frac{\sqrt{5}}{2}.$$

Upon replacing $Q_{(p)}$ and $Q_{(\nabla\phi)}$ by the corresponding Schur complements, the system has exactly three eigenvalues $\lambda = 1, \frac{1}{2} \pm \frac{\sqrt{5}}{2}$.

Proof:

Let $x = \begin{bmatrix} \mathbf{u} \\ \mathbf{J} \end{bmatrix}$ and $y = \begin{bmatrix} \mathbf{p} \\ \boldsymbol{\phi} \end{bmatrix}$. Define A, B, and Q by

$$\begin{bmatrix} A & B^t \\ B & 0 \end{bmatrix} \begin{bmatrix} \mathbf{x} \\ \mathbf{y} \end{bmatrix} := \begin{bmatrix} A_{(u)} & 0 & B_{(p)}^{t} & 0 \\ 0 & A_{(J)} & 0 & B_{(\phi)}^{t} \\ B_{(p)} & 0 & 0 & 0 \\ 0 & B_{(\phi)} & 0 & 0 \end{bmatrix} \begin{bmatrix} \mathbf{u} \\ \mathbf{J} \\ \mathbf{p} \\ \boldsymbol{\phi} \end{bmatrix}$$

$$= \lambda \begin{bmatrix} A_{(u)} & 0 & 0 & 0 \\ 0 & A_{(J)} & 0 & 0 \\ 0 & 0 & Q_{(p)} & 0 \\ 0 & 0 & 0 & Q_{(\nabla\phi)} \end{bmatrix} \begin{bmatrix} \mathbf{u} \\ \mathbf{J} \\ \mathbf{p} \\ \boldsymbol{\phi} \end{bmatrix} =: \lambda \begin{bmatrix} A & 0 \\ 0 & Q \end{bmatrix} \begin{bmatrix} \mathbf{x} \\ \mathbf{y} \end{bmatrix}.$$

Proving the last part of the theorem first, replace Q by the block diagonal matrix $BA^{-1}B^t$ of the pressure and potential Schur complements . The result follows from consideration of two cases: $\mathbf{y} = \mathbf{0}$ and $\mathbf{y} \neq \mathbf{0}$.

For $\mathbf{y} = \mathbf{0}$ we have $\mathbf{x} \neq \mathbf{0}$ else our eigenvector is the zero vector. Looking at the second row of the system: $A\mathbf{x} + B^t\mathbf{y} = \lambda A\mathbf{x}$, we see $A\mathbf{x} = \lambda A\mathbf{x}$. Using the positive definiteness of A, we have $\langle A\mathbf{x}, \mathbf{x}\rangle > 0$ and therefore $\lambda = 1$.

For $\mathbf{y} \neq \mathbf{0}$, we set the first and second row of the system equal to each other. From the second row of the system, we have $B\mathbf{x} = \lambda Q\mathbf{y} = \lambda BA^{-1}B^t\mathbf{y}$ and therefore

$$(\lambda - 1)\, B\mathbf{x} = (\lambda - 1)\, \lambda BA^{-1}B^t\mathbf{y}.$$

Solving the first row $A\mathbf{x} + B^t\mathbf{y} = \lambda A\mathbf{x}$ for $B^t\mathbf{y}$ and multiplying by BA^{-1} we have

$$B^t\mathbf{y} = (\lambda - 1)\, A\mathbf{x} \implies BA^{-1}B^t\mathbf{y} = (\lambda - 1)\, B\mathbf{x}.$$

Therefore, $BA^{-1}B^t\mathbf{y} = (\lambda - 1)\, \lambda BA^{-1}B^t\mathbf{y}$ and with $BA^{-1}B^t$ positive definite (from the last theorem) we have $\langle BA^{-1}B^t\mathbf{y}, \mathbf{y}\rangle > 0$ and

$$1 = (\lambda - 1)\, \lambda \quad \text{with} \quad \lambda = \frac{1}{2} \pm \frac{\sqrt{5}}{2}.$$

using the quadratic formula.

To determine the intervals from the first part of the theorem, we consider the two cases $\lambda < 0$ and $\lambda > 0$. Suppose that $\lambda < 0$ is an eigenvalue of the system. We claim this implies that $\mathbf{y} \neq \mathbf{0}$. In contradiction, suppose that $\mathbf{y} = \mathbf{0}$. Then $\mathbf{x} \neq \mathbf{0}$ to have a meaningful eigenvalue problem. Looking at the first row of the system, we have $A\mathbf{x} + B^t\mathbf{y} = \lambda A\mathbf{x}$. Since $\mathbf{y} = \mathbf{0}$, $A\mathbf{x} = \lambda A\mathbf{x}$. With A positive definite, and $\mathbf{x} \neq \mathbf{0}$ it must be that $\lambda = 1 > 0$, a contradiction.

The first row of the system $A\mathbf{x} + B^t\mathbf{y} = \lambda A\mathbf{x}$ also implies that $\mathbf{x} = \frac{1}{\lambda - 1}A^{-1}B^t\mathbf{y}$. We can substitute this result for $\mathbf{x}$ into the second row of the system $B\mathbf{x} = \lambda Q\mathbf{y}$, and obtain

$$\frac{1}{\lambda - 1}BA^{-1}B^t\mathbf{y} = \lambda Q\mathbf{y} \quad \text{and} \quad BA^{-1}B^t\mathbf{y} = \lambda\left(\lambda - 1\right)Q\mathbf{y} = -\lambda\left(1 - \lambda\right)Q\mathbf{y}.$$

The positive definiteness and spectral equivalence of the Schur complements with their corresponding mass matrices along with $\lambda < 0$ imply

$$-\lambda\left\langle Q\mathbf{y}, \mathbf{y}\right\rangle \leq -\lambda\left(1 - \lambda\right)\left\langle Q\mathbf{y}, \mathbf{y}\right\rangle = \left\langle BA^{-1}B\mathbf{y}, \mathbf{y}\right\rangle \leq \left\langle Q\mathbf{y}, \mathbf{y}\right\rangle.$$

With $\mathbf{y} \neq \mathbf{0}$ we have $\lambda \geq -1$. From the lower bounds of the spectral equivalences

$$-\lambda\left(1 - \lambda\right)\left\langle Q\mathbf{y}, \mathbf{y}\right\rangle = \left\langle BA^{-1}B^t\mathbf{y}, \mathbf{y}\right\rangle \geq \min\left(\beta_1, \beta_2\right)\left\langle Q\mathbf{y}, \mathbf{y}\right\rangle.$$

Hence, $\lambda^2 - \lambda - \min\left(\beta_1, \beta_2\right) \geq 0$. Factorizing, we have $\left(\lambda - \lambda_+\right)\left(\lambda - \lambda_-\right) \geq 0$, where

$$\lambda_\pm = \frac{1}{2} \pm \frac{\sqrt{1 + 4\min\left(\beta_1, \beta_2\right)}}{2}.$$

From $\lambda \geq \lambda_+$ or $\lambda \leq \lambda_-$, and we obtain the upper bound $\lambda \leq \frac{1}{2} - \frac{\sqrt{1+4\min(\beta_1,\beta_2)}}{2}$. With the bounds $-1 \leq \lambda \leq \frac{1}{2} - \frac{\sqrt{1+4\min(\beta_1,\beta_2)}}{2}$ established for $\lambda < 0$, we are ready to look at the last case $\lambda > 0$.

For $\lambda > 0$ we have that $\mathbf{x} \neq \mathbf{0}$. Suppose by contradiction that $\mathbf{x} = \mathbf{0}$. Then, having an eigenvalue problem with $\lambda > 0$ it must be that $\mathbf{y} \neq \mathbf{0}$. Taking an inner product of the second

row of the system $B\mathbf{x} = \mathbf{0} = \lambda Q\mathbf{y}$ with $\mathbf{y}$ implies that $\mathbf{y} = \mathbf{0}$, since $Q_{(\nabla\phi)}$ positive definite and $\lambda > 0$.

Equating the first and second row of the system by way of the inner product $\langle B^t\mathbf{y}, \mathbf{x}\rangle = \langle B\mathbf{x}, \mathbf{y}\rangle$, we have

$$(\lambda - 1)\langle A\mathbf{x}, \mathbf{x}\rangle = \lambda \langle Q\mathbf{y}, \mathbf{y}\rangle \geq 0.$$

And with $\mathbf{x} \neq \mathbf{0}$, we have $\lambda \geq 1$. For the upper bound, the second row provides $\mathbf{y} = \frac{1}{\lambda}Q^{-1}B\mathbf{x}$, and we substitute this into the first row

$$(\lambda - 1)A\mathbf{x} = B^t\mathbf{y} = \frac{1}{\lambda}B^tQ^{-1}B\mathbf{x}.$$

From the previous corollary, we have

$$(\lambda - 1)\langle A\mathbf{x}, \mathbf{x}\rangle = \frac{1}{\lambda}\left\langle \frac{1}{\lambda}B^tQ^{-1}B\mathbf{x}, \mathbf{x}\right\rangle \leq \frac{1}{\lambda}\langle A\mathbf{x}, \mathbf{x}\rangle$$

and $\mathbf{x} \neq \mathbf{0}$ implies that $\lambda^2 - \lambda - 1 \leq 0$. Completing the square, we have $\left(\lambda - \frac{1}{2}\right)^2 - \frac{\sqrt{5}}{2}^2 \leq 0$ and the difference of squares gives the upper bound $\lambda \leq \frac{1}{2} + \frac{\sqrt{5}}{2}$. $\square$

The theorem on the block-diagonal preconditioner can be made more general as in [37]. Rather than using A in the preconditioner, spectral equivalence of A with a simpler matrix is used in establishing eigenvalue bounds, However, the theorem above will allow us to make comparisons in the next chapter. In particular, we will see the effect of the preconditioner from the theorem on eigenvalues of the simplified system for a particular example.

Chapter 4

Computational Experiments and Results

4.1 Introduction to the Computational Environment

4.1.1 Choice of the Libraries

The deal.ii library was used to implement the finite element method, p4est was used to partition the domain to the nodes of the distributed memory cluster, and a GMRES implementation from Trilinos was used to approximate the solution of the linear system in parallel as well invoke part of the preconditioner. Freely available libraries were also used for mesh generation and solution visualization. The open source library Gmsh [43] was used to generate several meshes, and the open-source library VisIt [22, 23, 100] was used to visualize the approximated solution.

Successful meshes were generated using Gmsh with particular coding techniques applied to the Gmsh script file and alterations to output .msh files (removing all but volume elements). The techniques were necessary, since Gmsh generates meshes using triangles in two dimensions and tetrahedrons in three dimensions (n-simplices), where deal.ii works with meshes that are quadrilaterals in two dimensions and and hexahedrals in three dimensions. Therefore, using Gmsh required unconventional coding in its script language in order to obtain hexahedral three-dimensional meshes.

The need for care with Gmsh was first noticed with Navier-Stokes benchmark tests for flow around a cylinder discussed by Turek and Schaefer [87]. During these tests it became evident

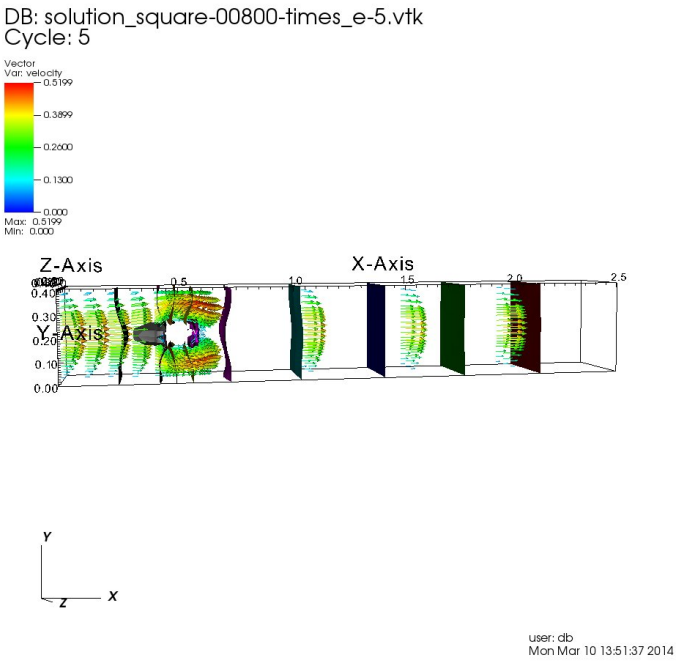

(a) Velocity Field with Presure Contours

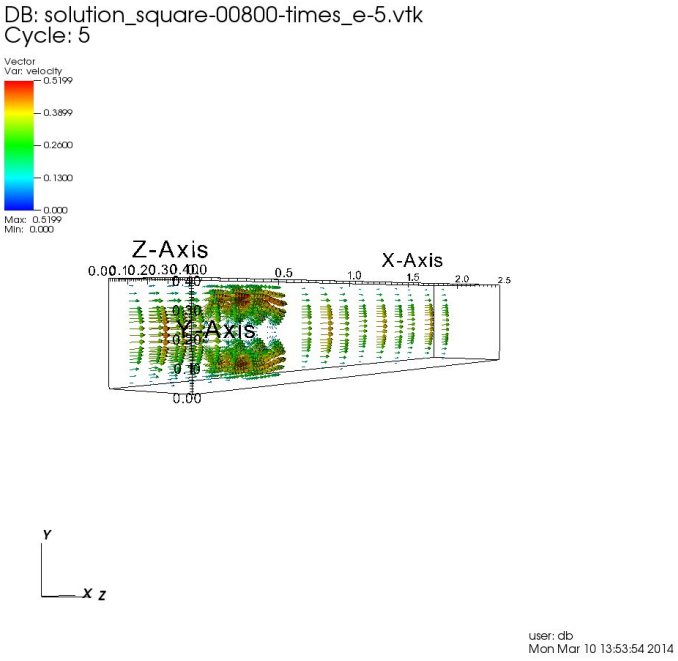

(b) Velocity Vector Field

Figure 4.1: Schafer Turek Benchmark

that boundary conditions were not being properly enforced for the velocity. Nonzero velocities were occurring on the boundary where zero velocities were prescribed. After troubleshooting the code, it became clear that the grid was causing problems. Some web research

concerning Gmsh and hexahedrals lead to editing of the Gmsh script files and the output .msh files. The problem with the boundary was fixed by removing elements in the output .msh file that were not volume elements (see GMSH manual `http://geuz.org/gmsh/`). Results comparable to Schafer and Turek were obtained as seen in the figure 4.1. With increasing library of meshes offered by newer versions of deal.ii and continued obstacles using Gmsh for generation, Gmsh was replaced by the deal.ii library for mesh generation toward the end of this research. In particular, code was added to the deal.ii library to create a toroidal mesh. A factor that appears to have influenced this decision was the activity of the mailing list. The depth of resources and documentation became important with increased investment in a library.

All of the visualization of data conducted during this research was performed using the library VisIt. VisIt was initially developed and is supported by the Lawrence Livermore National Lab. VisIt has decent documentation. However, the lack of documentation on movies with resolution providing crisp clarity have brought into consideration review of other libraries such as Paraview for comparison of capabilities and documentation.

4.1.2 Working with the Libraries

It should be mentioned that problems running code with the libraries can, do and have occurred during development. It is difficult to recall all bugs and problems encountered. They range from a variety of sources. Problems may occur in the installation process of the open-source libraries. This can be due to compiling a library with a faulty or unsupported compiler, attempting to link different libraries that have not been compiled with the same compiler, trying to link to versions of libraries that a particular library does not support, trying to link shared and static libraries, or not being able to properly locate and link to a compiler that has been installed by a system administrator. Bugs may also occur in the code being developed, such as a segmentation fault for an incorrectly set vector size. Bugs

may be found in the codes of the libraries that are being used, such as a bug encountered with the deal.ii PETSc vector values associated with ghost cells not being properly zeroed or a bug encountered with deal.ii function calls that work properly for serial code but corrupt for parallel code - as in mesh generation problems for an L-shaped domain. Bugs may occur that allow the code to compile and run but give unexpected results. An example is the approximate solution to the continuous pressure solutions of example 1 that gave discontinuous pressure contours. Rather than set the pressure at a node, the mean value pressure was calculated and then subtracted off the solution. This change in determining the unique solution eliminated the discontinuity appearing in the pressure contours. As the code was developed this problem eventually disappeared when both methods were retested. Attempts to recreate the bug have been unsuccessful. Most problems can be traced to a source, however some may disappear for uknown reasons with code development.

Bugs can occur outside of code run time, such as during visualization or mesh creation. An example of this type of problem is mentioned with the opensource software Gmsh opensource software when creating the flow around a cylinder to test out the Navier Stokes code while developing toward the MHD code. The problem appeared to be creating hexahedral elements using software designed to create tetrahedral elements. The problem was successfully overcome for a mesh used to model the flow around a cylinder in a rectangular duct. However, the problem was encountered again with the torus mesh with no apparent fix. Fortunately, deal.ii's mesh generation capabilities were developed enough to add code to the library to create a torus from hexhedral elements.

The use of multiple libraries can be forboding. The cause of an error may appear (and can be) difficult to determine or understand. In troubleshooting all the bugs encountered, the location of the bug was found first. Then, to understand the bug's behavior, adjustments to the code were made. Examples are changing the sample problem being tested or the size of a vector. The most common bugs occurred at interfaces between libraries. Important tips

to minimize work in tracking bugs are developing, programming, compiling and testing code frequently and in increments.

4.2 Example 1 - A Problem with an Exact Solution

The parallel finite element code was tested for expected convergence rates on two different domains: the cube $[0,1]^3$ and an L-shaped domain

$$[0,1]^3 \bigcup \left\{x + (0,1,0) \colon x \in [0,1]^3\right\} \bigcup \left\{x + (1,1,0) \colon x \in [0,1]^3\right\},$$

Using the example problem from [78]

$$\begin{aligned}
\mathbf{u}(x,y,z) &:= \begin{bmatrix} 0 \\ -\pi\cos(\pi x)\exp(-s)\left(\frac{1}{2}-z\right) \\ -\pi\cos(\pi x)\exp(-s)\left(y-\frac{1}{2}\right) \end{bmatrix} \\
\mathbf{J}(x,y,z) &:= \begin{bmatrix} 2\sin(\pi x)(1-s)\exp(-s) \\ -\pi\cos(\pi x)\exp(-s)\left(y-\frac{1}{2}\right) \\ -\pi\cos(\pi x)\exp(-s)\left(z-\frac{1}{2}\right) \end{bmatrix} \\
p(x,y,z) &:= -\frac{1}{2}\sin^2(\pi x)\, s\exp(-2s), \\
\phi(x,y,z) &:= \frac{2}{\pi}\cos(\pi x), \\
\mathbf{B}(x,y,z) &:= \begin{bmatrix} 1 \\ \sin(\pi x)\exp(-s)\left(\frac{1}{2}-z\right) \\ \sin(\pi x)\exp(-s)\left(y-\frac{1}{2}\right) \end{bmatrix}
\end{aligned}$$

with $\mathbf{r} = \left(0, y-\frac{1}{2}, z-\frac{1}{2}\right)$ and $s = |\mathbf{r}|^2 = \left(y-\frac{1}{2}\right)^2 + \left(z-\frac{1}{2}\right)^2$. Note that $\mathbf{u}$ and $\mathbf{B}$ are divergence free and $\nabla \times \mathbf{B} = \mathbf{J}$ (see Appendix D). The above set of equations is therefore a smooth solution to the velocity-current magnetohydrodynmaic equations with all parameters

η, ρ,σ, and μ equal to unity and the data $\mathbf{F}$, $\mathbf{E}$, $\mathbf{g}$, $\mathbf{J}_{ext}$, and $\mathbf{B}_{ext}$ defined by

$$\begin{aligned}\mathbf{F} &:= -\Delta\mathbf{u} + (\mathbf{u}\cdot\nabla)\,\mathbf{u} + \nabla p - \mathbf{J}\times\mathbf{B}, = -\begin{bmatrix}\nabla\cdot\nabla u_1\\ \nabla\cdot\nabla u_2\\ \nabla\cdot\nabla u_3\end{bmatrix} + \begin{bmatrix}\mathbf{u}\cdot\nabla u_1\\ \mathbf{u}\cdot\nabla u_2\\ \mathbf{u}\cdot\nabla u_3\end{bmatrix} + \begin{bmatrix}p_x\\ p_y\\ p_z\end{bmatrix} - \begin{bmatrix}J_2B_3 - J_3B_2\\ J_3B_1 - J_1B_3\\ J_1B_2 - J_2B_1\end{bmatrix}\\ &= \begin{bmatrix}0\\ \pi\cos(\pi x)\exp(-s)\left(z-\frac{1}{2}\right)\left(\pi^2+9-4s\right) + \sin^2(\pi x)\exp(-2s)\left(y-\frac{1}{2}\right)\\ -\pi^2\cos^2(\pi x)\exp(-2s)\left(y-\frac{1}{2}\right)\\ -\pi\cos(\pi x)\exp(-s)\left(y-\frac{1}{2}\right)\left(\pi^2+9-4s\right) + \sin^2(\pi x)\exp(-2s)\left(z-\frac{1}{2}\right)\\ -\pi^2\cos^2(\pi x)\exp(-2s)\left(z-\frac{1}{2}\right)\end{bmatrix}\end{aligned}$$

$$\mathbf{E} := \mathbf{J} + \nabla\phi - \mathbf{u}\times\mathbf{B} = \begin{bmatrix}2\sin(\pi x)\left((1-s)\exp(-s)-1\right)\\ 0\\ 0\end{bmatrix}$$

and

$$\mathbf{g} := \mathbf{u}\big|_{\Gamma}, \qquad \mathbf{J}_{ext} := \mathbf{J}\big|_{\mathbb{R}^3\setminus\overline{\Omega}}, \qquad \mathbf{B}_{ext} := \mathbf{i}.$$

Further, instead of integrating the Biot-Savart formula over $\mathbb{R}^3\setminus\overline{\Omega}$, the magnetic field induced by $\mathbf{J}_{ext}$ can be obtained from $\mathbf{B} - \mathbf{B}_{ext} - \mathcal{B}\left(\mathbf{J}\big|_{\Omega}\right)$. For uniqueness of the pressure and the electric potential, the exact solutions above for the pressure and potential were adjusted by a constant

$$\begin{aligned}p(x,y,z) &:= -\frac{1}{2}\sin^2(\pi x)\, s\exp(-2s) - \overline{p},\\ \phi(x,y,z) &:= \frac{2}{\pi}\cos(\pi x) - \frac{2}{\pi},\end{aligned}$$

where $\overline{p} = \frac{1}{\Omega}\int_{\Omega} -\frac{1}{2}\sin^2(\pi x)\, s\exp(-2s)dx$ was the mean pressure value of the exact solution over the domain Ω. For the electric potential ϕ one of the degrees of freedom on the $x = 0$ boundary of the domain $[0,1]^3$ was set to the value of the electric potential ϕ at $x = 0$ ($\phi(0) = 0$) by using the deal.ii constraint matrix.

The rates of convergence on the cube and the L-shaped domain are given in the tables 4.1 and 4.2.

Table 4.1: Errors and Convergence Rates for the Unit Cube Domain

Domain Infomation			**u**	**J**	p	ϕ
# Cells	**# DOFs**	**Cell size** (h)	**H^1-error**	**L^2-error**	**L^2-error**	**H^1-error**
			H^1-rate	**L^2-rate**	**L^2-rate**	**H^1-rate**
512	34,253	0.125	0.015004	0.000573	0.008111	0.006400
($8x8x8$)						
4096	253,205	0.0625	0.003751	0.000136	0.002031	0.001602
($16x16x16$)			2.000000	2.019216	1.999429	1.999674
32,768	1,945,637	0.03125	0.000938	0.000034	0.000508	0.000401
($32x32x32$)			1.999615	2.000000	1.999290	1.998200

Table 4.2: Errors and Convergence Rates for the Lshaped Domain

Domain Infomation			**u**	**J**	p	ϕ
# Cells	**# DOFs**	**Cell size** (h)	**H^1-error**	**L^2-error**	**L^2-error**	**H^1-error**
			H^1-rate	**L^2-rate**	**L^2-rate**	**H^1-rate**
24	2183	0.5	0.404921	0.146763	0.0154336	0.217988
($2x2x2$)						
192	13,969	0.25	0.102145	0.037215	0.00490111	0.00558378
($4x4x4$)			2.000000	2.076676	1.997737	1.998621
1536	44,508	0.125	0.02557343	0.00933088	0.000997906	0.0140478
($8x8x8$)			2.000001	2.019216	1.999429	1.999674

Visualizations of the numerical approximations to the solution of this example (see Figure 4.2) show symmetry about the line at the intersection of the planes $x = \frac{1}{2}$ and $y = \frac{1}{2}$. Note that to obtain illustrative perspectives in the plots for each variable, the point of view for each variable's plot is slightly different as indicated by the axes in the lower left corner. In particular, to compare the velocity vector field with the pressure contour plot, the pressure

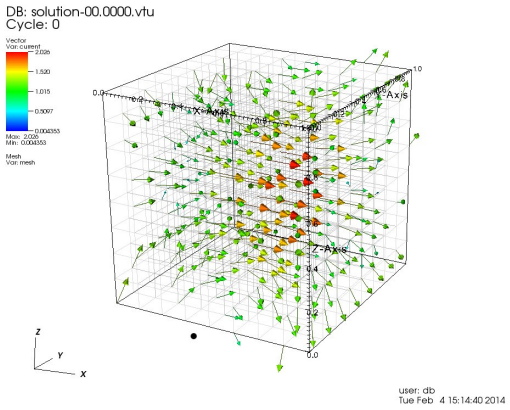

(a) Current in Cube Domain - Example 1

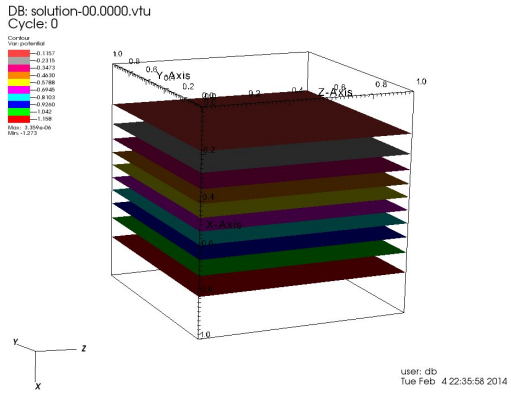

(b) Potential in Cube Domain - Example 1

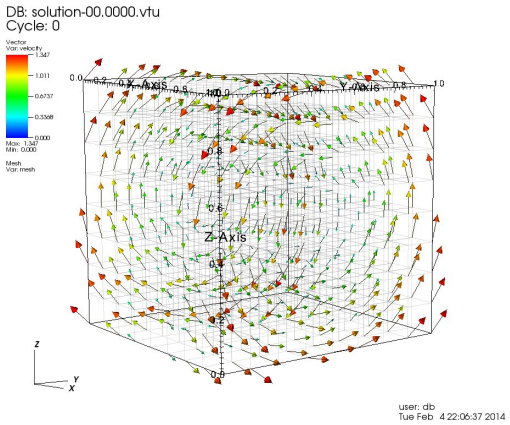

(c) Velocity in Cube Domain - Example 1

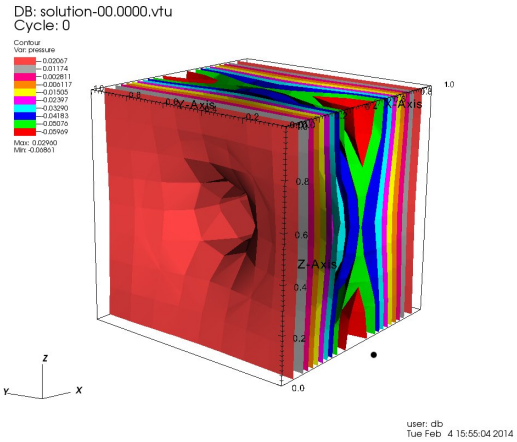

(d) Pressure in Cube Domain - Example 1

Figure 4.2: Example 1 for Cube Domain

plot would have to be rotated 90 degrees counter-clockwise around the z-axis. The symmetry in each plot would then match.

Approximate solutions to the problem on an L-shaped domain were also obtained. with graphs of the results shown in figure 4.3. From the figure, we see that the L-shaped domain extends the profiles of each approximated function occurring on the cube domain.

4.3 Example 2 - An Applied Problem

Approximate solutions to a second problem with more realistic conditions were also obtained for the unit cube and L-shaped domains. The problem prescribed a current entering at one

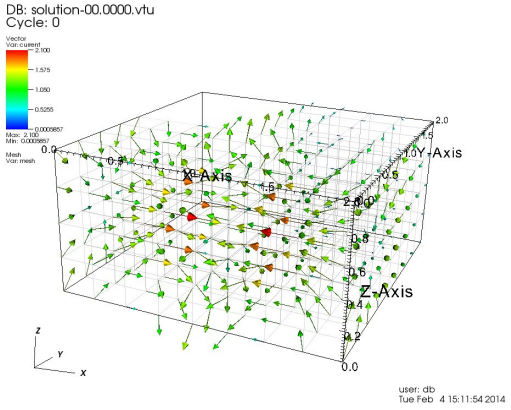

(a) Current in L-shaped Domain - Ex 1

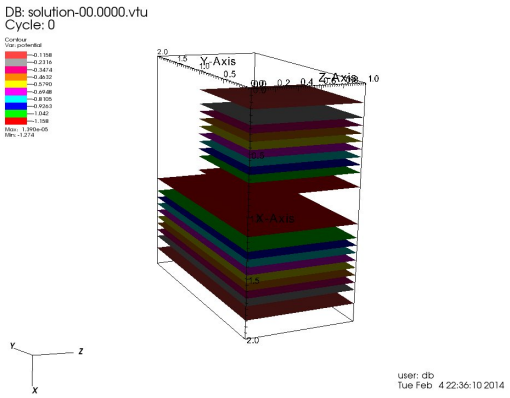

(b) Potential in L-shaped Domain - Ex 1

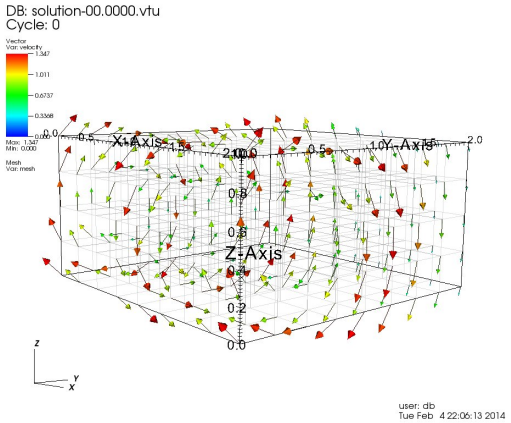

(c) Velocity in L-shaped Domain - Ex 1

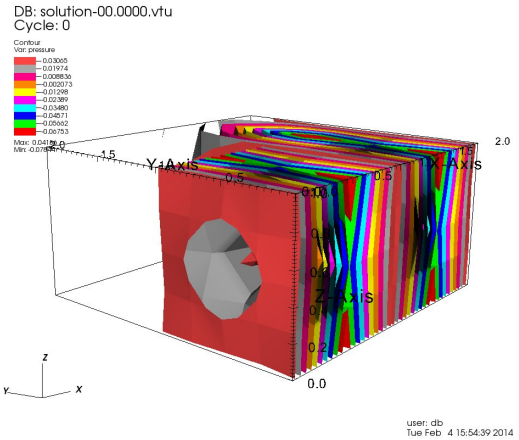

(d) Pressure in L-shaped Domain - Ex 1

Figure 4.3: Example 1 for Lshaped Domain

end (part of a domain face parallel to the z-axis) of the domain and exiting at the an end opposite to the entrance. The Dirichlet boundary conditions for the velocity were zero and the external magnetic field was zero for the problem as well. The magnitude of the current entering and exiting the domain through the boundary was fixed at $|\mathbf{J_{ext}}| = 100$. In order to obtain a unique solution for the electric potential and pressure, the problem was handled similar to the previous problem with an exact solution. In particular, the pressure mean value was calculated in a post process and subtracted from the solved pressure solution. The results can be seen in Figures 4.4, 4.5 and 5.2.

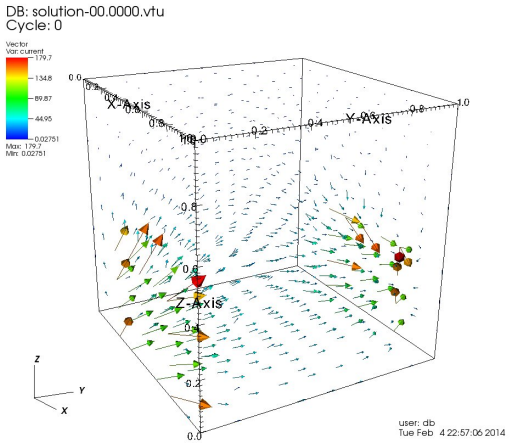

(a) Current in Cube Domain - Example 2

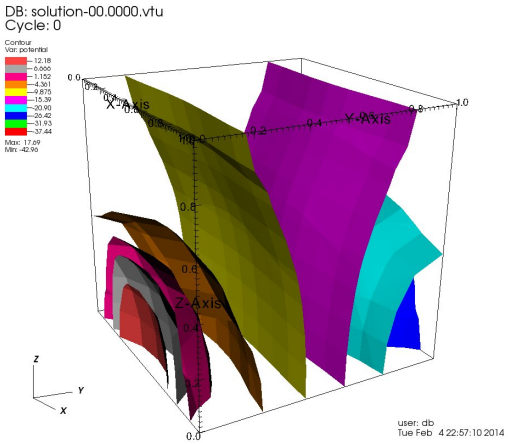

(b) Potential in Cube Domain - Example 2

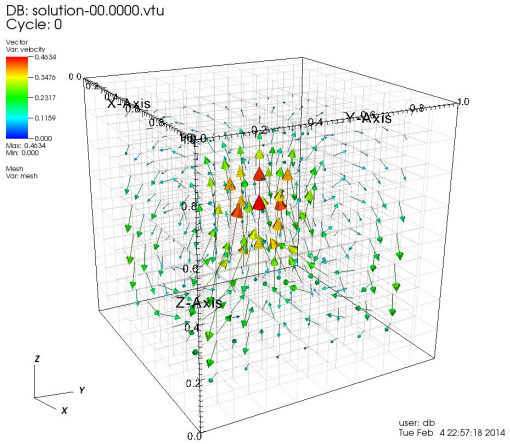

(c) Velocity in Cube Domain - Example 2

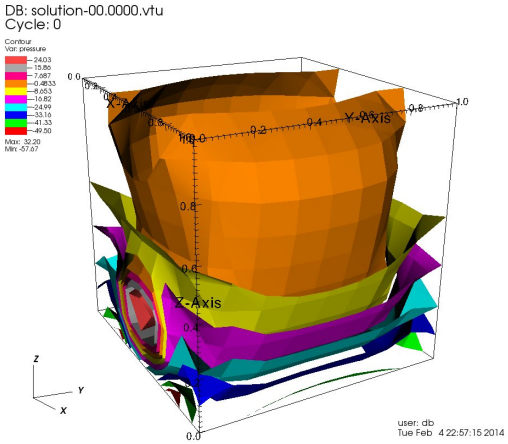

(d) Pressure in Cube Domain - Example 2

Figure 4.4: Example 2 for Cube Domain

The current density vector field plots exhibit the current entering and exiting the domain, as indicated above. This can be seen for both the cube and L-shaped domains, where the current

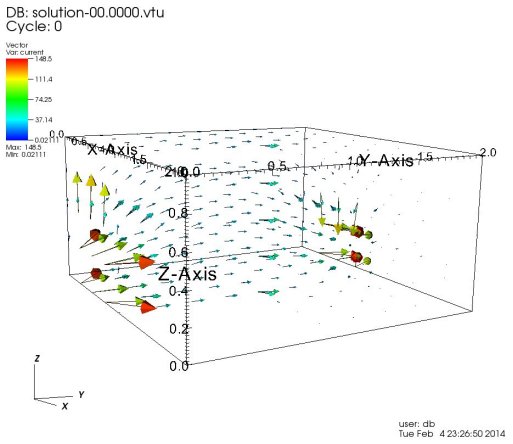

(a) Current in L-shaped Domain - Ex 2

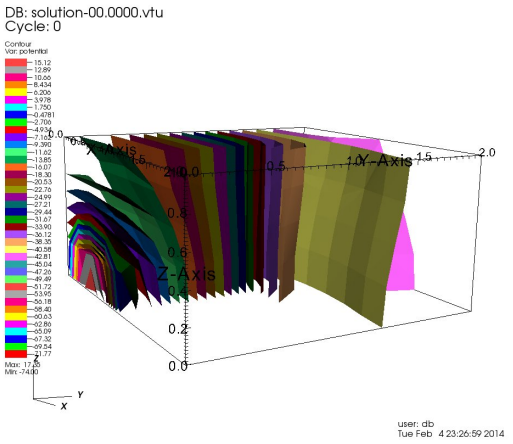

(b) Potential in L-shaped Domain - Ex 2

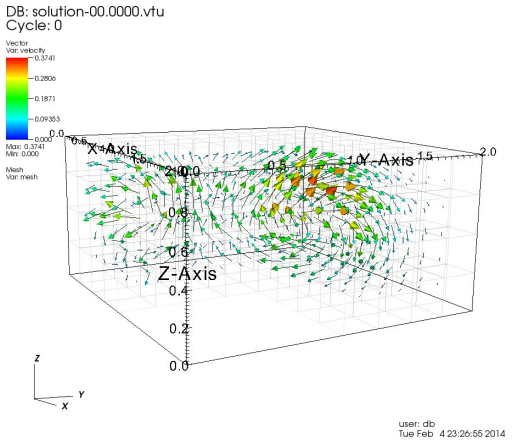

(c) Velocity in L-shaped Domain - Ex 2

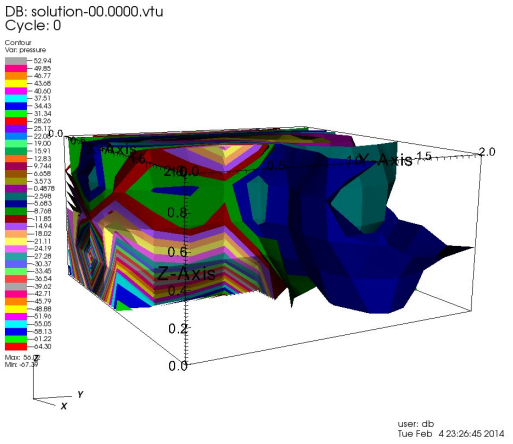

(d) Pressure in L-shaped Domain - Ex 2

Figure 4.5: Example 2 for Lshaped Domain

travels into and out of the domain in the same direction. Since the external magnetic field is zero, the induced magnetic field described by the Biot-Savart formula is the only contributor to the forces experienced by the fluid - the Lorentz force $\mathbf{J} \times \mathbf{B}$ in the momentum equation.

In the vector field plot for the velocity, we can see that maximum fluid speeds are occurring in the center of the domain with an upward direction. Again, the only driving force for this flow is the Lorentz force $\mathbf{J} \times \mathbf{B}$ due to the induced magnetic field. In consideration of the Biot-Savart formula and the symmetry of the current-density in the domain, we see that the upward maximum velocity occurring in the center may be expected. The BiotSavart formula provides for large contributions to the induced magnetic field in regions where the

magnitudes $\mathbf{J}(\mathbf{y})$ of the current are large as well as where the distances $|\mathbf{x}-\mathbf{y}|$ are small. We see that the current magnitudes are largest at the boundary. In calculating the Biot-Savart integrand at the center of the domain $\mathbf{x} = (1/2, 1/2, 1/2)$ and incorporating the negative sign from outside the integral, vectors pointing in the direction of the negative x-axis for both exiting and entering currents on the boundary are obtained. Likewise, close to the center of the domain y where the distance $|\mathbf{x}-\mathbf{y}|$ to the center $\mathbf{x}$ is small, the negative cross-product of the integrand again gives a direction toward the negative x-axis. With the induced magnetic field at the center having this direction, we can determine the body force acting on the fluid at this location by taking the cross product of this field with the current moving in the direction of the positive y-axis. This cross product yields an upward-pointing Lorentz force in the positive z-direction. This upward body force acting on the fluid does indeed correspond to the upward velocity profile seen at the center of the domain. Further, the contributions noted on both sides of the plane $y = 1/2$ can only occur near the center of the cube and imply a maximum magnitude there. The lack of domain symmetry with respect to the entering and exiting current density of the L-shaped domain makes it harder to argue the velocity profiles seen for this case.

4.3.1 Preconditioning Results

Returning to the second problem with the more realistic conditions and the cube domain, we compare the expected theoretical results to computed computational results for the eigenvalues of this problem. Recall the form of our preconditioner

$$P = \begin{bmatrix} A_{(u)}^{-1} & 0 & 0 & 0 \\ 0 & Q_{(p)}^{-1} & 0 & 0 \\ 0 & 0 & A_{(J)}^{-1} & 0 \\ 0 & 0 & 0 & Q_{(\nabla\phi)}^{-1} \end{bmatrix},$$

where $Q_{(p)}$ is the pressure mass matrix and $Q_{(\nabla\phi)}$ is the laplacian mass matrix.

For each eigenvalue plot, we have considered the second iteration in the Picard iteration sequence. We plot the eigenvalues on the complex plane for the unit cube refined once in each direction to yield 8 cells. We start with the plot of the eigenvalues of the system matrix before preconditioning, shown in 4.6. From this plot, we can see that the eigenvalues are not clustered in groups, especially near the origin. We may expect that the number of GMRES iterations to convergence to be high, and indeed without a preconditioner GMRES fails converge (for the default tolerance and maximum number of iterations).

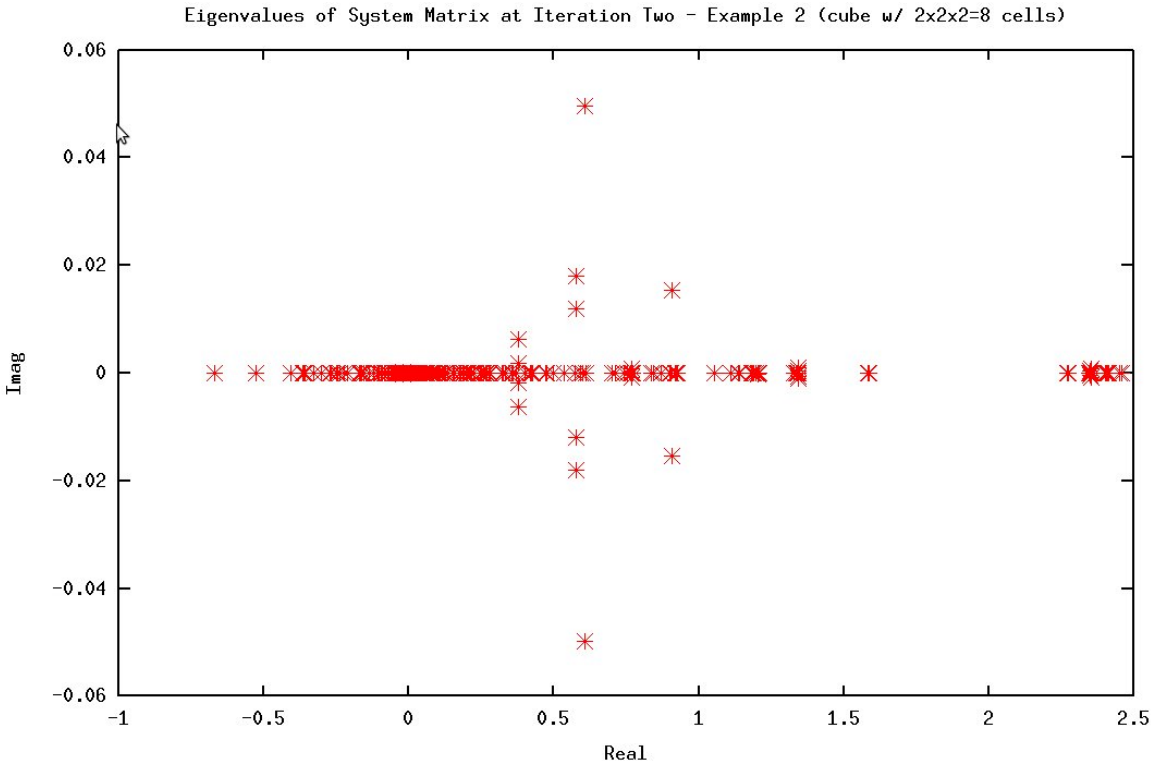

Figure 4.6: Eigenvalues for System Matrix

Next, we examine the eigenvalue plot in figure 4.7 for simplified system of theorem 3.4 after applying our preconditioner. From the plot, we can see clustering in three locations. Looking closely, we see the locations are exactly the eigenvalues stated in the last part of the theorem when constructing the preconditioner by using the Schur complements instead of the mass

matrices. It appears that constructing with the mass matrices gives the same result. Roughly twenty eigenvalues are located away from the three clusters. These eigenvalues are believed to be due to the velocity boundary conditions enforced by deal.ii by way of the system matrix [12, 1]. Further, a zero eigenvalue can be seen in the graph. This was determined to be due to the null space of the pressure having dimension one. We note that GMRES did not have a problem with convergence for such a system.

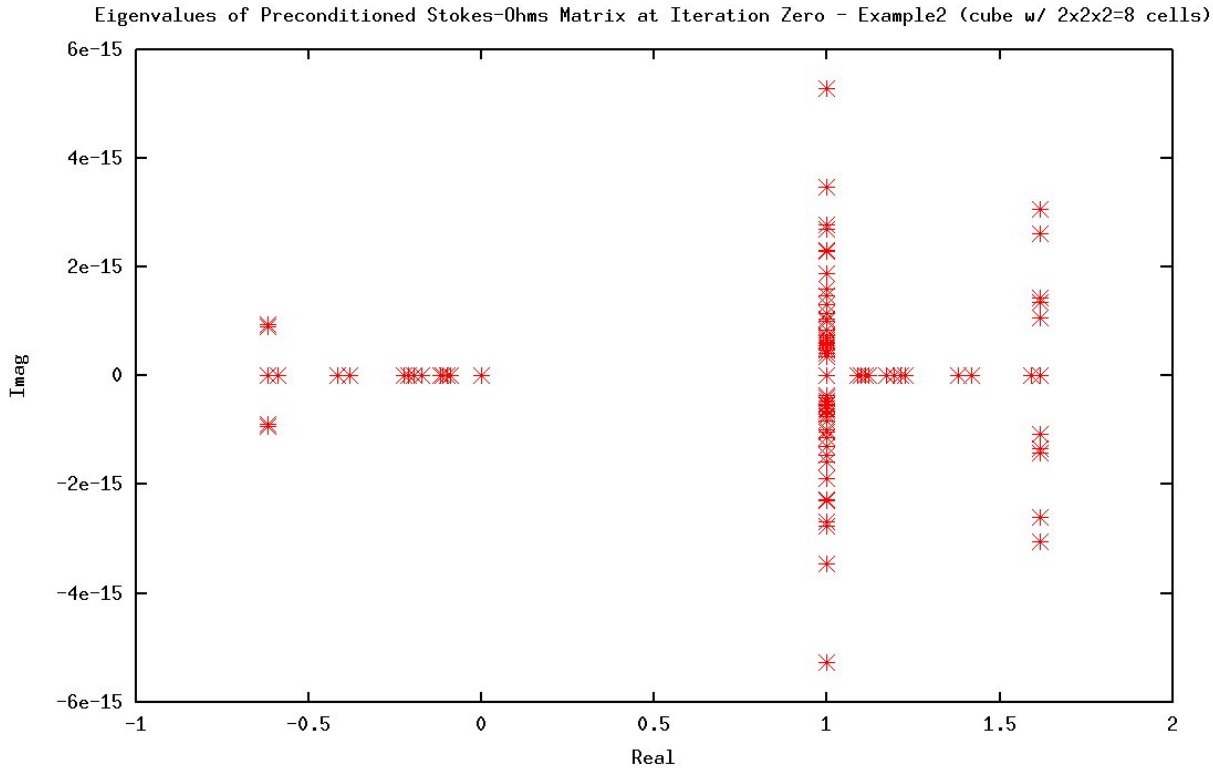

Figure 4.7: Eigenvalues for Preconditioned Stokes-Ohms System

Finally, we look at the effects of preconditioning on the eigenvalues for the simplified system with the inertial term, figure 4.8, and for the simplified system with both the inertial term and Lorentz force terms (the entire system matrix), figure 4.9. From these plots, we see that clustering of eigenvalues is still occurring, though not as well as for only the simplified system. We note that GMRES still converged with less than 100 iterations.

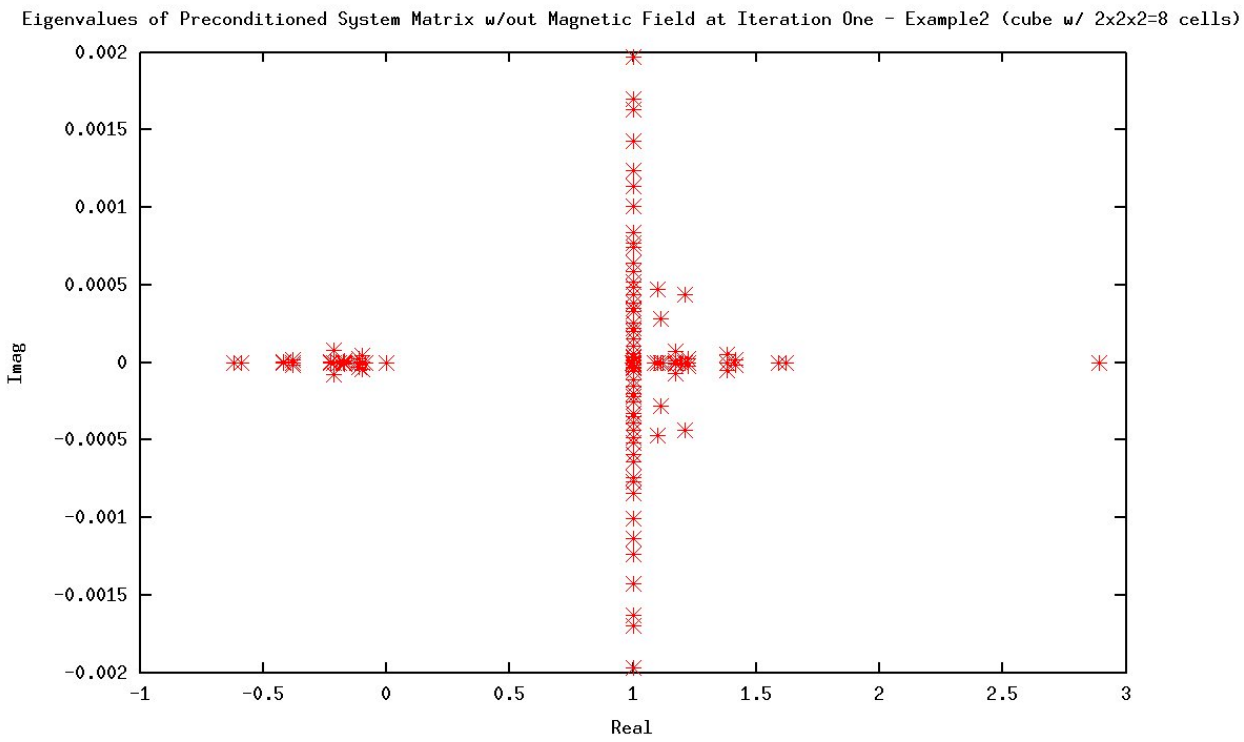

Figure 4.8: Eigenvalues for Preconditioned Stokes-Ohms System with Inertial Term

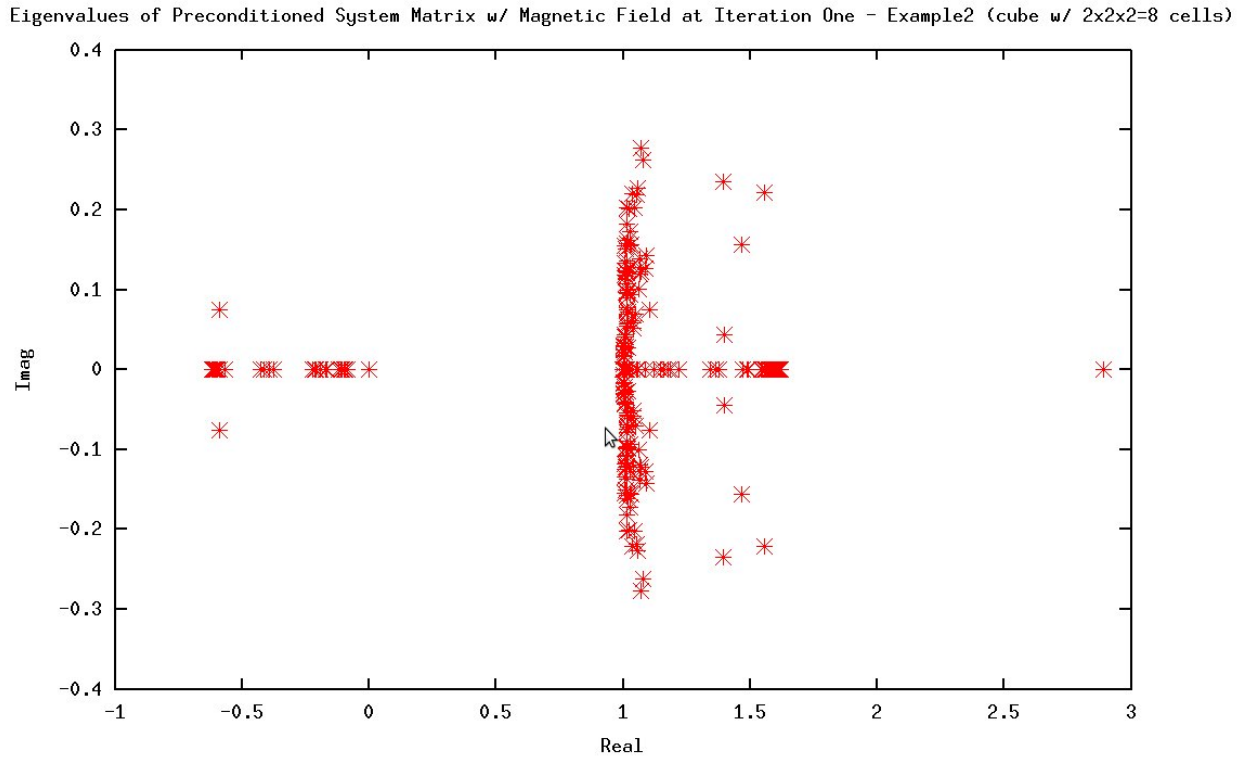

Figure 4.9: Eigenvalues for Preconditioned System Matrix

Chapter 5

Conclusion and Future Work

5.1 Summary

We have implemented a parallel, object-oriented, finite element code that utilizes open-source, academic and government software libraries. The code is capable of approximating the solution to the velocity-current MHD equations on high performance computer clusters. We have established a preconditioner that permits using GMRES to approximate the solution to the system of equations iteratively. We have successfully tested the code on the unit cube and an L-shaped domain for two problem types. For the problem with an exact solution we have obtained expected orders of convergence [78]. We have also successfully run the code with millions of unknowns on a 64 node distributed memory architecture at the Alabama Supercomputer Center DMC. From these results and opportunities to discuss our work, we have a couple different directions that we would like to develop in the future that will be outlined in the upcoming sections.

5.2 Torus Domain

Discussions with physicists have indicated a potential for the velocity-current equations to model plasma in fusion reactors. Two general types of fusion reactors are stellarators (named after the devices purpose of harnessing the power of a stellar object - the sun) and tokomaks (a Russion acronym, due to its origin). The main difference between a tokomak and a stellarator are their methods of generating the magnetic fields that confine the plasma. The stellarator uses two magnetic fields generated by currents running through coils that

surround the plasma. The tokomak generates one field by running current through a set of coils encircling the plasma, but creates the second field by sending current through the plasma. Our system of equations appears to apply naturally to the tokamak reactor design, with a current being applied to the domain to create the second magnetic field. We note that research on fusion energy is active, with fusion energy being an engineering grand challenge problem for the 21st century and grants being available through the NSF on fusion energy research. In fact, the ITER (International Thermonuclear Experimental Reactor) project located in the south of France is the largest tokomak reactor in the world and has been designed to be the first full scale fusion power plant. We can see that With the domain of a tokomak being essentially a torus, we have interest in approximating solutions to our equations for a toroidal domain. We have started testing out equations on this domain. In particular, we are testing the first problem from chapter 3, having an exact solution, on a quarter torus. Results at this time are located in in the figure 5.1 and table 5.1.

Table 5.1: Errors and Convergence Rates for the Quarter Torus Domain

Domain Infomation			**u**	**J**	p	ϕ
# Cells	**# DOFs**	**Cell size** (h)	$\mathbf{H}^1$**-error**	$\mathbf{L}^2$**-error**	$\mathbf{L}^2$**-error**	$\mathbf{H}^1$**-error**
			$\mathbf{H}^1$**-rate**	$\mathbf{L}^2$**-rate**	$\mathbf{L}^2$**-rate**	$\mathbf{H}^1$**-rate**
80	5553	h_1	0.132016	0.0270524	0.0257992	0.0828241
640	40,261	$\frac{1}{2}h_1$	0.0349727	0.00647049	0.0134858	0.0214727
			1.916412	2.063810	0.935884	1.947547
5120	306,597	$\frac{1}{4}h_1$	0.00894921	0.00164881	0.0129277	0.00552349
			1.966397	1.972450	0.060975	1.958852

From the convergence table for the quarter-torus we see the expected rates of approximation, except for the pressure. Work continues on this problem to understand the problematic rate of convergence for the pressure. We have seen a similar situation with the L-shaped domain and will be testing our code with this in mind.

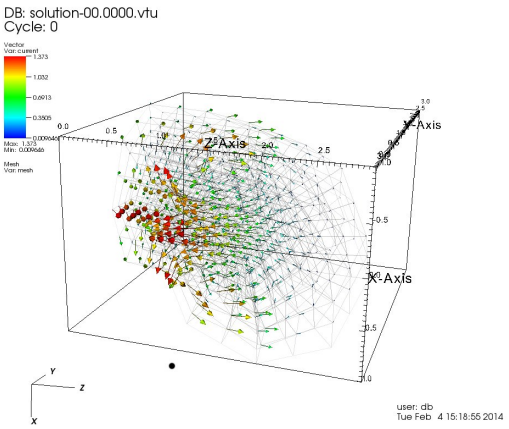

(a) Current in Torus Domain - Ex 1

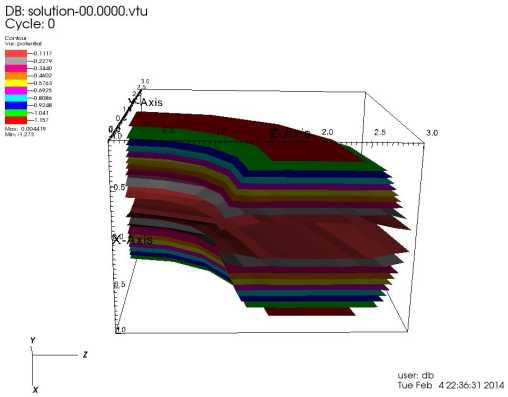

(b) Potential in Torus Domain - Ex 1

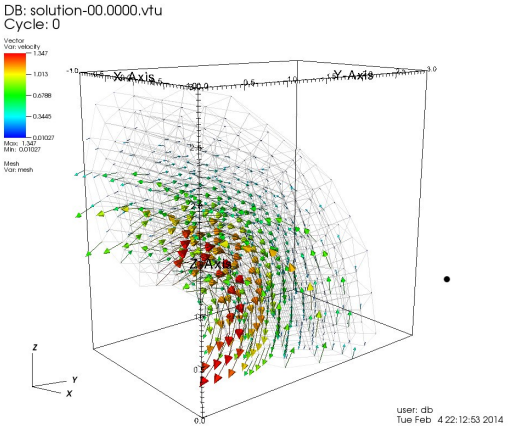

(c) Velocity in Torus Domain - Ex 1

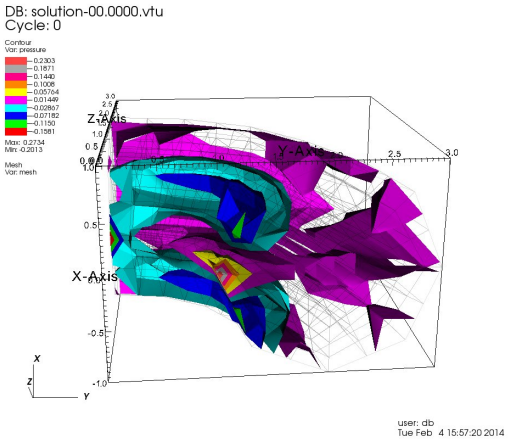

(d) Pressure in Torus Domain - Ex 1

Figure 5.1: Example 1 for Lshaped Domain

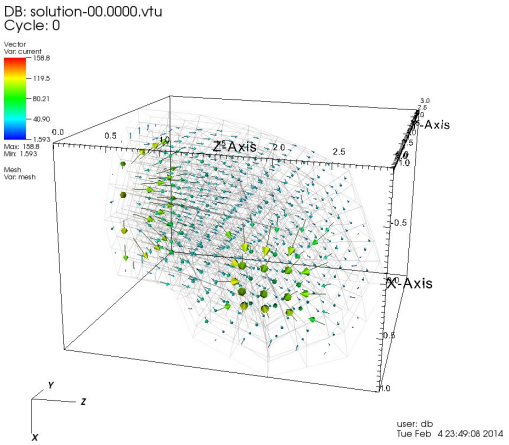

(a) Current in Torus Domain - Ex 2

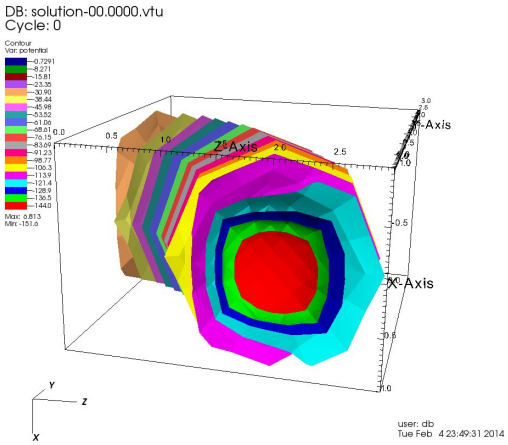

(b) Potential in Torus Domain - Ex 2

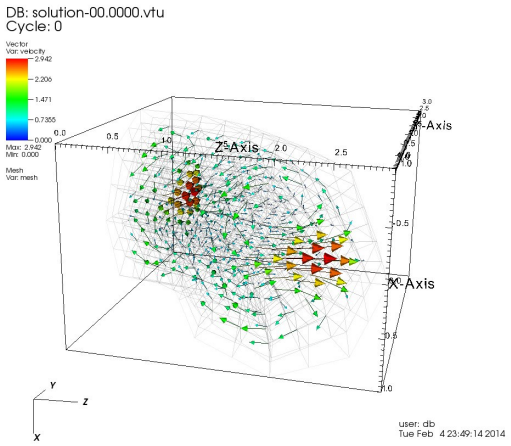

(c) Velocity in Torus Domain - Ex 2

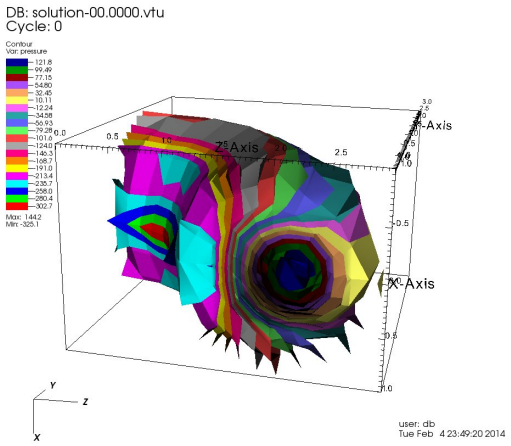

(d) Pressure in Torus Domain - Ex 2

Figure 5.2: Example 2 for Torus Domain

We have also obtained results on the quarter-torus domain for the second example of chapter 3. In this case the current can be seen entering and exiting through the cross-sections of the torus (see Figure 5.2), with the directions of entry and departure perpendicular to each other. The predictions for the velocity and the pressure are interesting. According to the velocity vector field, the fluid does not appear to be cycling through to torus in the xy-plane, but rather the movement is vertical and along the torus's radial cross-sections. At the angle of capture of the velocity graph, this may be difficult to see. The layers of the pressure contours also correspond to the movement of the fluid into and out of the torus' radial axis, with high pressures located along that axis.

Finally, we have started numerical approximations of the equations on a full torus. Related to the second example of chapter three with the velocity at the boundary being zero and the current entering and exiting a particular part of the domain, we have the results seen in figure 5.3

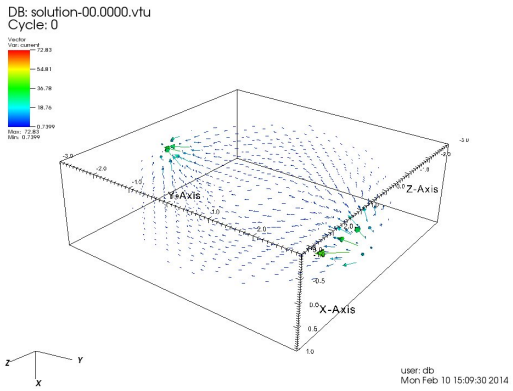

(a) Current in Full Torus Domain - Ex 2

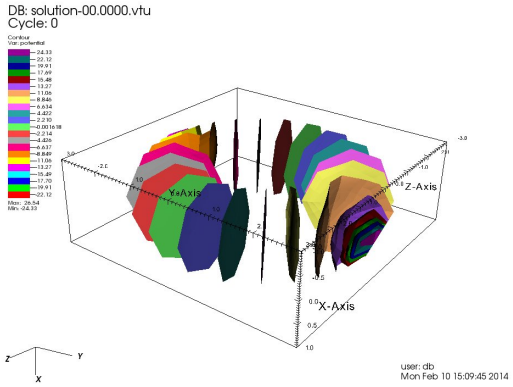

(b) Potential in Full Torus Domain - Ex 2

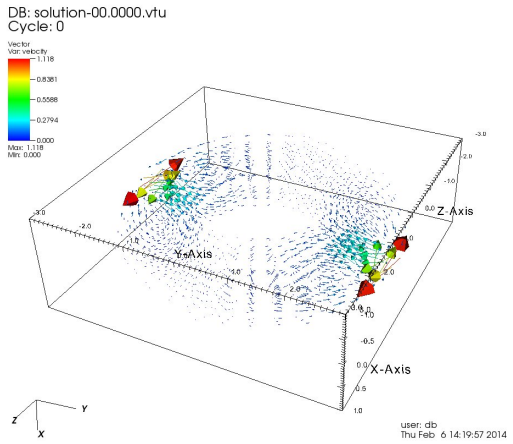

(c) Velocity in Full Torus Domain - Ex 2

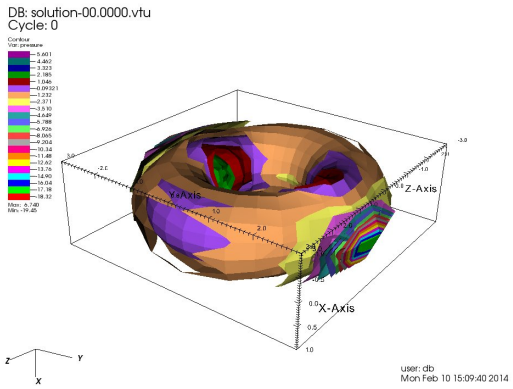

(d) Pressure in Full Torus Domain - Ex 2

Figure 5.3: Example 2 for Full Torus Domain

5.3 Code Speedup

Another research direction is the consideration of code bottlenecks. We have started work in this direction by comparing the three slowest components of the code: the assembly of the equation system, the solution of the system and the calculation of the Biot-Savart integral at each quadrature point during the assembly. In the plots in figure 5.4, we quickly see that the slowest component of the code during runtime is the calculation of the Biot-Savart integral.

Figure 5.4 considers strong scaling, where the problem size (the number of unknowns or domain refinement) has been fixed and the number of processors is varied. We recall that the speedup for a parallel program under a fixed problem size is the ratio of the parallel

program's time over the sequential program's time. Ideally, if two processors are used instead of one, then the time to complete a portion of code should decrease by a factor of two, and the speedup would be 2. In our observations, as we double the number of processors we use to numerically approximation the solution to the equations of fixed mesh size, we see (in the plot on the left in figure 5.4) that the time to completion is roughly halved for each of the components of the code being considered. Recall that parallel efficiency is the ratio of speedup over the number of processors, and that ideal efficiency has a value of 1. We conclude from the graphs that the libraries being used in the assembly (deal.ii) and the solution (trilinos) of the system of equations have good parallel efficiency in this range of processors for this particular problem size. From the graphs as well, the in-house MPI code for the BiotSavart integral also exhibits the same level of efficiency in this processor range. To see the speedup and efficiency more clearly, we use a log-log plot with a base of two. Doubling the number of processors corresponds to incrementing by one unit on the x-axis, and halving the cpu time corresponds to a decrease on the y-axis by one unit. We expect in the ideal case that an increment of one unit along the x-axis would result in a decrease of one unit along the y-axis, and that we would see a linear trend in the log-log plot with a slope of negative one. The plot on the right in figure 5.4 does indeed show trends close to ideal.

With the three slowest components working near optimal efficiency with respect to strong scaling observations, we would like to address the slowest component of the code, the Biot-Savart integral. The Biot-Savart integral calculates the magnetic field induced by the current density in the domain. The code does this using quadrature. Each processor contains information - previous current densities and quadrature points - needed to perform the quadrature calculation over the domain for a particular location x in

$$\mathbf{B}\left(\mathbf{J}_{n-1}\right)(x) = -\frac{\mu}{4\pi}\int_{\Omega}\frac{x-y}{|x-y|^3}\times\mathbf{J_{n-1}}\left(y\right)dy$$

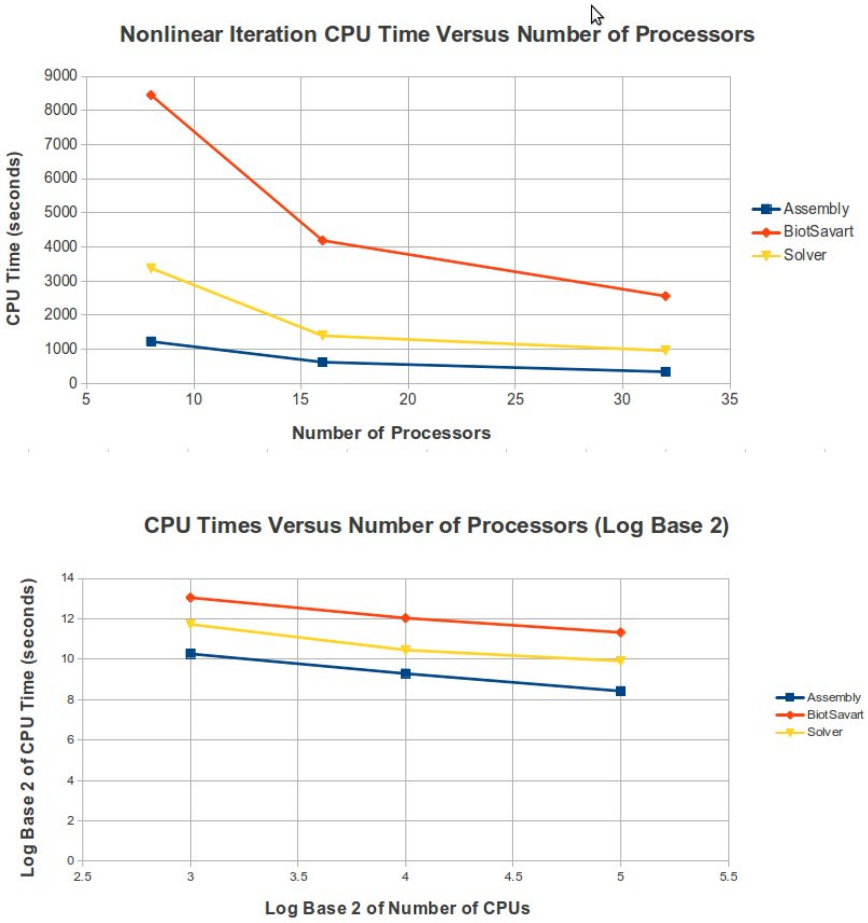

Figure 5.4: CPU Time Versus Number of Processors

to determine the value of the Biot-Savart integral at that particular location. With all the information readily available on each processor (after a numerical solve), the major component of the calculation is the MPI communication between processors. To see if we can shorten the time to approximate the induced magnetic field at these locations, we consider approximating the solution to the magnetic field in the Maxwell equations

$$\nabla \cdot \mathbf{B} = 0 \quad \text{and} \quad \nabla \times \mathbf{B} = \mathbf{J}_{(n-1)} \quad \text{on } \Omega$$

with the boundary condition

$$\mathbf{B} \cdot \mathbf{n} = \mathbf{B}\left(\mathbf{J}_{n-1}\right) \cdot \mathbf{n}$$

by a parallel finite element method, using deal.ii. We approximate the solution to the system of equations using the least squares finite element method [67, 19]. Just as with the solution method using only the Biot-Savart integral, the obtained magnetic field values are used in the next solve for the four uknowns $\mathbf{J}$, $\mathbf{u}$, p, ϕ. For the first example problem from chapter three with exact solutions, we look at strong scaling using this method, and compare this to the Biot-Savart method. Note that the method using only the Biot-Savart integral was optimized to make the comparison as fair as possible - leading to considerable reductions that can be seen when comparing figure 5.5 to 5.4. However, even with optimizations to the communication occurring during the Biot-Savart method, we can see that the solution of the div-curl system is almost an order of magnitude faster and appears to parallelize well.

As can be seen in the figure 5.5, we even tested an approximation to the BiotSavart integral method, where we used the fact that the denominator in the integrand of the BiotSavart integral caused the magnetic field values to be small with large distances between x and y. This method was a first step toward a fast multipole method for the integral [24, 47, 13, 46, 93, 64]. However, the least squares finite element method to calculate the induced magnetic field in the domain outperformed this simplifying approximation to the quadrature method for the BiotSavart integral. This div-curl finite element solver for the induced magnetic field seems to be a natural direction for future work. For future work, we would like to do some analysis on this code and extend this code to domains that are nonconvex. A major issue is the possible occurrence of singularities in such a domains [26]. Hence, the geometry of the domain must be taken into consideration [27, 14, 63, 28] with the possible use of the discontinuous finite element method. It may also be of interest to address the problem from the point of view of finite element exterior calculus [61, 6, 4, 5].

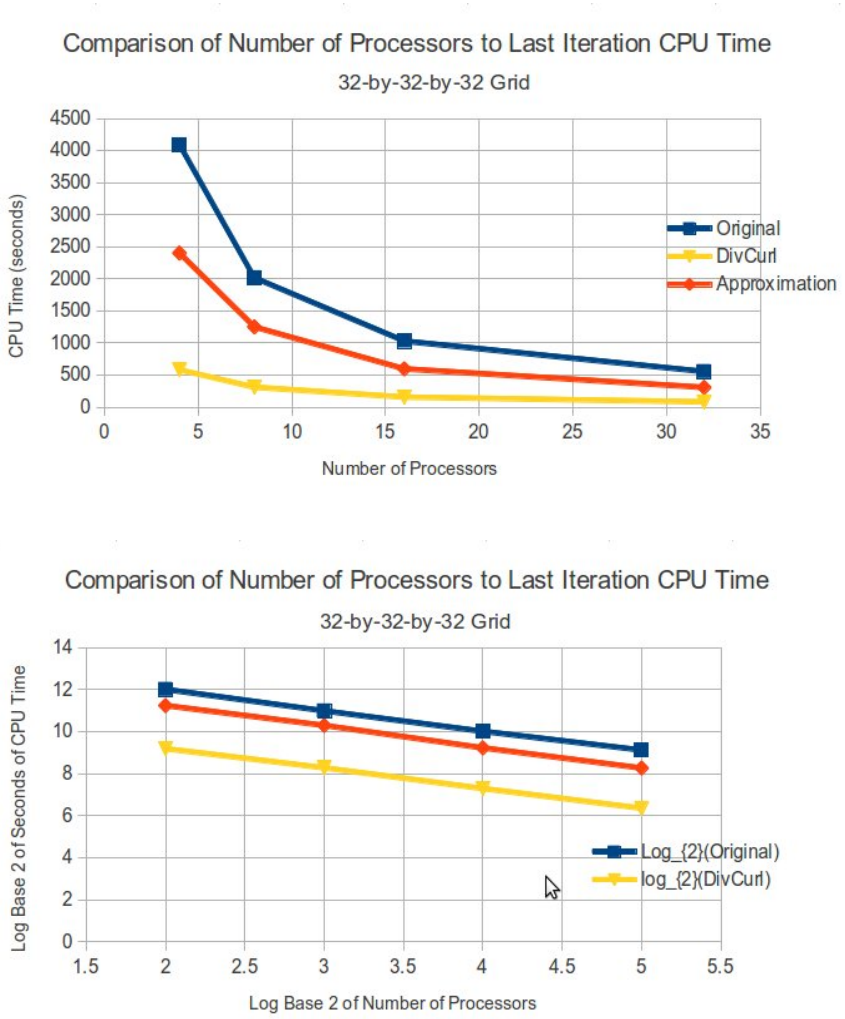

Figure 5.5: CPU Time Versus Number of Processors

Appendices

Appendix A

Weak Formulation and Identities

A.1 Navier-Stokes Identities

Here, we go over the identities

$$\begin{aligned}
\int_\Omega \mathbf{v}\cdot\nabla p &= -\int_\Omega p\nabla\cdot\mathbf{v} + \int_{\partial\Omega} p\mathbf{n}\cdot\mathbf{v} \\
-\int_\Omega \mathbf{v}\cdot\nabla^2\mathbf{u} &= \int_\Omega \nabla\mathbf{u}\colon\nabla\mathbf{v} - \int_{\partial\Omega}(\mathbf{n}\cdot\nabla\mathbf{u})\cdot\mathbf{v} \\
\rho\int_\Omega((\mathbf{u}\cdot\nabla)\,\mathbf{u})\cdot\mathbf{v} &= \frac{\rho}{2}\left(\int_\Omega((\mathbf{u}\cdot\nabla)\,\mathbf{u})\cdot\mathbf{v} - \int_\Omega((\mathbf{u}\cdot\nabla)\,\mathbf{v})\cdot\mathbf{u}\right)
\end{aligned}$$

to write Navier-Stokes equations in the form below.

$$\begin{aligned}
\int_\Omega \mathbf{F}\cdot\mathbf{v} &= -\eta\int_\Omega \Delta\mathbf{u}\cdot\mathbf{v} + \rho\int_\Omega((\mathbf{u}\cdot\nabla)\,\mathbf{u})\cdot\mathbf{v} + \int_\Omega \nabla p\cdot\mathbf{v} \\
&= \eta\int_\Omega \nabla\mathbf{u}\colon\nabla\mathbf{v} + \frac{\rho}{2}\left(\int_\Omega((\mathbf{u}\cdot\nabla)\,\mathbf{u})\cdot\mathbf{v} - \int_\Omega((\mathbf{u}\cdot\nabla)\,\mathbf{v})\cdot\mathbf{u}\right) - \int_\Omega p\nabla\cdot\mathbf{v}
\end{aligned}$$

A.1.1 Pressure Term

We weaken the pressure in the term $\int_\Omega \nabla p\cdot\mathbf{v}$ by using

$$\begin{aligned}
\frac{\partial}{\partial x}(\mathbf{v}\cdot\mathbf{a}) &= \frac{\partial}{\partial x}(v_1a_1 + v_2a_2 + v_3a_3) \\
&= v_1\frac{\partial a_1}{\partial x} + \frac{\partial v_1}{\partial x}a_1 + v_2\frac{\partial a_2}{\partial x} + \frac{\partial v_2}{\partial x}a_2 + v_3\frac{\partial a_3}{\partial x} + \frac{\partial v_3}{\partial x}a_3
\end{aligned}$$

$$= \mathbf{v} \cdot \left(\frac{\partial}{\partial x} \mathbf{a} \right) + \left(\frac{\partial}{\partial x} \mathbf{v} \right) \cdot \mathbf{a}$$

to form the identity

$$\begin{aligned} \nabla \cdot (p\mathbf{v}) &= \left\langle \frac{\partial p v_1}{\partial x}, \frac{\partial p v_2}{\partial y}, \frac{\partial p v_3}{\partial z} \right\rangle \\ &= \left\langle p\frac{\partial v_1}{\partial x} + v_1 \frac{\partial p}{\partial x}, p\frac{\partial v_2}{\partial y} + v_2 \frac{\partial p}{\partial y}, p\frac{\partial v_3}{\partial z} + v_3 \frac{\partial p}{\partial z} \right\rangle \\ &= \mathbf{v} \cdot \nabla p + p \nabla \cdot \mathbf{v}. \end{aligned}$$

Using this result with the divergence theorem $\int_\Omega \nabla \cdot \mathbf{v} = \int_{\partial\Omega} \mathbf{v} \cdot \mathbf{n}$ we have

$$\begin{aligned} \int_\Omega \mathbf{v} \cdot \nabla p &= -\int_\Omega p \nabla \cdot \mathbf{v} + \int_\Omega \nabla \cdot (p\mathbf{v}) \\ &= -\int_\Omega p \nabla \cdot \mathbf{v} + \int_{\partial\Omega} p\mathbf{n} \cdot \mathbf{v} \end{aligned}$$

A.1.2 Diffusion Term

The diffusion term $\int_\Omega \nabla^2 \mathbf{u} \cdot \mathbf{v}$ is weakened using integration by parts and the identity

$$\nabla \cdot (\nabla \vec{u} \cdot \vec{v}) = \nabla \vec{u} \colon \nabla \vec{v} + \vec{v} \cdot \nabla^2 \vec{u}$$

Writing the gradient of the velocity vector in matrix form

$$\nabla \mathbf{u} = \begin{bmatrix} \frac{\partial}{\partial x} \\ \frac{\partial}{\partial y} \\ \frac{\partial}{\partial z} \end{bmatrix} \begin{bmatrix} u_1 & u_2 & u_3 \end{bmatrix} = \begin{bmatrix} \frac{\partial u_1}{\partial x} & \frac{\partial u_2}{\partial x} & \frac{\partial u_3}{\partial x} \\ \frac{\partial u_1}{\partial y} & \frac{\partial u_2}{\partial y} & \frac{\partial u_3}{\partial y} \\ \frac{\partial u_1}{\partial z} & \frac{\partial u_2}{\partial z} & \frac{\partial u_3}{\partial z} \end{bmatrix} \tag{A.1}$$

The diffusion term can then be written as

$$\begin{aligned}
\Delta\mathbf{u} &= \nabla^2\mathbf{u} = \nabla\cdot(\nabla\mathbf{u}) = \begin{bmatrix} \frac{\partial}{\partial x_1} & \frac{\partial}{\partial x_2} & \frac{\partial}{\partial x_3} \end{bmatrix} \begin{bmatrix} u_{1,x} & u_{2,x} & u_{3,x} \\ u_{1,y} & u_{2,y} & u_{3,y} \\ u_{1,z} & u_{2,z} & u_{3,z} \end{bmatrix} \\
&= \begin{bmatrix} \frac{\partial^2 u_1}{\partial x^2} + \frac{\partial^2 u_1}{\partial y^2} + \frac{\partial^2 u_1}{\partial z^2} \\ \frac{\partial^2 u_2}{\partial x^2} + \frac{\partial^2 u_2}{\partial y^2} + \frac{\partial^2 u_2}{\partial z^2} \\ \frac{\partial^2 u_3}{\partial x^2} + \frac{\partial^2 u_3}{\partial y^2} + \frac{\partial^2 u_3}{\partial z^2} \end{bmatrix} = \begin{bmatrix} \nabla\cdot\nabla u_1 \\ \nabla\cdot\nabla u_2 \\ \nabla\cdot\nabla u_3 \end{bmatrix} = \left\langle \nabla^2 u_1, \nabla^2 u_2, \nabla^2 u_3 \right\rangle
\end{aligned}$$

Here we will write the tensor-tensor product $\nabla\mathbf{u} : \nabla\mathbf{v}$ as

$$\begin{aligned}
\nabla\mathbf{u} : \nabla\mathbf{v} &= \begin{bmatrix} \frac{\partial u_1}{\partial x} & \frac{\partial u_2}{\partial x} & \frac{\partial u_3}{\partial x} \\ \frac{\partial u_1}{\partial y} & \frac{\partial u_2}{\partial y} & \frac{\partial u_3}{\partial y} \\ \frac{\partial u_1}{\partial z} & \frac{\partial u_2}{\partial z} & \frac{\partial u_3}{\partial z} \end{bmatrix} : \begin{bmatrix} \frac{\partial v_1}{\partial x} & \frac{\partial v_2}{\partial x} & \frac{\partial v_3}{\partial x} \\ \frac{\partial v_1}{\partial y} & \frac{\partial v_2}{\partial y} & \frac{\partial v_3}{\partial y} \\ \frac{\partial v_1}{\partial z} & \frac{\partial v_2}{\partial z} & \frac{\partial v_3}{\partial z} \end{bmatrix} \\
&= u_{1,x}v_{1,x} + u_{1,y}v_{1,y} + u_{1,z}v_{1,z} + u_{1,x}v_{2,x} + u_{2,y}v_{2,y} + u_{2,z}v_{2,z} \\
&\qquad + u_{3,x}v_{3,x} + u_{3,y}v_{3,y} + u_{3,z}v_{3,z} \\
&= (\nabla u_1\cdot\nabla v_1) + (\nabla u_2\cdot\nabla v_2) + (\nabla u_3\cdot\nabla v_3)
\end{aligned} \tag{A.2}$$

Consider the divergence of the tensor-vector product $\nabla\mathbf{u}\cdot\mathbf{v}$

$$\begin{aligned}
\nabla\cdot(\nabla\mathbf{u}\cdot\mathbf{v}) &= \nabla\cdot\left(\begin{pmatrix} \frac{\partial u_1}{\partial x} & \frac{\partial u_2}{\partial x} & \frac{\partial u_3}{\partial x} \\ \frac{\partial u_1}{\partial y} & \frac{\partial u_2}{\partial y} & \frac{\partial u_3}{\partial y} \\ \frac{\partial u_1}{\partial z} & \frac{\partial u_2}{\partial z} & \frac{\partial u_3}{\partial z} \end{pmatrix}\cdot\mathbf{v}\right) = \nabla\cdot\left\langle \left(\frac{\partial}{\partial x}\mathbf{u}\right)\cdot\mathbf{v}, \left(\frac{\partial}{\partial y}\mathbf{u}\right)\cdot\mathbf{v}, \left(\frac{\partial}{\partial z}\mathbf{u}\right)\cdot\mathbf{v} \right\rangle \\
&= \frac{\partial}{\partial x}\left(\frac{\partial}{\partial x}\mathbf{u}\cdot\mathbf{v}\right) + \frac{\partial}{\partial y}\left(\frac{\partial}{\partial y}\mathbf{u}\cdot\mathbf{v}\right) + \frac{\partial}{\partial z}\left(\frac{\partial}{\partial z}\mathbf{u}\cdot\mathbf{v}\right) \\
&= \left(\frac{\partial^2\mathbf{u}}{\partial x^2}\cdot\mathbf{v} + \frac{\partial\mathbf{v}}{\partial x}\cdot\frac{\partial\mathbf{u}}{\partial x}\right) + \left(\frac{\partial^2\mathbf{u}}{\partial y^2}\cdot\mathbf{v} + \frac{\partial\mathbf{v}}{\partial y}\cdot\frac{\partial\mathbf{u}}{\partial y}\right)\left(\frac{\partial^2\mathbf{u}}{\partial z^2}\cdot\mathbf{v} + \frac{\partial\mathbf{v}}{\partial z}\cdot\frac{\partial\mathbf{u}}{\partial z}\right) \\
&= \mathbf{v}\cdot\langle\nabla\cdot\nabla u_1, \nabla\cdot\nabla u_2, \nabla\cdot\nabla u_3\rangle + (\nabla v_1\cdot\nabla u_1 + \nabla v_2\cdot\nabla u_2 + \nabla v_3\cdot\nabla u_3) \\
&= \mathbf{v}\cdot\left\langle\nabla^2 u_1, \nabla^2 u_2, \nabla^2 u_3\right\rangle + \nabla\mathbf{v}\colon\nabla\mathbf{u} = \mathbf{v}\cdot\nabla^2\mathbf{u} + \nabla\mathbf{v}\colon\nabla\mathbf{u}
\end{aligned}$$

Hence,

$$\int_\Omega \nabla \cdot (\nabla \mathbf{u} \cdot \mathbf{v}) = \int_\Omega \mathbf{v} \cdot (\nabla \cdot \nabla \mathbf{u}) + \int_\Omega \nabla \mathbf{u} \colon \nabla \mathbf{v}$$

With the help of the divergence thereom, we can rewrite the diffusion term $-\int_\Omega \nabla^2 \mathbf{u} \cdot \mathbf{v}$ in Navier Stokes

$$\begin{aligned} -\int_\Omega \mathbf{v} \cdot \nabla^2 \mathbf{u} &= \int_\Omega \nabla \mathbf{u} \colon \nabla \mathbf{v} - \int_\Omega \nabla \cdot (\nabla \mathbf{u} \cdot \mathbf{v}) \\ &= \int_\Omega \nabla \mathbf{u} \colon \nabla \mathbf{v} - \int_{\partial\Omega} (\nabla \mathbf{u} \cdot \mathbf{v}) \cdot \mathbf{n} \\ &= \int_\Omega \nabla \mathbf{u} \colon \nabla \mathbf{v} - \int_{\partial\Omega} (\mathbf{n} \cdot \nabla \mathbf{u}) \cdot \mathbf{v}. \end{aligned}$$

The last equality is true since

$$\begin{aligned} (\nabla \mathbf{u} \cdot \mathbf{v}) \cdot \mathbf{n} &= \left(\begin{pmatrix} \frac{\partial u_1}{\partial x} & \frac{\partial u_2}{\partial x} & \frac{\partial u_3}{\partial x} \\ \frac{\partial u_1}{\partial y} & \frac{\partial u_2}{\partial y} & \frac{\partial u_3}{\partial y} \\ \frac{\partial u_1}{\partial z} & \frac{\partial u_2}{\partial z} & \frac{\partial u_3}{\partial z} \end{pmatrix} \cdot \mathbf{v} \right) \cdot \mathbf{n} = \begin{pmatrix} \mathbf{v} \cdot \frac{\partial}{\partial x} \mathbf{u} \\ \mathbf{v} \cdot \frac{\partial}{\partial y} \mathbf{u} \\ \mathbf{v} \cdot \frac{\partial}{\partial z} \mathbf{u} \end{pmatrix} \cdot \mathbf{n} \\ &= n_1 \mathbf{v} \cdot \frac{\partial}{\partial x} \mathbf{u} + n_2 \mathbf{v} \cdot \frac{\partial}{\partial y} \mathbf{u} + n_3 \mathbf{v} \cdot \frac{\partial}{\partial z} \mathbf{u} = \left(n_1 \frac{\partial}{\partial x} \mathbf{u} + n_2 \frac{\partial}{\partial y} \mathbf{u} + n_3 \frac{\partial}{\partial z} \mathbf{u} \right) \cdot \mathbf{v} \\ &= \left(\mathbf{n} \cdot \left\langle \frac{\partial}{\partial x} \mathbf{u}, \frac{\partial}{\partial y} \mathbf{u}, \frac{\partial}{\partial z} \mathbf{u} \right\rangle \right) \cdot \mathbf{v} = \left(\mathbf{n} \cdot \begin{pmatrix} \frac{\partial u_1}{\partial x} & \frac{\partial u_2}{\partial x} & \frac{\partial u_3}{\partial x} \\ \frac{\partial u_1}{\partial y} & \frac{\partial u_2}{\partial y} & \frac{\partial u_3}{\partial y} \\ \frac{\partial u_1}{\partial z} & \frac{\partial u_2}{\partial z} & \frac{\partial u_3}{\partial z} \end{pmatrix} \right) \cdot \mathbf{v} \\ &= (\mathbf{n} \cdot \nabla \mathbf{u}) \cdot \mathbf{v} \end{aligned}$$

A.1.3 Advection Term

For the advection term, we wish to show

$$\rho \int_\Omega ((\mathbf{u} \cdot \nabla)\, \mathbf{u}) \cdot \mathbf{v} = \frac{\rho}{2} \left(\int_\Omega ((\mathbf{u} \cdot \nabla)\, \mathbf{u}) \cdot \mathbf{v} - \int_\Omega ((\mathbf{u} \cdot \nabla)\, \mathbf{v}) \cdot \mathbf{u} \right)$$

To start,

$$\begin{aligned}\rho\int_\Omega\left(\left(\mathbf{u}\cdot\nabla\right)\mathbf{u}\right)\cdot\mathbf{v} &= \frac{\rho}{2}\int_\Omega\left(\left(\mathbf{u}\cdot\nabla\right)\mathbf{u}\right)\cdot\mathbf{v}+\frac{\rho}{2}\int_\Omega\left(\left(\mathbf{u}\cdot\nabla\right)\mathbf{u}\right)\cdot\mathbf{v}\\ &= \frac{\rho}{2}\left(\int_\Omega\left(\left(\mathbf{u}\cdot\nabla\right)\mathbf{u}\right)\cdot\mathbf{v}+\int_\Omega\left(\left(\mathbf{u}\cdot\nabla\right)\mathbf{u}\right)\cdot\mathbf{v}\right)\end{aligned}$$

We wish to show that

$$-\int_\Omega\left(\left(\mathbf{u}\cdot\nabla\right)\mathbf{u}\right)\cdot\mathbf{v}=\int_\Omega\left(\left(\mathbf{u}\cdot\nabla\right)\mathbf{v}\right)\cdot\mathbf{u}$$

we have that

$$\begin{aligned}\left(\left(\mathbf{u}\cdot\nabla\right)\mathbf{u}\right)\cdot\mathbf{v} &= \begin{bmatrix}u_1\frac{\partial u_1}{\partial x}+u_2\frac{\partial u_1}{\partial y}+u_3\frac{\partial u_1}{\partial z}\\ u_1\frac{\partial u_2}{\partial x}+u_2\frac{\partial u_2}{\partial y}+u_3\frac{\partial u_2}{\partial z}\\ u_1\frac{\partial u_3}{\partial x}+u_2\frac{\partial u_3}{\partial y}+u_3\frac{\partial u_3}{\partial z}\end{bmatrix}\cdot\mathbf{v}\\ &= v_1\left(u_1\frac{\partial u_1}{\partial x}+u_2\frac{\partial u_1}{\partial y}+u_3\frac{\partial u_1}{\partial z}\right)+v_2\left(u_1\frac{\partial u_2}{\partial x}+u_2\frac{\partial u_2}{\partial y}+u_3\frac{\partial u_2}{\partial z}\right)\\ &\quad+v_3\left(u_1\frac{\partial u_3}{\partial x}++u_2\frac{\partial u_3}{\partial y}+u_3\frac{\partial u_3}{\partial z}\right)\end{aligned}\tag{A.3}$$

and that

$$\begin{aligned}\left(\left(\mathbf{u}\cdot\nabla\right)\mathbf{v}\right)\cdot\mathbf{u} &= \begin{bmatrix}u_1\frac{\partial v_1}{\partial x}+u_2\frac{\partial v_1}{\partial y}+u_3\frac{\partial v_1}{\partial z}\\ u_1\frac{\partial v_2}{\partial x}+u_2\frac{\partial v_2}{\partial y}+u_3\frac{\partial v_2}{\partial z}\\ u_1\frac{\partial v_3}{\partial x}+u_2\frac{\partial v_3}{\partial y}+u_3\frac{\partial v_3}{\partial z}\end{bmatrix}\cdot\mathbf{u}\\ &= u_1\left(u_1\frac{\partial v_1}{\partial x}+u_2\frac{\partial v_1}{\partial y}+u_3\frac{\partial v_1}{\partial z}\right)+u_2\left(u_1\frac{\partial v_2}{\partial x}+u_2\frac{\partial v_2}{\partial y}+u_3\frac{\partial v_2}{\partial z}\right)\\ &\quad+v_3\left(u_1\frac{\partial v_3}{\partial x}++u_2\frac{\partial v_3}{\partial y}+u_3\frac{\partial v_3}{\partial z}\right)\end{aligned}\tag{A.4}$$

Using Integration-By-Parts and assuming that $\mathbf{u}\big|_\Gamma=\mathbf{0}$, we have

$$\int_\Omega u_1\frac{\partial u_1}{\partial x_1}v_1 = \int_\Omega\left(u_1v_1\right)\frac{\partial u_1}{\partial x_1}=-\int_\Omega\frac{\partial\left(v_1u_1\right)}{\partial x_1}u_1+\int_\Gamma v_1u_1u_1dS$$

$$= \quad -\int_\Omega \frac{\partial\left(v_1 u_1\right)}{\partial x_1} u_1 = -\int_\Omega v_1 \frac{\partial\left(u_1\right)}{\partial x_1} u_1 - \int_\Omega u_1 \frac{\partial\left(v_1\right)}{\partial x_1} u_1$$

Therefore,

$$\begin{aligned}
&\int_\Omega v_1 \left(u_1 \frac{\partial u_1}{\partial x} + u_2 \frac{\partial u_1}{\partial y} + u_3 \frac{\partial u_1}{\partial z}\right) + \int_\Omega v_2 \left(u_1 \frac{\partial u_2}{\partial x} + u_2 \frac{\partial u_2}{\partial y} + u_3 \frac{\partial u_2}{\partial z}\right) \\
&\qquad\qquad + \int_\Omega v_3 \left(u_1 \frac{\partial u_3}{\partial x} + + u_2 \frac{\partial u_3}{\partial y} + u_3 \frac{\partial u_3}{\partial z}\right) \\
&= -\int_\Omega v_1 \frac{\partial u_1}{\partial x} u_1 - \int_\Omega u_1 \frac{\partial v_1}{\partial x} u_1 - \int_\Omega v_1 \frac{\partial u_2}{\partial y} u_1 - \int_\Omega u_2 \frac{\partial v_1}{\partial y} u_1 - \int_\Omega v_1 \frac{\partial u_3}{\partial z} u_1 - \int_\Omega u_3 \frac{\partial v_1}{\partial z} u_1 \\
&\quad - \int_\Omega v_2 \frac{\partial u_1}{\partial x} u_2 - \int_\Omega u_1 \frac{\partial v_2}{\partial x} u_2 - \int_\Omega v_2 \frac{\partial u_2}{\partial y} u_2 - \int_\Omega u_2 \frac{\partial v_2}{\partial y} u_2 - \int_\Omega v_2 \frac{\partial u_3}{\partial z} u_2 - \int_\Omega u_3 \frac{\partial v_2}{\partial z} u_2 \\
&\quad - \int_\Omega v_3 \frac{\partial u_1}{\partial x} u_3 - \int_\Omega u_1 \frac{\partial v_3}{\partial x} u_3 - \int_\Omega v_3 \frac{\partial u_2}{\partial y} u_3 - \int_\Omega u_2 \frac{\partial v_3}{\partial y} u_3 - \int_\Omega v_3 \frac{\partial u_3}{\partial z} u_3 - \int_\Omega u_3 \frac{\partial v_3}{\partial z} u_3
\end{aligned} \tag{A.5}$$

Therefore, collecting terms we have

$$\begin{aligned}
&\int_\Omega v_1 \left(u_1 \frac{\partial u_1}{\partial x} + u_2 \frac{\partial u_1}{\partial y} + u_3 \frac{\partial u_1}{\partial z}\right) + \int_\Omega v_2 \left(u_1 \frac{\partial u_2}{\partial x} + u_2 \frac{\partial u_2}{\partial y} + u_3 \frac{\partial u_2}{\partial z}\right) \\
&\qquad\qquad + \int_\Omega v_3 \left(u_1 \frac{\partial u_3}{\partial x} + + u_2 \frac{\partial u_3}{\partial y} + u_3 \frac{\partial u_3}{\partial z}\right) \\
&= -\left(\int_\Omega u_1 \frac{\partial v_1}{\partial x} u_1 + \int_\Omega u_2 \frac{\partial v_1}{\partial y} u_1 + \int_\Omega u_3 \frac{\partial v_1}{\partial z} u_1\right) - \left(\int_\Omega v_1 \frac{\partial u_1}{\partial x} u_1 + \int_\Omega v_1 \frac{\partial u_2}{\partial y} u_1 + \int_\Omega v_1 \frac{\partial u_3}{\partial z} u_1\right) \\
&\quad - \left(\int_\Omega u_1 \frac{\partial v_2}{\partial x} u_2 + \int_\Omega u_2 \frac{\partial v_2}{\partial y} u_2 + \int_\Omega u_3 \frac{\partial v_2}{\partial z} u_2\right) - \left(\int_\Omega v_2 \frac{\partial u_1}{\partial x} u_2 + \int_\Omega v_2 \frac{\partial u_2}{\partial y} u_2 + \int_\Omega v_2 \frac{\partial u_3}{\partial z} u_2\right) \\
&\quad - \left(\int_\Omega u_1 \frac{\partial v_3}{\partial x} u_3 + \int_\Omega u_2 \frac{\partial v_3}{\partial y} u_3 + \int_\Omega u_3 \frac{\partial v_3}{\partial z} u_3\right) - \left(\int_\Omega v_3 \frac{\partial u_1}{\partial x} u_3 + \int_\Omega v_3 \frac{\partial u_2}{\partial y} u_3 + \int_\Omega v_3 \frac{\partial u_3}{\partial z} u_3\right)
\end{aligned} \tag{A.6}$$

Writing this in vector notation, we have

$$\begin{aligned}\int_\Omega \left((\mathbf{u}\cdot\nabla)\,\mathbf{u}\right)\cdot\mathbf{v} &= \int_\Omega (\mathbf{u}\cdot\nabla u_1)\,v_1 + (\mathbf{u}\cdot\nabla u_2)\,v_2 + (\mathbf{u}\cdot\nabla u_3)\,v_3 \\ &= -\int_\Omega (\mathbf{u}\cdot\nabla v_1)\,u_1 - \int_\Omega v_1\,(\nabla\cdot\mathbf{u})\,u_1 - \int_\Omega (\mathbf{u}\cdot\nabla v_2)\,u_2 - \int_\Omega v_2\,(\nabla\cdot\mathbf{u})\,u_2 \\ &\qquad - \int_\Omega (\mathbf{u}\cdot\nabla v_3)\,u_3 - \int_\Omega v_3\,(\nabla\cdot\mathbf{u})\,u_3 \\ &= -\int_\Omega (\mathbf{u}\cdot\nabla v_1)\,u_1 - \int_\Omega (\mathbf{u}\cdot\nabla v_2)\,u_2 - \int_\Omega (\mathbf{u}\cdot\nabla v_3)\,u_3 = -\int_\Omega \left((\mathbf{u}\cdot\nabla)\,\mathbf{v}\right)\cdot\mathbf{u} \end{aligned} \tag{A.7}$$

Hence,

$$\begin{aligned}\rho\int_\Omega \left((\mathbf{u}\cdot\nabla)\,\mathbf{u}\right)\cdot\mathbf{v} &= \frac{\rho}{2}\left(\int_\Omega \left((\mathbf{u}\cdot\nabla)\,\mathbf{u}\right)\cdot\mathbf{v} + \int_\Omega \left((\mathbf{u}\cdot\nabla)\,\mathbf{u}\right)\cdot\mathbf{v}\right) \\ &= \frac{\rho}{2}\left(\int_\Omega \left((\mathbf{u}\cdot\nabla)\,\mathbf{u}\right)\cdot\mathbf{v} - \int_\Omega \left((\mathbf{u}\cdot\nabla)\,\mathbf{v}\right)\cdot\mathbf{u}\right)\end{aligned}$$

A.2 Ohms Law

We wish to show

$$\int_\Omega (\mathbf{u}\times\mathbf{B})\cdot\mathbf{K} = -\int_\Omega (\mathbf{K}\times\mathbf{B})\cdot\mathbf{u}.$$

This amounts to show that for any vector $\mathbf{a}$, $\mathbf{b}$, and $\mathbf{c}$

$$\int_\Omega (\mathbf{a}\times\mathbf{b})\cdot\mathbf{c} = -\int_\Omega (\mathbf{c}\times\mathbf{b})\cdot\mathbf{a} \tag{A.8}$$

To start, recall that the cross product between two vectors $\mathbf{a}$ and $\mathbf{b}$ is

$$\mathbf{a} \times \mathbf{b} = \langle a_1, a_2, a_3 \rangle \times \langle b_1, b_2, b_3 \rangle = \begin{vmatrix} \mathbf{i} & \mathbf{j} & \mathbf{k} \\ a_1 & a_2 & a_3 \\ b_1 & b_2 & b_3 \end{vmatrix} = \begin{vmatrix} a_2 & a_3 \\ b_2 & b_3 \end{vmatrix} \mathbf{i} - \begin{vmatrix} a_1 & a_3 \\ b_1 & b_3 \end{vmatrix} \mathbf{j} + \begin{vmatrix} a_1 & a_2 \\ b_1 & b_2 \end{vmatrix} \mathbf{k}$$

$$= (a_2 b_3 - a_3 b_2)\,\mathbf{i} - (a_1 b_3 - a_3 b_1)\,\mathbf{j} + (a_1 b_2 - a_2 b_1)\,\mathbf{k} \quad \text{(A.9)}$$

Now, we wish to show that the identity

$$\int_\Omega (\mathbf{a} \times \mathbf{b}) \cdot \mathbf{c} = -\int_\Omega (\mathbf{c} \times \mathbf{b}) \cdot \mathbf{a} \quad \text{(A.10)}$$

is true.

First, note that $\mathbf{a} \cdot (\mathbf{b} \times \mathbf{c}) = (\mathbf{a} \times \mathbf{b}) \cdot \mathbf{c}$

$$\begin{aligned} \mathbf{a} \cdot (\mathbf{b} \times \mathbf{c}) &= \langle a_1, a_2, a_3 \rangle \cdot (\langle b_1, b_2, b_3 \rangle \times \langle c_1, c_2, c_3 \rangle) \\ &= \langle a_1, a_2, a_3 \rangle \cdot ((b_2 c_3 - b_3 c_2)\,\mathbf{i} - (b_1 c_3 - b_3 c_1)\,\mathbf{j} + (b_1 c_2 - b_2 c_1)\,\mathbf{k}) \\ &= a_1 (b_2 c_3 - b_3 c_2) - a_2 (b_1 c_3 - b_3 c_1) + a_3 (b_1 c_2 - b_2 c_1) \\ &= a_1 b_2 c_3 - a_1 b_3 c_2 - a_2 b_1 c_3 + a_2 b_3 c_1 + a_3 b_1 c_2 - a_3 b_2 c_1 \\ &= (a_2 b_3 - a_3 b_2)\, c_1 - (a_1 b_3 - a_3 b_1)\, c_2 + (a_1 b_2 - a_2 b_1)\, c_3 = (\mathbf{a} \times \mathbf{b}) \cdot \mathbf{c} \end{aligned} \quad \text{(A.11)}$$

Since $\mathbf{a} \times \mathbf{b} = -\mathbf{b} \times \mathbf{a}$ and $\mathbf{a} \cdot \mathbf{b} = \mathbf{b} \cdot \mathbf{a}$

$$(\mathbf{a} \times \mathbf{b}) \cdot \mathbf{c} = \mathbf{a} \cdot (\mathbf{b} \times \mathbf{c}) = (\mathbf{b} \times \mathbf{c}) \cdot \mathbf{a} = -\,(\mathbf{c} \times \mathbf{b}) \cdot \mathbf{a} \quad \text{(A.12)}$$

Therefore,

$$\int_{\Omega} (\mathbf{a} \times \mathbf{b}) \cdot \mathbf{c} = -\int_{\Omega} (\mathbf{c} \times \mathbf{b}) \cdot \mathbf{a} \tag{A.13}$$

Appendix B

Newton's Method Linearization

Recalling Newton's method

$$\mathbf{X}^{(k+1)} = \mathbf{X}^{(k)} - \frac{\mathbf{H}\left(\mathbf{X}^{(k)}\right)}{\mathbf{H}'\left(\mathbf{X}^{(k)}\right)} \tag{B.1}$$

with

$$\mathbf{H}(\mathbf{X}) = \begin{bmatrix} \eta\Delta\mathbf{u}_1 + \rho\left(\mathbf{u}\cdot\nabla\right)\mathbf{u}_1 + \frac{\partial p}{\partial x} - \left(\mathbf{J}_2\mathbf{B}_3 - \mathbf{J}_3\mathbf{B}_2\right) - \mathbf{F}_1 \\ \eta\Delta\mathbf{u}_2 + \rho\left(\mathbf{u}\cdot\nabla\right)\mathbf{u}_2 + \frac{\partial p}{\partial y} + \left(\mathbf{J}_1\mathbf{B}_3 - \mathbf{J}_3\mathbf{B}_1\right) - \mathbf{F}_2 \\ \eta\Delta\mathbf{u}_3 + \rho\left(\mathbf{u}\cdot\nabla\right)\mathbf{u}_3 + \frac{\partial p}{\partial z} - \left(\mathbf{J}_1\mathbf{B}_2 - \mathbf{J}_2\mathbf{B}_1\right) - \mathbf{F}_3 \\ \sigma^{-1}\mathbf{J}_1 + \frac{\partial \phi}{\partial x} - \left(\mathbf{u}_2\mathbf{B}_3 - \mathbf{u}_3\mathbf{B}_2\right) - \mathbf{E}_1 \\ \sigma^{-1}\mathbf{J}_2 + \frac{\partial \phi}{\partial y} - \left(\mathbf{u}_1\mathbf{B}_3 - \mathbf{u}_3\mathbf{B}_1\right) - \mathbf{E}_2 \\ \sigma^{-1}\mathbf{J}_3 + \frac{\partial \phi}{\partial z} - \left(\mathbf{u}_1\mathbf{B}_2 - \mathbf{u}_2\mathbf{B}_1\right) - \mathbf{E}_3 \\ \frac{\partial \mathbf{u}_1}{\partial x} + \frac{\partial \mathbf{u}_2}{\partial y} + \frac{\partial \mathbf{u}_3}{\partial z} \\ \frac{\partial \mathbf{J}_1}{\partial x} + \frac{\partial \mathbf{J}_2}{\partial y} + \frac{\partial \mathbf{J}_3}{\partial z} \end{bmatrix}$$

and the variable $\mathbf{X} = (\mathbf{u}_1, \mathbf{u}_2, \mathbf{u}_3, p, \mathbf{J}_1, \mathbf{J}_2, \mathbf{J}_3, \phi)$ obtained from the equations

$$\begin{aligned} -\eta\Delta\mathbf{u} + \rho\left(\mathbf{u}\cdot\nabla\right)\mathbf{u} + \nabla p - \mathbf{J}\times\mathbf{B} &= \mathbf{F} \\ \sigma^{-1}\mathbf{J} + \nabla\phi - \mathbf{u}\times\mathbf{B} &= \mathbf{E}, \\ \nabla\cdot\mathbf{u} = 0 \qquad \text{and} \qquad \nabla\cdot\mathbf{J} &= 0. \end{aligned}$$

Also recall the Gateaux deritave

$$H'_G\left(\mathbf{X}^{(k)}\right)(\Delta\mathbf{X}) = \lim_{\epsilon\to 0}\frac{\mathbf{H}\left(\mathbf{X}^{(k)} + \epsilon\Delta\mathbf{X}\right) - \mathbf{H}\left(\mathbf{X}^{(k)}\right)}{\epsilon}, \tag{B.2}$$

where $\Delta\mathbf{X} = \mathbf{X}^{(k+1)} - \mathbf{X}^{(k)}$ and $\epsilon\Delta\mathbf{X} = \epsilon\left(\Delta\mathbf{u}_1, \Delta\mathbf{u}_2, \Delta\mathbf{u}_3, \Delta p, \Delta\mathbf{J}_1, \Delta\mathbf{J}_2, \Delta\mathbf{J}_3\right)$. Note that Δ will be used for increment as opposed to using it for the Laplacian.

Since

$$\begin{aligned}
\mathbf{B} &= \mathbf{B}_0 + \mathcal{B}(\mathbf{J}) \\
&= \mathbf{B}_0 - \frac{\mu}{4\pi}\int_\Omega \frac{\mathbf{x}-\mathbf{y}}{|\mathbf{x}-\mathbf{y}|^3} \times \mathbf{J}(\mathbf{y})\, d\mathbf{y} = \begin{bmatrix} (\mathbf{B}_0)_1 - \frac{\mu}{4\pi}\int_\Omega \frac{(\mathbf{x}_2-\mathbf{y}_2)\mathbf{J}_3(\mathbf{y})-(\mathbf{x}_3-\mathbf{y}_3)\mathbf{J}_2(\mathbf{y})}{|\mathbf{x}-\mathbf{y}|^3} d\mathbf{y} \\ (\mathbf{B}_0)_2 - \frac{\mu}{4\pi}\int_\Omega \frac{(\mathbf{x}_1-\mathbf{y}_1)\mathbf{J}_3(\mathbf{y})-(\mathbf{x}_3-\mathbf{y}_3)\mathbf{J}_1(\mathbf{y})}{|\mathbf{x}-\mathbf{y}|^3} d\mathbf{y} \\ (\mathbf{B}_0)_3 - \frac{\mu}{4\pi}\int_\Omega \frac{(\mathbf{x}_1-\mathbf{y}_1)\mathbf{J}_2(\mathbf{y})-(\mathbf{x}_2-\mathbf{y}_2)\mathbf{J}_1(\mathbf{y})}{|\mathbf{x}-\mathbf{y}|^3} d\mathbf{y} \end{bmatrix}
\end{aligned}$$

we have

$$\mathbf{H}\left(\mathbf{X}^{(k)}\right) = \begin{bmatrix} \eta\nabla\cdot\nabla\mathbf{u}_1^{(k)} + \rho\left(\mathbf{u}^{(k)}\cdot\nabla\right)\mathbf{u}_1^{(k)} + \frac{\partial p^{(k)}}{\partial x} \\ -\mathbf{J}_2^{(k)}\left((\mathbf{B}_0)_3 - \frac{\mu}{4\pi}\int_\Omega \frac{(\mathbf{x}_1-\mathbf{y}_1)\mathbf{J}_2^{(k)}-(\mathbf{x}_2-\mathbf{y}_2)\mathbf{J}_1^{(k)}}{|\mathbf{x}-\mathbf{y}|^3}d\mathbf{y}\right) \\ +\mathbf{J}_3^{(k)}\left((\mathbf{B}_0)_2 - \frac{\mu}{4\pi}\int_\Omega \frac{(\mathbf{x}_1-\mathbf{y}_1)\mathbf{J}_3^{(k)}-(\mathbf{x}_3-\mathbf{y}_3)\mathbf{J}_1^{(k)}}{|\mathbf{x}-\mathbf{y}|^3}d\mathbf{y}\right) - \mathbf{F}_1 \\ \\ \eta\nabla\cdot\nabla\mathbf{u}_2^{(k)} + \rho\left(\mathbf{u}^{(k)}\cdot\nabla\right)\mathbf{u}_2^{(k)} + \frac{\partial p^{(k)}}{\partial y} \\ +\mathbf{J}_1^{(k)}\left((\mathbf{B}_0)_3 - \frac{\mu}{4\pi}\int_\Omega \frac{(\mathbf{x}_1-\mathbf{y}_1)\mathbf{J}_2^{(k)}-(\mathbf{x}_2-\mathbf{y}_2)\mathbf{J}_1^{(k)}}{|\mathbf{x}-\mathbf{y}|^3}d\mathbf{y}\right) \\ -\mathbf{J}_3^{(k)}\left((\mathbf{B}_0)_1 - \frac{\mu}{4\pi}\int_\Omega \frac{(\mathbf{x}_2-\mathbf{y}_2)\mathbf{J}_3^{(k)}-(\mathbf{x}_3-\mathbf{y}_3)\mathbf{J}_2^{(k)}}{|\mathbf{x}-\mathbf{y}|^3}d\mathbf{y}\right) - \mathbf{F}_2 \\ \\ \eta\nabla\cdot\nabla\mathbf{u}_3^{(k)} + \rho\left(\mathbf{u}^{(k)}\cdot\nabla\right)\mathbf{u}_3^{(k)} + \frac{\partial p^{(k)}}{\partial z} \\ -\mathbf{J}_1^{(k)}\left((\mathbf{B}_0)_2 - \frac{\mu}{4\pi}\int_\Omega \frac{(\mathbf{x}_1-\mathbf{y}_1)\mathbf{J}_3^{(k)}-(\mathbf{x}_3-\mathbf{y}_3)\mathbf{J}_1^{(k)}}{|\mathbf{x}-\mathbf{y}|^3}d\mathbf{y}\right) \\ +\mathbf{J}_2^{(k)}\left((\mathbf{B}_0)_1 - \frac{\mu}{4\pi}\int_\Omega \frac{(\mathbf{x}_2-\mathbf{y}_2)\mathbf{J}_3^{(k)}-(\mathbf{x}_3-\mathbf{y}_3)\mathbf{J}_2^{(k)}}{|\mathbf{x}-\mathbf{y}|^3}d\mathbf{y}\right) - \mathbf{F}_3 \\ \\ \sigma^{-1}\mathbf{J}_1^{(k)} + \frac{\partial\phi^{(k)}}{\partial x} - \mathbf{u}_2^{(k)}\left((\mathbf{B}_0)_3 - \frac{\mu}{4\pi}\int_\Omega \frac{(\mathbf{x}_1-\mathbf{y}_1)\mathbf{J}_2^{(k)}-(\mathbf{x}_2-\mathbf{y}_2)\mathbf{J}_1^{(k)}}{|\mathbf{x}-\mathbf{y}|^3}d\mathbf{y}\right) \\ +\mathbf{u}_3^{(k)}\left((\mathbf{B}_0)_2 - \frac{\mu}{4\pi}\int_\Omega \frac{(\mathbf{x}_1-\mathbf{y}_1)\mathbf{J}_3^{(k)}-(\mathbf{x}_3-\mathbf{y}_3)\mathbf{J}_1^{(k)}}{|\mathbf{x}-\mathbf{y}|^3}d\mathbf{y}\right) - \mathbf{E}_1 \\ \\ \sigma^{-1}\mathbf{J}_2^{(k)} + \frac{\partial\phi^{(k)}}{\partial y} - \mathbf{u}_1^{(k)}\left((\mathbf{B}_0)_3 - \frac{\mu}{4\pi}\int_\Omega \frac{(\mathbf{x}_1-\mathbf{y}_1)\mathbf{J}_2^{(k)}-(\mathbf{x}_2-\mathbf{y}_2)\mathbf{J}_1^{(k)}}{|\mathbf{x}-\mathbf{y}|^3}d\mathbf{y}\right) \\ +\mathbf{u}_3^{(k)}\left((\mathbf{B}_0)_1 - \frac{\mu}{4\pi}\int_\Omega \frac{(\mathbf{x}_2-\mathbf{y}_2)\mathbf{J}_3^{(k)}-(\mathbf{x}_3-\mathbf{y}_3)\mathbf{J}_2^{(k)}}{|\mathbf{x}-\mathbf{y}|^3}d\mathbf{y}\right) - \mathbf{E}_2 \\ \\ \sigma^{-1}\mathbf{J}_3^{(k)} + \frac{\partial\phi^{(k)}}{\partial z} - \mathbf{u}_1^{(k)}\left((\mathbf{B}_0)_2 - \frac{\mu}{4\pi}\int_\Omega \frac{(\mathbf{x}_1-\mathbf{y}_1)\mathbf{J}_3^{(k)}-(\mathbf{x}_3-\mathbf{y}_3)\mathbf{J}_1^{(k)}}{|\mathbf{x}-\mathbf{y}|^3}d\mathbf{y}\right) \\ +\mathbf{u}_2^{(k)}\left((\mathbf{B}_0)_1 - \frac{\mu}{4\pi}\int_\Omega \frac{(\mathbf{x}_2-\mathbf{y}_2)\mathbf{J}_3^{(k)}-(\mathbf{x}_3-\mathbf{y}_3)\mathbf{J}_2^{(k)}}{|\mathbf{x}-\mathbf{y}|^3}d\mathbf{y}\right) - \mathbf{E}_3 \\ \\ \frac{\partial\mathbf{u}_1^{(k)}}{\partial x} + \frac{\partial\mathbf{u}_2^{(k)}}{\partial y} + \frac{\partial\mathbf{u}_3^{(k)}}{\partial z} \\ \\ \frac{\partial\mathbf{J}_1^{(k)}}{\partial x} + \frac{\partial\mathbf{J}_2^{(k)}}{\partial y} + \frac{\partial\mathbf{J}_3^{(k)}}{\partial z} \end{bmatrix}$$

and

$$
\mathbf{H}\left(\mathbf{X}^{(k)}+\epsilon\Delta\mathbf{X}\right)=\left[\begin{array}{c}
\eta\nabla\cdot\nabla\left(\mathbf{u}_1^{(k)}+\epsilon\Delta\mathbf{u}_1\right)+\rho\left(\left(\mathbf{u}^{(k)}+\epsilon\Delta\mathbf{u}\right)\cdot\nabla\right)\left(\mathbf{u}_1^{(k)}+\epsilon\Delta\mathbf{u}_1\right)\\
+\frac{\partial\left(p^{(k)}+\epsilon\Delta p\right)}{\partial x}-\left(\mathbf{J}_2^{(k)}+\epsilon\Delta\mathbf{J}_2\right)\left((\mathbf{B}_0)_3-\frac{\mu}{4\pi}\int_\Omega\frac{(\mathbf{x}_1-\mathbf{y}_1)\left(\mathbf{J}_2^{(k)}+\epsilon\Delta\mathbf{J}_2\right)-(\mathbf{x}_2-\mathbf{y}_2)\left(\mathbf{J}_1^{(k)}+\epsilon\Delta\mathbf{J}_1\right)}{|\mathbf{x}-\mathbf{y}|^3}d\mathbf{y}\right)\\
+\left(\mathbf{J}_3^{(k)}+\epsilon\Delta\mathbf{J}_3\right)\left((\mathbf{B}_0)_2-\frac{\mu}{4\pi}\int_\Omega\frac{(\mathbf{x}_1-\mathbf{y}_1)\left(\mathbf{J}_3^{(k)}+\epsilon\Delta\mathbf{J}_3\right)-(\mathbf{x}_3-\mathbf{y}_3)\left(\mathbf{J}_1^{(k)}+\epsilon\Delta\mathbf{J}_1\right)}{|\mathbf{x}-\mathbf{y}|^3}d\mathbf{y}\right)-\mathbf{F}_1\\
\\
\eta\nabla\cdot\nabla\left(\mathbf{u}_2^{(k)}+\epsilon\Delta\mathbf{u}_2\right)+\rho\left(\left(\mathbf{u}^{(k)}+\epsilon\Delta\mathbf{u}\right)\cdot\nabla\right)\left(\mathbf{u}_2^{(k)}+\epsilon\Delta\mathbf{u}_2\right)+\frac{\partial\left(p^{(k)}+\epsilon\Delta p\right)}{\partial y}\\
+\left(\mathbf{J}_1^{(k)}+\epsilon\Delta\mathbf{J}_1\right)\left((\mathbf{B}_0)_3-\frac{\mu}{4\pi}\int_\Omega\frac{(\mathbf{x}_1-\mathbf{y}_1)\left(\mathbf{J}_2^{(k)}+\epsilon\Delta\mathbf{J}_2\right)-(\mathbf{x}_2-\mathbf{y}_2)\left(\mathbf{J}_1^{(k)}+\epsilon\Delta\mathbf{J}_1\right)}{|\mathbf{x}-\mathbf{y}|^3}d\mathbf{y}\right)\\
-\left(\mathbf{J}_3^{(k)}+\epsilon\Delta\mathbf{J}_3\right)\left((\mathbf{B}_0)_1-\frac{\mu}{4\pi}\int_\Omega\frac{(\mathbf{x}_2-\mathbf{y}_2)\left(\mathbf{J}_3^{(k)}+\epsilon\Delta\mathbf{J}_3\right)-(\mathbf{x}_3-\mathbf{y}_3)\left(\mathbf{J}_2^{(k)}+\epsilon\Delta\mathbf{J}_2\right)}{|\mathbf{x}-\mathbf{y}|^3}d\mathbf{y}\right)-\mathbf{F}_2\\
\\
\eta\nabla\cdot\nabla\left(\mathbf{u}_3^{(k)}+\epsilon\Delta\mathbf{u}_3\right)+\rho\left(\left(\mathbf{u}^{(k)}+\epsilon\Delta\mathbf{u}\right)\cdot\nabla\right)\left(\mathbf{u}_3^{(k)}+\epsilon\Delta\mathbf{u}_3\right)+\frac{\partial\left(p^{(k)}+\epsilon\Delta p\right)}{\partial z}\\
-\left(\mathbf{J}_1^{(k)}+\epsilon\Delta\mathbf{J}_1\right)\left((\mathbf{B}_0)_2-\frac{\mu}{4\pi}\int_\Omega\frac{(\mathbf{x}_1-\mathbf{y}_1)\left(\mathbf{J}_3^{(k)}+\epsilon\Delta\mathbf{J}_3\right)-(\mathbf{x}_3-\mathbf{y}_3)\left(\mathbf{J}_1^{(k)}+\epsilon\Delta\mathbf{J}_1\right)}{|\mathbf{x}-\mathbf{y}|^3}d\mathbf{y}\right)\\
+\left(\mathbf{J}_2^{(k)}+\epsilon\Delta\mathbf{J}_2\right)\left((\mathbf{B}_0)_1-\frac{\mu}{4\pi}\int_\Omega\frac{(\mathbf{x}_2-\mathbf{y}_2)\left(\mathbf{J}_3^{(k)}+\epsilon\Delta\mathbf{J}_3\right)-(\mathbf{x}_3-\mathbf{y}_3)\left(\mathbf{J}_2^{(k)}+\epsilon\Delta\mathbf{J}_2\right)}{|\mathbf{x}-\mathbf{y}|^3}d\mathbf{y}\right)-\mathbf{F}_3\\
\\
\sigma^{-1}\left(\mathbf{J}_1^{(k)}+\epsilon\Delta\mathbf{J}_1\right)+\frac{\partial\left(\phi^{(k)}+\epsilon\Delta\phi\right)}{\partial x}\\
-\left(\mathbf{u}_2^{(k)}+\epsilon\Delta\mathbf{u}_2\right)\left((\mathbf{B}_0)_3-\frac{\mu}{4\pi}\int_\Omega\frac{(\mathbf{x}_1-\mathbf{y}_1)\left(\mathbf{J}_2^{(k)}+\epsilon\Delta\mathbf{J}_2\right)-(\mathbf{x}_2-\mathbf{y}_2)\left(\mathbf{J}_1^{(k)}+\epsilon\Delta\mathbf{J}_1\right)}{|\mathbf{x}-\mathbf{y}|^3}d\mathbf{y}\right)\\
+\left(\mathbf{u}_3^{(k)}+\epsilon\Delta\mathbf{u}_3\right)\left((\mathbf{B}_0)_2-\frac{\mu}{4\pi}\int_\Omega\frac{(\mathbf{x}_1-\mathbf{y}_1)\left(\mathbf{J}_3^{(k)}+\epsilon\Delta\mathbf{J}_3\right)-(\mathbf{x}_3-\mathbf{y}_3)\left(\mathbf{J}_1^{(k)}+\epsilon\Delta\mathbf{J}_1\right)}{|\mathbf{x}-\mathbf{y}|^3}d\mathbf{y}\right)-\mathbf{E}_1\\
\\
\sigma^{-1}\left(\mathbf{J}_2^{(k)}+\epsilon\Delta\mathbf{J}_2\right)+\frac{\partial\left(\phi^{(k)}+\epsilon\Delta\phi\right)}{\partial y}\\
-\left(\mathbf{u}_1^{(k)}+\epsilon\Delta\mathbf{u}_1\right)\left((\mathbf{B}_0)_3-\frac{\mu}{4\pi}\int_\Omega\frac{(\mathbf{x}_1-\mathbf{y}_1)\left(\mathbf{J}_2^{(k)}+\epsilon\Delta\mathbf{J}_2\right)-(\mathbf{x}_2-\mathbf{y}_2)\left(\mathbf{J}_1^{(k)}+\epsilon\Delta\mathbf{J}_1\right)}{|\mathbf{x}-\mathbf{y}|^3}d\mathbf{y}\right)\\
+\left(\mathbf{u}_3^{(k)}+\epsilon\Delta\mathbf{u}_3\right)\left((\mathbf{B}_0)_1-\frac{\mu}{4\pi}\int_\Omega\frac{(\mathbf{x}_2-\mathbf{y}_2)\left(\mathbf{J}_3^{(k)}+\epsilon\Delta\mathbf{J}_3\right)-(\mathbf{x}_3-\mathbf{y}_3)\left(\mathbf{J}_2^{(k)}+\epsilon\Delta\mathbf{J}_2\right)}{|\mathbf{x}-\mathbf{y}|^3}d\mathbf{y}\right)-\mathbf{E}_2\\
\\
\sigma^{-1}\left(\mathbf{J}_3^{(k)}+\epsilon\Delta\mathbf{J}_3\right)+\frac{\partial\left(\phi^{(k)}+\epsilon\Delta\phi\right)}{\partial z}\\
-\left(\mathbf{u}_1^{(k)}+\epsilon\Delta\mathbf{u}_1\right)\left((\mathbf{B}_0)_2-\frac{\mu}{4\pi}\int_\Omega\frac{(\mathbf{x}_1-\mathbf{y}_1)\left(\mathbf{J}_3^{(k)}+\epsilon\Delta\mathbf{J}_3\right)-(\mathbf{x}_3-\mathbf{y}_3)\left(\mathbf{J}_1^{(k)}+\epsilon\Delta\mathbf{J}_1\right)}{|\mathbf{x}-\mathbf{y}|^3}d\mathbf{y}\right)\\
+\left(\mathbf{u}_2^{(k)}+\epsilon\Delta\mathbf{u}_2\right)\left((\mathbf{B}_0)_1-\frac{\mu}{4\pi}\int_\Omega\frac{(\mathbf{x}_2-\mathbf{y}_2)\left(\mathbf{J}_3^{(k)}+\epsilon\Delta\mathbf{J}_3\right)-(\mathbf{x}_3-\mathbf{y}_3)\left(\mathbf{J}_2^{(k)}+\epsilon\Delta\mathbf{J}_2\right)}{|\mathbf{x}-\mathbf{y}|^3}d\mathbf{y}\right)-\mathbf{E}_3\\
\\
\frac{\partial\left(\mathbf{u}_1^{(k)}+\epsilon\Delta\mathbf{u}_1\right)}{\partial x}+\frac{\partial\left(\mathbf{u}_2^{(k)}+\epsilon\Delta\mathbf{u}_2\right)}{\partial y}+\frac{\partial\left(\mathbf{u}_3^{(k)}+\epsilon\Delta\mathbf{u}_3\right)}{\partial z}\\
\\
\frac{\partial\left(\mathbf{J}_1^{(k)}+\epsilon\Delta\mathbf{J}_1\right)}{\partial x}+\frac{\partial\left(\mathbf{J}_2^{(k)}+\epsilon\Delta\mathbf{J}_2\right)}{\partial y}+\frac{\partial\left(\mathbf{J}_3^{(k)}+\epsilon\Delta\mathbf{J}_3\right)}{\partial z}
\end{array}\right]
$$

Then, since

$$\begin{aligned}\rho\left(\left(\mathbf{u}^{(k)}+\epsilon\Delta\mathbf{u}\right)\cdot\nabla\right)\left(\mathbf{u}_1^{(k)}+\epsilon\Delta\mathbf{u}_1\right) &= \rho\left(\left(\mathbf{u}^{(k)}+\epsilon\Delta\mathbf{u}\right)\cdot\nabla\right)\mathbf{u}_1^{(k)}+\rho\left(\left(\mathbf{u}^{(k)}+\epsilon\Delta\mathbf{u}\right)\cdot\nabla\right)\epsilon\Delta\mathbf{u}_1\\ &= \rho\left(\mathbf{u}^{(k)}\cdot\nabla\right)\mathbf{u}_1^{(k)}+\rho\left(\epsilon\Delta\mathbf{u}\cdot\nabla\right)\mathbf{u}_1^{(k)}+\rho\left(\mathbf{u}^{(k)}\cdot\nabla\right)\epsilon\Delta\mathbf{u}_1\\ &\quad +\rho\left(\epsilon\Delta\mathbf{u}\cdot\nabla\right)\epsilon\Delta\mathbf{u}_1\end{aligned}$$

$$\begin{aligned}&\left(\mathbf{J}_2^{(k)}+\epsilon\Delta\mathbf{J}_2\right)\left((\mathbf{B}_0)_3-\frac{\mu}{4\pi}\int_\Omega\frac{(\mathbf{x}_1-\mathbf{y}_1)\left(\mathbf{J}_2^{(k)}+\epsilon\Delta\mathbf{J}_2\right)-(\mathbf{x}_2-\mathbf{y}_2)\left(\mathbf{J}_1^{(k)}+\epsilon\Delta\mathbf{J}_1\right)}{|\mathbf{x}-\mathbf{y}|^3}d\mathbf{y}\right)\\ &\quad=\mathbf{J}_2^{(k)}\left((\mathbf{B}_0)_3-\frac{\mu}{4\pi}\int_\Omega\frac{(\mathbf{x}_1-\mathbf{y}_1)\left(\mathbf{J}_2^{(k)}+\epsilon\Delta\mathbf{J}_2\right)-(\mathbf{x}_2-\mathbf{y}_2)\left(\mathbf{J}_1^{(k)}+\epsilon\Delta\mathbf{J}_1\right)}{|\mathbf{x}-\mathbf{y}|^3}d\mathbf{y}\right)\\ &\qquad+\epsilon\Delta\mathbf{J}_2\left((\mathbf{B}_0)_3-\frac{\mu}{4\pi}\int_\Omega\frac{(\mathbf{x}_1-\mathbf{y}_1)\left(\mathbf{J}_2^{(k)}+\epsilon\Delta\mathbf{J}_2\right)-(\mathbf{x}_2-\mathbf{y}_2)\left(\mathbf{J}_1^{(k)}+\epsilon\Delta\mathbf{J}_1\right)}{|\mathbf{x}-\mathbf{y}|^3}d\mathbf{y}\right)\\ &\quad=\mathbf{J}_2^{(k)}\left((\mathbf{B}_0)_3-\frac{\mu}{4\pi}\int_\Omega\frac{(\mathbf{x}_1-\mathbf{y}_1)\mathbf{J}_2^{(k)}-(\mathbf{x}_2-\mathbf{y}_2)\mathbf{J}_1^{(k)}}{|\mathbf{x}-\mathbf{y}|^3}d\mathbf{y}\right)\\ &\qquad+\epsilon\mathbf{J}_2^{(k)}\left(0-\frac{\mu}{4\pi}\int_\Omega\frac{(\mathbf{x}_1-\mathbf{y}_1)\Delta\mathbf{J}_2-(\mathbf{x}_2-\mathbf{y}_2)\Delta\mathbf{J}_1}{|\mathbf{x}-\mathbf{y}|^3}d\mathbf{y}\right)\\ &\qquad\quad+\epsilon\Delta\mathbf{J}_2\left((\mathbf{B}_0)_3-\frac{\mu}{4\pi}\int_\Omega\frac{(\mathbf{x}_1-\mathbf{y}_1)\mathbf{J}_2^{(k)}-(\mathbf{x}_2-\mathbf{y}_2)\mathbf{J}_1^{(k)}}{|\mathbf{x}-\mathbf{y}|^3}d\mathbf{y}\right)\\ &\qquad\quad\quad+\epsilon\Delta\mathbf{J}_2\left(0-\frac{\mu}{4\pi}\int_\Omega\frac{(\mathbf{x}_1-\mathbf{y}_1)\epsilon\Delta\mathbf{J}_2-(\mathbf{x}_2-\mathbf{y}_2)\epsilon\Delta\mathbf{J}_1}{|\mathbf{x}-\mathbf{y}|^3}d\mathbf{y}\right)\end{aligned}$$

$$\lim_{\epsilon\to0}\frac{\mathbf{H}\left(\mathbf{X}^{(k)}+\epsilon\Delta\mathbf{X}\right)-\mathbf{H}\left(\mathbf{X}^{(k)}\right)}{\epsilon}$$

$$
= \begin{bmatrix}
-\eta\nabla\cdot\nabla\left(\Delta\mathbf{u}_1\right)+\rho\left(\Delta\mathbf{u}\cdot\nabla\right)\mathbf{u}_1^{(k)}+\rho\left(\mathbf{u}^{(k)}\cdot\nabla\right)\Delta\mathbf{u}_1+\frac{\partial\Delta p}{\partial x} \\
-\mathbf{J}_2^{(k)}\left(0-\frac{\mu}{4\pi}\int_\Omega\frac{(\mathbf{x}_1-\mathbf{y}_1)\Delta\mathbf{J}_2-(\mathbf{x}_2-\mathbf{y}_2)\Delta\mathbf{J}_1}{|\mathbf{x}-\mathbf{y}|^3}d\mathbf{y}\right)-\Delta\mathbf{J}_2\left((\mathbf{B}_0)_3-\frac{\mu}{4\pi}\int_\Omega\frac{(\mathbf{x}_1-\mathbf{y}_1)\mathbf{J}_2^{(k)}-(\mathbf{x}_2-\mathbf{y}_2)\mathbf{J}_1^{(k)}}{|\mathbf{x}-\mathbf{y}|^3}d\mathbf{y}\right) \\
+\mathbf{J}_3^{(k)}\left(0-\frac{\mu}{4\pi}\int_\Omega\frac{(\mathbf{x}_1-\mathbf{y}_1)\Delta\mathbf{J}_3-(\mathbf{x}_3-\mathbf{y}_3)\Delta\mathbf{J}_1}{|\mathbf{x}-\mathbf{y}|^3}d\mathbf{y}\right)+\Delta\mathbf{J}_3^{(k)}\left((\mathbf{B}_0)_2-\frac{\mu}{4\pi}\int_\Omega\frac{(\mathbf{x}_1-\mathbf{y}_1)\mathbf{J}_3^{(k)}-(\mathbf{x}_3-\mathbf{y}_3)\mathbf{J}_1^{(k)}}{|\mathbf{x}-\mathbf{y}|^3}d\mathbf{y}\right) \\
\\
\eta\nabla\cdot\nabla\Delta\mathbf{u}_2+\rho\left(\Delta\mathbf{u}\cdot\nabla\right)\mathbf{u}_2^{(k)}+\rho\left(\mathbf{u}^{(k)}\cdot\nabla\right)\Delta\mathbf{u}_2+\frac{\partial\Delta p}{\partial y} \\
+\mathbf{J}_1^{(k)}\left(0-\frac{\mu}{4\pi}\int_\Omega\frac{(\mathbf{x}_1-\mathbf{y}_1)\Delta\mathbf{J}_2-(\mathbf{x}_2-\mathbf{y}_2)\Delta\mathbf{J}_1}{|\mathbf{x}-\mathbf{y}|^3}d\mathbf{y}\right)+\Delta\mathbf{J}_1^{(k)}\left((\mathbf{B}_0)_3-\frac{\mu}{4\pi}\int_\Omega\frac{(\mathbf{x}_1-\mathbf{y}_1)\mathbf{J}_2^{(k)}-(\mathbf{x}_2-\mathbf{y}_2)\mathbf{J}_1^{(k)}}{|\mathbf{x}-\mathbf{y}|^3}d\mathbf{y}\right) \\
-\mathbf{J}_3^{(k)}\left(0-\frac{\mu}{4\pi}\int_\Omega\frac{(\mathbf{x}_2-\mathbf{y}_2)\Delta\mathbf{J}_3-(\mathbf{x}_3-\mathbf{y}_3)\Delta\mathbf{J}_2}{|\mathbf{x}-\mathbf{y}|^3}d\mathbf{y}\right)-\Delta\mathbf{J}_3^{(k)}\left((\mathbf{B}_0)_1-\frac{\mu}{4\pi}\int_\Omega\frac{(\mathbf{x}_2-\mathbf{y}_2)\mathbf{J}_3^{(k)}-(\mathbf{x}_3-\mathbf{y}_3)\mathbf{J}_2^{(k)}}{|\mathbf{x}-\mathbf{y}|^3}d\mathbf{y}\right) \\
\\
\eta\nabla\cdot\nabla\Delta\mathbf{u}_3+\rho\left(\Delta\mathbf{u}\cdot\nabla\right)\mathbf{u}_3^{(k)}+\rho\left(\mathbf{u}^{(k)}\cdot\nabla\right)\Delta\mathbf{u}_3+\frac{\partial\Delta p}{\partial z} \\
-\mathbf{J}_1^{(k)}\left(0-\frac{\mu}{4\pi}\int_\Omega\frac{(\mathbf{x}_1-\mathbf{y}_1)\Delta\mathbf{J}_3-(\mathbf{x}_3-\mathbf{y}_3)\Delta\mathbf{J}_1}{|\mathbf{x}-\mathbf{y}|^3}d\mathbf{y}\right)-\Delta\mathbf{J}_1\left((\mathbf{B}_0)_2-\frac{\mu}{4\pi}\int_\Omega\frac{(\mathbf{x}_1-\mathbf{y}_1)\mathbf{J}_3^{(k)}-(\mathbf{x}_3-\mathbf{y}_3)\mathbf{J}_1^{(k)}}{|\mathbf{x}-\mathbf{y}|^3}d\mathbf{y}\right) \\
+\mathbf{J}_2^{(k)}\left(0-\frac{\mu}{4\pi}\int_\Omega\frac{(\mathbf{x}_2-\mathbf{y}_2)\Delta\mathbf{J}_3-(\mathbf{x}_3-\mathbf{y}_3)\Delta\mathbf{J}_2}{|\mathbf{x}-\mathbf{y}|^3}d\mathbf{y}\right)+\Delta\mathbf{J}_2^{(k)}\left((\mathbf{B}_0)_1-\frac{\mu}{4\pi}\int_\Omega\frac{(\mathbf{x}_2-\mathbf{y}_2)\mathbf{J}_3^{(k)}-(\mathbf{x}_3-\mathbf{y}_3)\mathbf{J}_2^{(k)}}{|\mathbf{x}-\mathbf{y}|^3}d\mathbf{y}\right) \\
\\
\sigma^{-1}\Delta\mathbf{J}_1+\frac{\partial\Delta\phi}{\partial x} \\
-\mathbf{u}_2^{(k)}\left(0-\frac{\mu}{4\pi}\int_\Omega\frac{(\mathbf{x}_1-\mathbf{y}_1)\Delta\mathbf{J}_2-(\mathbf{x}_2-\mathbf{y}_2)\Delta\mathbf{J}_1}{|\mathbf{x}-\mathbf{y}|^3}d\mathbf{y}\right)-\Delta\mathbf{u}_2\left((\mathbf{B}_0)_3-\frac{\mu}{4\pi}\int_\Omega\frac{(\mathbf{x}_1-\mathbf{y}_1)\mathbf{J}_2^{(k)}-(\mathbf{x}_2-\mathbf{y}_2)\mathbf{J}_1^{(k)}}{|\mathbf{x}-\mathbf{y}|^3}d\mathbf{y}\right) \\
+\mathbf{u}_3^{(k)}\left(0-\frac{\mu}{4\pi}\int_\Omega\frac{(\mathbf{x}_1-\mathbf{y}_1)\Delta\mathbf{J}_3-(\mathbf{x}_3-\mathbf{y}_3)\Delta\mathbf{J}_1}{|\mathbf{x}-\mathbf{y}|^3}d\mathbf{y}\right)+\Delta\mathbf{u}_3\left((\mathbf{B}_0)_2-\frac{\mu}{4\pi}\int_\Omega\frac{(\mathbf{x}_1-\mathbf{y}_1)\mathbf{J}_3^{(k)}-(\mathbf{x}_3-\mathbf{y}_3)\mathbf{J}_1^{(k)}}{|\mathbf{x}-\mathbf{y}|^3}d\mathbf{y}\right) \\
\\
\sigma^{-1}\Delta\mathbf{J}_2+\frac{\partial\Delta\phi}{\partial y} \\
-\mathbf{u}_1^{(k)}\left(0-\frac{\mu}{4\pi}\int_\Omega\frac{(\mathbf{x}_1-\mathbf{y}_1)\Delta\mathbf{J}_2-(\mathbf{x}_2-\mathbf{y}_2)\Delta\mathbf{J}_1}{|\mathbf{x}-\mathbf{y}|^3}d\mathbf{y}\right)-\Delta\mathbf{u}_1\left((\mathbf{B}_0)_3-\frac{\mu}{4\pi}\int_\Omega\frac{(\mathbf{x}_1-\mathbf{y}_1)\mathbf{J}_2^{(k)}-(\mathbf{x}_2-\mathbf{y}_2)\mathbf{J}_1^{(k)}}{|\mathbf{x}-\mathbf{y}|^3}d\mathbf{y}\right) \\
+\mathbf{u}_3^{(k)}\left(0-\frac{\mu}{4\pi}\int_\Omega\frac{(\mathbf{x}_2-\mathbf{y}_2)\Delta\mathbf{J}_3-(\mathbf{x}_3-\mathbf{y}_3)\Delta\mathbf{J}_2}{|\mathbf{x}-\mathbf{y}|^3}d\mathbf{y}\right)+\Delta\mathbf{u}_3\left((\mathbf{B}_0)_1-\frac{\mu}{4\pi}\int_\Omega\frac{(\mathbf{x}_2-\mathbf{y}_2)\mathbf{J}_3^{(k)}-(\mathbf{x}_3-\mathbf{y}_3)\mathbf{J}_2^{(k)}}{|\mathbf{x}-\mathbf{y}|^3}d\mathbf{y}\right) \\
\\
\sigma^{-1}\Delta\mathbf{J}_3+\frac{\partial\Delta\phi}{\partial z} \\
-\mathbf{u}_1^{(k)}\left(0-\frac{\mu}{4\pi}\int_\Omega\frac{(\mathbf{x}_1-\mathbf{y}_1)\Delta\mathbf{J}_3-(\mathbf{x}_3-\mathbf{y}_3)\Delta\mathbf{J}_1}{|\mathbf{x}-\mathbf{y}|^3}d\mathbf{y}\right)-\Delta\mathbf{u}_1\left((\mathbf{B}_0)_2-\frac{\mu}{4\pi}\int_\Omega\frac{(\mathbf{x}_1-\mathbf{y}_1)\mathbf{J}_3^{(k)}-(\mathbf{x}_3-\mathbf{y}_3)\mathbf{J}_1^{(k)}}{|\mathbf{x}-\mathbf{y}|^3}d\mathbf{y}\right) \\
+\mathbf{u}_2^{(k)}\left(0-\frac{\mu}{4\pi}\int_\Omega\frac{(\mathbf{x}_2-\mathbf{y}_2)\Delta\mathbf{J}_3-(\mathbf{x}_3-\mathbf{y}_3)\Delta\mathbf{J}_2}{|\mathbf{x}-\mathbf{y}|^3}d\mathbf{y}\right)+\Delta\mathbf{u}_2\left((\mathbf{B}_0)_1-\frac{\mu}{4\pi}\int_\Omega\frac{(\mathbf{x}_2-\mathbf{y}_2)\mathbf{J}_3^{(k)}-(\mathbf{x}_3-\mathbf{y}_3)\mathbf{J}_2^{(k)}}{|\mathbf{x}-\mathbf{y}|^3}d\mathbf{y}\right) \\
\\
\frac{\partial\Delta\mathbf{u}_1}{\partial x}+\frac{\partial\Delta\mathbf{u}_2}{\partial y}+\frac{\partial\Delta\mathbf{u}_3}{\partial z} \\
\\
\frac{\partial\Delta\mathbf{J}_1}{\partial x}+\frac{\partial\Delta\mathbf{J}_2}{\partial y}+\frac{\partial\Delta\mathbf{J}_3}{\partial z}
\end{bmatrix}
$$

$$= \begin{bmatrix} \nabla \cdot \nabla (\Delta \mathbf{u}) + \rho ((\Delta \mathbf{u}) \cdot \nabla) \mathbf{u}^{(k)} + \rho \left(\mathbf{u}^{(k)} \cdot \nabla\right) (\Delta \mathbf{u}) + \nabla (\Delta p) - \mathbf{J}^{(k)} \times \mathcal{B} (\Delta \mathbf{J}) - (\Delta \mathbf{J}) \times \mathbf{B} \left(\mathbf{J}^{(k)}\right) \\ \sigma^{-1} (\Delta \mathbf{J}) + \nabla (\Delta \phi) - \mathbf{u}^{(k)} \times \mathcal{B} (\Delta \mathbf{J}) - (\Delta \mathbf{u}) \times \mathbf{B} \left(\mathbf{J}^{(k)}\right) \\ \nabla \cdot (\Delta \mathbf{u}) \\ \nabla \cdot (\Delta \mathbf{J}) \end{bmatrix}$$

So, we have

$$\mathbf{H}'_G \left(\mathbf{X}^{(k)}\right) (\Delta \mathbf{X}) = \begin{bmatrix} \nabla \cdot \nabla (\Delta \mathbf{u}) + \rho ((\Delta \mathbf{u}) \cdot \nabla) \mathbf{u}^{(k)} + \rho \left(\mathbf{u}^{(k)} \cdot \nabla\right) (\Delta \mathbf{u}) + \nabla (\Delta p) \\ -\mathbf{J}^{(k)} \times \mathcal{B} (\Delta \mathbf{J}) - (\Delta \mathbf{J}) \times \mathbf{B} \left(\mathbf{J}^{(k)}\right) \\ \sigma^{-1} (\Delta \mathbf{J}) + \nabla (\Delta \phi) - \mathbf{u}^{(k)} \times \mathcal{B} (\Delta \mathbf{J}) - (\Delta \mathbf{u}) \times \mathbf{B} \left(\mathbf{J}^{(k)}\right) \\ \nabla \cdot (\Delta \mathbf{u}) \\ \nabla \cdot (\Delta \mathbf{J}) \end{bmatrix} \tag{B.3}$$

Recalling $\Delta \mathbf{X} = \mathbf{X}^{(k+1)} - \mathbf{X}^{(k)}$, $\Delta \mathbf{X} = (\Delta \mathbf{u}_1, \Delta \mathbf{u}_2, \Delta \mathbf{u}_3, \Delta p, \Delta \mathbf{J}_1, \Delta \mathbf{J}_2, \Delta \mathbf{J}_3)$, and Newton's method $\mathbf{H}' \left(\mathbf{X}^{(k)}\right) (\Delta \mathbf{X}) = -\mathbf{H} \left(\mathbf{X}^{(k)}\right)$, we have

$$\begin{bmatrix} -\eta \nabla \cdot \nabla \mathbf{u}^{(k+1)} + \rho \left(\mathbf{u}^{(k+1)} \cdot \nabla\right) \mathbf{u}^{(k)} + \rho \left(\mathbf{u}^{(k)} \cdot \nabla\right) \mathbf{u}^{(k+1)} + \nabla p^{(k+1)} - \mathbf{J}^{(k)} \times \mathcal{B} \left(\mathbf{J}^{(k+1)}\right) - \mathbf{J}^{(k+1)} \times \mathbf{B} \left(\mathbf{J}^{(k)}\right) \\ \sigma^{-1} \mathbf{J}^{(k+1)} + \nabla \phi^{(k+1)} - \mathbf{u}^{(k)} \times \mathcal{B} \left(\mathbf{J}^{(k+1)}\right) - \mathbf{u}^{(k+1)} \times \mathbf{B} \left(\mathbf{J}^{(k)}\right) \\ \nabla \cdot \mathbf{u}^{(k+1)} \\ \nabla \cdot \mathbf{J}^{(k+1)} \end{bmatrix}$$

$$- \begin{bmatrix} -\eta \nabla \cdot \nabla \mathbf{u}^{(k)} + \rho \left(\mathbf{u}^{(k)} \cdot \nabla\right) \mathbf{u}^{(k)} + \rho \left(\mathbf{u}^{(k)} \cdot \nabla\right) \mathbf{u}^{(k)} + \nabla p^{(k)} - \mathbf{J}^{(k)} \times \mathcal{B} \left(\mathbf{J}^{(k)}\right) - \mathbf{J}^{(k)} \times \mathbf{B} \left(\mathbf{J}^{(k)}\right) \\ \sigma^{-1} \mathbf{J}^{(k)} + \nabla \phi^{(k)} - \mathbf{u}^{(k)} \times \mathcal{B} \left(\mathbf{J}^{(k)}\right) - \mathbf{u}^{(k)} \times \mathbf{B} \left(\mathbf{J}^{(k)}\right) \\ \nabla \cdot \mathbf{u}^{(k)} \\ \nabla \cdot \mathbf{J}^{(k)} \end{bmatrix} = -\mathbf{H} \left(\mathbf{X}^{(k)}\right)$$

Therefore

$$\begin{bmatrix} -\eta\nabla\cdot\nabla\mathbf{u}^{(k+1)}+\rho\left(\mathbf{u}^{(k+1)}\cdot\nabla\right)\mathbf{u}^{(k)}-\rho\left(\mathbf{u}^{(k)}\cdot\nabla\right)\mathbf{u}^{(k)}+\rho\left(\mathbf{u}^{(k)}\cdot\nabla\right)\mathbf{u}^{(k+1)} \\ +\nabla p^{(k+1)}-\mathbf{J}^{(k)}\times\mathcal{B}\left(\mathbf{J}^{(k+1)}\right)+\mathbf{J}^{(k)}\times\mathcal{B}\left(\mathbf{J}^{(k)}\right)-\mathbf{J}^{(k+1)}\times\mathbf{B}\left(\mathbf{J}^{(k)}\right) \\ \\ \sigma^{-1}\mathbf{J}^{(k+1)}+\nabla\phi^{(k+1)}-\mathbf{u}^{(k)}\times\mathcal{B}\left(\mathbf{J}^{(k+1)}\right)+\mathbf{u}^{(k)}\times\mathcal{B}\left(\mathbf{J}^{(k)}\right)-\mathbf{u}^{(k+1)}\times\mathbf{B}\left(\mathbf{J}^{(k)}\right) \\ \\ \nabla\cdot\mathbf{u}^{(k+1)} \\ \\ \nabla\cdot\mathbf{J}^{(k+1)} \end{bmatrix} = \begin{bmatrix} \mathbf{F} \\ \\ \mathbf{E} \\ \\ 0 \\ \\ 0 \end{bmatrix}$$

Appendix C

Iterative Solvers

C.1 Conjugate Gradient (CG) Method

We recall the conjugate gradient method from the point of view of steepest descent, where we try to find the minimum of the function $\phi(x) = \frac{1}{2}x^tAx - x^tb$ where $b \in \mathbb{R}^n$ and $A \in \mathbb{R}^{n\times n}$ is symmetric positive definite. With $\nabla\phi\,(x) = \left[\frac{\partial}{\partial x_1}\phi(x), \ldots, \frac{\partial}{\partial x_k}\phi(x), \ldots, \frac{\partial}{\partial x_n}\phi(x)\right]$, consider

$$\begin{aligned}
\frac{\partial}{\partial x_k}\phi(x) &= \frac{\partial}{\partial x_k}\left(\frac{1}{2}x^tAx - x^tb\right) = \frac{\partial}{\partial x_k}\left(\frac{1}{2}\langle Ax, x\rangle - \langle b, x\rangle\right) \\
&= \frac{\partial}{\partial x_k}\left(\frac{1}{2}\sum_{i=1}^{n} x_i \sum_{j=1}^{n} a_{ij}x_j - \sum_{i=1}^{n} b_i x_i\right) \\
&= \frac{1}{2}\sum_{i=1}^{n}\sum_{j=1}^{n} a_{ij}x_j\frac{\partial}{\partial x_k}x_i + \frac{1}{2}\sum_{i=1}^{n}\sum_{j=1}^{n} a_{ij}x_i\frac{\partial}{\partial x_k}x_j - \sum_{i=1}^{n} b_i\frac{\partial}{\partial x_k}x_i \\
&= \frac{1}{2}\sum_{j=1}^{n} a_{kj}x_j + \frac{1}{2}\sum_{i=1}^{n} x_i a_{ik} - b_k = \sum_{j=1}^{n} a_{kj}x_j - b_k = \mathrm{row}_k\,(A)\,x - b_k
\end{aligned}$$

Then $\nabla\phi(x) = Ax - b$ and an extreme value is attained when $\nabla\phi = 0$, $Ax = b$, and we have solve our system of equations. Recalling that at a location x_n, a function decreases greatest in the opposite direction of its gradient $-\nabla\phi(x_n) = b - Ax_n = r_n$ and in the direction of steepest descent. If the gradient is nonzero, we can decrease $\phi(x_n)$ by moving in the direction of r_n. Due to the symmetry and positive definiteness of A, the quadratic form $\phi(x)$ will attain a minimum at some location $x_n + \alpha r_n$ in this direction. A good example to illustrate $\phi(x)$ is when $n = 2$, $x = (x_1, x_2)$, and $\phi(x)$ is the elliptic paraboloid. To determine

α and the location of the minimum in the direction r_n, we find the critical value of

$$\begin{aligned}\tilde{\phi}(\alpha) &= \phi(x_n + \alpha r_n) \\ &= \frac{1}{2}(x_n \alpha r_n)^t A(x_n \alpha r_n) - (x_n + \alpha r_n)^t b \\ &= \frac{1}{2}\langle Ax_n, x_n\rangle + \alpha\langle Ax_n, r_n\rangle + \alpha^2\langle Ar_n, r_n\rangle - \langle b, x_n\rangle - \alpha\langle b, r_n\rangle .\end{aligned}$$

Differentiating,

$$\begin{aligned}\frac{\partial}{\partial\alpha}\tilde{\phi}(\alpha) &= \langle Ax_n, r_n\rangle + 2\alpha\langle Ar_n, r_n\rangle - \alpha\langle b, r_n\rangle \\ &= \langle Ax_n - b, r_n\rangle + 2\alpha\langle Ar_n, r_n\rangle = -\langle r_n, r_n\rangle + 2\alpha\langle Ar_n, r_n\rangle .\end{aligned}$$

Setting the derivative to zero, $\frac{\partial}{\partial\alpha}\tilde{\phi}(\alpha) = 0$, we have $\alpha = \frac{\langle r_n, r_n\rangle}{2\langle Ar_n, r_n\rangle}$. The steepest descent algorithm is given below.

Method of Steepest Descent

```
int k = 0;
vector x_k;                          // initial guess x_0
vector r_k = b - Ax_k;               // initial residual r_0
while r_k ≠ 0
   k = k + 1;
  α_k = ⟨r_{k-1}, r_{k-1}⟩ / ⟨Ar_{k-1}, r_{k-1}⟩;
  x_k = x_{k-1} + α_k r_{k-1};
  r_k = b - Ax_k;
```

However, if the matrix A is ill-conditioned, the method of determining search directions using the gradients and steepest descent may not be the most efficient in terms of the number of iterations to convergence. By bringing the structure of A into the algorithm to more effectively determine search directions we can obtain the conjugate gradient method

[44] shown below. With $\beta_k = 0$ the conjugate gradient algorithm returns to the method of steepest descent.

Conjugate Gradient (CG) Method

```
int k = 0;
vector x_k;                          // initial guess x_0
vector r_k = b - A x_k;              // initial residual r_0
while r_k ≠ 0
  k = k + 1;
    if k = 1
      p_1 = r_0
    else
      β_k = ⟨r_{k-1}, r_{k-1}⟩ / ⟨r_{k-2}, r_{k-2}⟩;
      p_k = r_{k-1} + β_k p_{k-1}
    end
  α_k = ⟨r_{k-1}, r_{k-1}⟩ / ⟨A p_k, p_k⟩;
  x_k = x_{k-1} + α_k p_k;
  r_k = r_{k-1} - α A p_k;
```

The operations per iteration for this algorithm are two inner products, one matrix-vector product, three scalar-vector products, two scalar-scalar multiplications and three additions. If the system matrix A is sparse with m nonzeros per row and $m << n$, then the resulting number of floating point operations per iteration is $O(n)$.

C.2 Generalized Minimal Residual (GMRES) Method

The GMRES method was developed as an extension of the Minimal Residual Method to treat systems of equations that were not necessary symmetric, where the minimal residual method had extended the conjugate gradient method to symmetric indefinite systems. The

GMRES algorithm iteratively solves the system $Ax = b$ using two major steps. The first is the orthonormalization of the Krylov vectors $\{b, Ab, A^2b, \ldots, A^{n-1}b\}$ spanning a Krylov space. The second step is a least squares solution to the best approximation x_n in this space with respect to the minimization of the size of the residual $\|r_n\| = \|b - Ax_n\|$. The algorithm is given below.

Generalized Minimal Residual (GMRES) Method

```
vector r_0 = b - A x_0;
scalar γ = ||r_0||_2;
vector v_1 = r_0 / γ ;    // first orthonormal vector of Krylov space
for j = 1, ..., m          // orthonomalizing Krylov vectors
  w = A v_j;
  for i = 1, ..., j
    h_{i,j} = ⟨w, v_i⟩      // projecting w onto previous vectors v_i
    w = w - h_{i,j} v_i     // orthogonalizing w w.r.t. v_i
  end
  h_{j+1,j} = ||w||_2;
  v_{j+1} = w / h_{j+1,j};    // normalizing w
end
V_m = [v_1, ..., v_m];
H̃_m = [h_{i,j}]  (1 ≤ i ≤ j+1, 1 ≤ j ≤ m);
y_m = min_y ||γ e_1 - H̃_m y||_2; x_m = x_0 + V_m y_m;
if (||r_m||_2 = ||b - A x_m||_2 < ε)
  stop;
else
  x_0 = x_m; return to start;
end
```

To take a closer look at the least squares solve at the end of the algorithm, consider the matrices V_m, V_{m+1}, and $\tilde{H}_m$ formed by the algorithm

$$V_{m+1} = \begin{bmatrix} | & | & & | & | \\ v_1 & v_2 & \dots & v_m & v_{m+1} \\ | & | & & | & | \end{bmatrix} \quad \text{and} \quad \tilde{H}_m = \begin{bmatrix} h_{1,1} & \dots & \dots & h_{1,n} \\ h_{2,1} & h_{2,2} & \dots & h_{2,n} \\ 0 & \ddots & \ddots & \vdots \\ \vdots & \ddots & h_{m,m-1} & h_{m,m} \\ 0 & \dots & 0 & h_{m+1,m} \end{bmatrix}$$

Looking closely at the algorithm, we can identify the matrix equation $AV_m = V_{m+1}\tilde{H}_m$ with the Gram-Schmidt orthonormalization process. Indeed, the equality of the first columns resulting from the matrix products in the equation yield the first orthonormalized vector

$$Av_1 = h_{11}v_1 + h_{21}v_2 \implies v_2 = \frac{1}{h_{21}}\left(Av_1 - h_{11}v_1\right).$$

Continuing in a similar manner we see

$$Av_2 = h_{12}v_1 + h_{22}v_2 + h_{32}v_3 \implies v_3 = \frac{1}{h_{32}}\left(Av_2 - h_{12}v_1 - h_{22}v_2\right).$$

With the matrix equation $AV_m = V_{m+1}\tilde{H}_m$, we elaborate on the least squares step at the end of the algorithm. Recall that we wish to minimize the l_2 norm of the residual vector r_m and that our approximate solution x_m for the m^{th} iteration resides in the space $x_0 + \mathcal{K}_m = x_0 + \text{span}\left\{v_1, Av_1, ..., A^{m-1}v_1\right\}$, where $v_1 = \frac{r_0}{\gamma} = \frac{b - Ax_0}{\|b - Ax_0\|_2}$. Further, the vectors $v_1, v_2, \dots v_m$ form an orthonormal basis for $\mathcal{K}_m$. Therefore, for some $y \in \mathbb{R}^m$, such that x_m is a linear combination of the orthonormal basis, we have

$$\begin{aligned} \|r_m\|_2^2 &= \|b - Ax_m\|_2^2 = \|b - A\left(x_0 + V_m y\right)\|_2^2 = \|r_0 - AV_m y\|_2^2 \\ &= \left\|\gamma v_1 - V_{m+1}\tilde{H}_m y\right\|_2^2 = \left\|V_{m+1}\left(\gamma e_1 - \tilde{H}_m y\right)\right\|_2^2 = \left\|\gamma e_1 - \tilde{H}_m y\right\|_2^2 \end{aligned}$$

$$= \left\| Q_m \gamma e_1 - Q_m \tilde{H}_m y \right\|_2^2 = \left\| \tilde{g} - \tilde{R}_m y \right\|_2^2 = |\tilde{g}_{m+1}|^2 + \|g - R_m y\|_2^2 ,$$

where e_1 is the standard Euclidean basis vector in the first coordinate direction, V_{m+1} being orthonormal is norm preserving, and Q_m is the product of Givens rotations that put the upper Hessenberg matrix $\tilde{H}_m$ in upper right-triangular form $\tilde{R}_m$. Since the last row of $\tilde{R}_m$ is therefore a row of zeros, the last row of $\tilde{g} - \tilde{R}_m y$ will be equal to the last element of $\tilde{g}$ - $\tilde{g}_{m+1}$. Defining g and R_m to be all but the last row of $\tilde{g}$ and $\tilde{R}_m$, respectively, we obtain the last equality. Noting that R_m is invertible, we see there is a y such that $g - R_m y = 0$ and therefore $\|r_m\|_2^2 = |\tilde{g}_{m+1}|^2$.

Looking at the operation count for one iteration of GMRES, we see that the algorithm starts off with a vector subtraction (n flops), a vector inner product, a square root and a scalar division ($n + 2$ flops). We assume that A is sparse with approximately $k << n$ nonzeros per row and that the dimension of the Krylov space $m << n$ as well. A Gram-Schmidt orthogonalization iteration consists of a matrix-vector product (kn flops), a vector inner product ($jn < mn$ flops), vector subtraction ($jn < mn$ flops), another vector inner product with a square root and a scalar division ($n+2$ flops). This is carried out m times. If $m^2 << n$ then the Gram-Schmidt operations are $O(m^2 n) = O(n)$. The least squares methods consists of Givens rotations ($O(m^2)$ flops each) and backsolve to obtain y ($O(m^2)$ flops. Therefore, with $m^2 << n$ the GMRES flop count is $O(n)$.

Appendix D

Exact Solution

Recall the first example of chapter 4 having the exact solution given below.

$$
\begin{aligned}
\mathbf{u}(x,y,z) &:= \begin{bmatrix} 0 \\ -\pi\cos(\pi x)\exp(-s)\left(\frac{1}{2}-z\right) \\ -\pi\cos(\pi x)\exp(-s)\left(y-\frac{1}{2}\right) \end{bmatrix} \\
\mathbf{J}(x,y,z) &:= \begin{bmatrix} 2\sin(\pi x)(1-s)\exp(-s) \\ -\pi\cos(\pi x)\exp(-s)\left(y-\frac{1}{2}\right) \\ -\pi\cos(\pi x)\exp(-s)\left(z-\frac{1}{2}\right) \end{bmatrix} \\
p(x,y,z) &:= -\frac{1}{2}\sin^2(\pi x)\, s\exp(-2s), \\
\phi(x,y,z) &:= \frac{2}{\pi}\cos(\pi x), \\
\mathbf{B}(x,y,z) &:= \begin{bmatrix} 1 \\ \sin(\pi x)\exp(-s)\left(\frac{1}{2}-z\right) \\ \sin(\pi x)\exp(-s)\left(y-\frac{1}{2}\right) \end{bmatrix}
\end{aligned}
$$

with $\mathbf{r} = \left(0, y-\frac{1}{2}, z-\frac{1}{2}\right)$ and $s = |\mathbf{r}|^2 = \left(y-\frac{1}{2}\right)^2 + \left(z-\frac{1}{2}\right)^2$. Note that $\mathbf{u}$ and $\mathbf{B}$ are divergence free and $\nabla \times \mathbf{B} = \mathbf{J}$

$$
\begin{aligned}
\nabla \cdot B &= B_{1,x} + B_{2,y} + B_{3,z} \\
&= \frac{\partial}{\partial x}(1) + \frac{\partial}{\partial y}\sin(\pi x)\exp(-s)\left(\frac{1}{2}-z\right) + \frac{\partial}{\partial z}\sin(\pi x)\exp(-s)\left(y-\frac{1}{2}\right) \\
&= 0 + \sin(\pi x)\left(\frac{1}{2}-z\right)\frac{\partial}{\partial y}\exp\left(-\left(y-\frac{1}{2}\right)^2-\left(z-\frac{1}{2}\right)^2\right) + \sin(\pi x)\left(y-\frac{1}{2}\right)\frac{\partial}{\partial z}\exp\left(-\left(y-\frac{1}{2}\right)^2-\left(z-\frac{1}{2}\right)^2\right)
\end{aligned}
$$

$$= \quad -2\sin(\pi x)\left(\frac{1}{2}-z\right)\left(y-\frac{1}{2}\right)\exp(-s) - 2\sin(\pi x)\left(y-\frac{1}{2}\right)\left(z-\frac{1}{2}\right)\exp(-s) = 0$$

$$\begin{aligned}
\nabla \cdot u &= u_{1,x} + u_{2,y} + u_{3,z} \\
&= \frac{\partial}{\partial x}(0) - \pi\frac{\partial}{\partial y}\cos(\pi x)\exp(-s)\left(\frac{1}{2}-z\right) - \pi\frac{\partial}{\partial z}\cos(\pi x)\exp(-s)\left(y-\frac{1}{2}\right) \\
&= 0 - \pi\cos(\pi x)\left(\frac{1}{2}-z\right)\frac{\partial}{\partial y}\exp\left(-\left(y-\frac{1}{2}\right)^2 - \left(z-\frac{1}{2}\right)^2\right) - \pi\cos(\pi x)\left(y-\frac{1}{2}\right)\frac{\partial}{\partial z}\exp\left(-\left(y-\frac{1}{2}\right)^2 - \left(z-\frac{1}{2}\right)^2\right) \\
&= 2\pi\cos(\pi x)\left(\frac{1}{2}-z\right)\left(y-\frac{1}{2}\right)\exp(-s) + 2\pi\cos(\pi x)\left(y-\frac{1}{2}\right)\left(z-\frac{1}{2}\right)\exp(-s) = 0
\end{aligned}$$

and $\nabla \times \mathbf{B} = \mathbf{J}$:

$$\begin{aligned}
\nabla \times B &= \begin{bmatrix} B_{3,y} - B_{2,z} \\ B_{1,z} - B_{3,x} \\ B_{2,x} - B_{1,y} \end{bmatrix} = \begin{bmatrix} \frac{\partial}{\partial y}\sin(\pi x)\exp(-s)\left(y-\frac{1}{2}\right) - \frac{\partial}{\partial z}\sin(\pi x)\exp(-s)\left(\frac{1}{2}-z\right) \\ \frac{\partial}{\partial z}(1) - \frac{\partial}{\partial x}\sin(\pi x)\exp(-s)\left(y-\frac{1}{2}\right) \\ \frac{\partial}{\partial x}\sin(\pi x)\exp(-s)\left(\frac{1}{2}-z\right) - \frac{\partial}{\partial y}(1) \end{bmatrix} \\
&= \begin{bmatrix} \sin(\pi x)\frac{\partial}{\partial y}\exp(-s)\left(y-\frac{1}{2}\right) - \sin(\pi x)\frac{\partial}{\partial z}\exp(-s)\left(\frac{1}{2}-z\right) \\ -\pi\cos(\pi x)\exp(-s)\left(y-\frac{1}{2}\right) \\ -\pi\cos(\pi x)\exp(-s)\left(z-\frac{1}{2}\right) \end{bmatrix} \\
&= \begin{bmatrix} \sin(\pi x)\exp(-s)\left(1-2\left(y-\frac{1}{2}\right)^2\right) - \sin(\pi x)\exp(-s)\left(-1+2\left(z-\frac{1}{2}\right)^2\right) \\ -\pi\cos(\pi x)\exp(-s)\left(y-\frac{1}{2}\right) \\ -\pi\cos(\pi x)\exp(-s)\left(z-\frac{1}{2}\right) \end{bmatrix} \\
&= \begin{bmatrix} 2(1-s)\sin(\pi x)\exp(-s) \\ -\pi\cos(\pi x)\exp(-s)\left(y-\frac{1}{2}\right) \\ -\pi\cos(\pi x)\exp(-s)\left(z-\frac{1}{2}\right) \end{bmatrix} = J,
\end{aligned}$$

$$
\begin{aligned}
\mathbf{F} &:= -\Delta\mathbf{u} + (\mathbf{u}\cdot\nabla)\,\mathbf{u} + \nabla p - \mathbf{J}\times\mathbf{B}, \\
&= -\begin{bmatrix} \nabla\cdot\nabla u_1 \\ \nabla\cdot\nabla u_2 \\ \nabla\cdot\nabla u_3 \end{bmatrix} + \begin{bmatrix} \mathbf{u}\cdot\nabla u_1 \\ \mathbf{u}\cdot\nabla u_2 \\ \mathbf{u}\cdot\nabla u_3 \end{bmatrix} + \begin{bmatrix} p_x \\ p_y \\ p_z \end{bmatrix} - \begin{bmatrix} J_2B_3 - J_3B_2 \\ J_3B_1 - J_1B_3 \\ J_1B_2 - J_2B_1 \end{bmatrix} \\
&= \begin{bmatrix} -u_{1,xx} - u_{1,yy} - u_{1,zz} + u_1\frac{\partial u_1}{\partial x} + u_2\frac{\partial u_1}{\partial y} + u_3\frac{\partial u_1}{\partial z} + p_x - J_2B_3 + J_3B_2 \\ -u_{2,xx} - u_{2,yy} - u_{2,zz} + u_1\frac{\partial u_2}{\partial x} + u_2\frac{\partial u_2}{\partial y} + u_3\frac{\partial u_2}{\partial z} + p_y - J_3B_1 + J_1B_3 \\ -u_{3,xx} - u_{3,yy} - u_{3,zz} + u_1\frac{\partial u_3}{\partial x} + u_2\frac{\partial u_3}{\partial y} + u_3\frac{\partial u_3}{\partial z} + p_z - J_1B_2 + J_2B_1 \end{bmatrix} \\
&= \begin{bmatrix} -0 + 0 - \pi s\sin(\pi x)\cos(\pi x)\exp(-2s) + \pi s\sin(\pi x)\cos(\pi x)\exp(-2s) \\ -\pi\cos(\pi x)\exp(-s)\left(\frac{1}{2} - z\right)\left(\pi^2 + 8 - 4s\right) - \pi^2\cos^2(\pi x)\exp(-2s)\left(y - \frac{1}{2}\right) \\ \qquad + \sin^2(\pi x)\exp(-2s)\left(y - \frac{1}{2}\right)(2s-1) + \pi\cos(\pi x)\exp(-s)\left(z - \frac{1}{2}\right) \\ \qquad + 2\,(1-s)\sin^2(\pi x)\exp(-2s)\left(y - \frac{1}{2}\right) \\ -\pi\cos(\pi x)\exp(-s)\left(y - \frac{1}{2}\right)\left(\pi^2 + 8 - 4s\right) - \pi^2\cos^2(\pi x)\exp(-2s)\left(z - \frac{1}{2}\right) \\ \qquad + \sin^2(\pi x)\exp(-2s)\left(z - \frac{1}{2}\right)(2s-1) - 2\,(1-s)\sin^2(\pi x)\exp(-2s)\left(\frac{1}{2} - z\right) \\ \qquad -\pi\cos(\pi x)\exp(-s)\left(y - \frac{1}{2}\right) \end{bmatrix} \\
&= \begin{bmatrix} 0 \\ \pi\cos(\pi x)\exp(-s)\left(z - \frac{1}{2}\right)\left(\pi^2 + 9 - 4s\right) + \sin^2(\pi x)\exp(-2s)\left(y - \frac{1}{2}\right) \\ \qquad -\pi^2\cos^2(\pi x)\exp(-2s)\left(y - \frac{1}{2}\right) \\ -\pi\cos(\pi x)\exp(-s)\left(y - \frac{1}{2}\right)\left(\pi^2 + 9 - 4s\right) + \sin^2(\pi x)\exp(-2s)\left(z - \frac{1}{2}\right) \\ \qquad -\pi^2\cos^2(\pi x)\exp(-2s)\left(z - \frac{1}{2}\right) \end{bmatrix} \\
\mathbf{E} &:= \mathbf{J} + \nabla\phi - \mathbf{u}\times\mathbf{B} \\
&= \begin{bmatrix} 2\sin(\pi x)(1-s)\exp(-s) - 2\sin(\pi x) - 0 \\ -\pi\cos(\pi x)\exp(-s)\left(y - \frac{1}{2}\right) + 0 + \pi\cos(\pi x)\exp(-s)\left(y - \frac{1}{2}\right) \\ -\pi\cos(\pi x)\exp(-s)\left(z - \frac{1}{2}\right) + 0 - \pi\cos(\pi x)\exp(-s)\left(\frac{1}{2} - z\right) \end{bmatrix} \\
&= \begin{bmatrix} 2\sin(\pi x)\left((1-s)\exp(-s) - 1\right) \\ 0 \\ 0 \end{bmatrix}
\end{aligned}
$$

and

$$\mathbf{g} := \mathbf{u}\big|_{\Gamma}, \qquad \mathbf{J}_{ext} := \mathbf{J}\big|_{\mathbb{R}^3\setminus\overline{\Omega}}, \qquad \mathbf{B}_{ext} := \mathbf{i}.$$

To determine $\mathbf{F}$ and $\mathbf{E}$ we form the components of the laplacian

$$\begin{aligned}
u_{2,xx} &= \frac{\partial}{\partial x}\left(\frac{\partial}{\partial x}\left(-\pi\cos(\pi x)\exp(-s)\left(\frac{1}{2}-z\right)\right)\right) = \frac{\partial}{\partial x}\left(\pi^2\sin(\pi x)\exp(-s)\left(\frac{1}{2}-z\right)\right)\\
&= \pi^3\cos(\pi x)\exp(-s)\left(\frac{1}{2}-z\right)\\
u_{2,yy} &= \frac{\partial}{\partial y}\left(\frac{\partial}{\partial y}\left(-\pi\cos(\pi x)\exp(-s)\left(\frac{1}{2}-z\right)\right)\right) = \frac{\partial}{\partial y}\left(-\pi\cos(\pi x)\left(\frac{1}{2}-z\right)\left(-2\left(y-\frac{1}{2}\right)\exp(-s)\right)\right)\\
&= \frac{\partial}{\partial y}\left(2\pi\cos(\pi x)\exp(-s)\left(y-\frac{1}{2}\right)\left(\frac{1}{2}-z\right)\right) = 2\pi\cos(\pi x)\left(\frac{1}{2}-z\right)\left(\exp(-s)-2\left(y-\frac{1}{2}\right)^2\exp(-s)\right)\\
&= -2\pi\cos(\pi x)\exp(-s)\left(z-\frac{1}{2}\right)\left(1-2\left(y-\frac{1}{2}\right)^2\right)\\
u_{2,zz} &= \frac{\partial}{\partial z}\left(\frac{\partial}{\partial z}\left(-\pi\cos(\pi x)\exp(-s)\left(\frac{1}{2}-z\right)\right)\right) = \frac{\partial}{\partial z}\left(-\pi\cos(\pi x)\left(-\exp(-s)+\left(\frac{1}{2}-z\right)\left(-2\left(z-\frac{1}{2}\right)\exp(-s)\right)\right)\right)\\
&= \frac{\partial}{\partial z}\left(\pi\cos(\pi x)\exp(-s)\left(1-2\left(z-\frac{1}{2}\right)^2\right)\right)\\
&= \pi\cos(\pi x)\left(-4\left(z-\frac{1}{2}\right)\exp(-s)+\left(1-2\left(z-\frac{1}{2}\right)^2\right)\left(-2\left(z-\frac{1}{2}\right)\right)\exp(-s)\right)\\
&= -2\pi\cos(\pi x)\exp(-s)\left(z-\frac{1}{2}\right)\left(3-2\left(z-\frac{1}{2}\right)^2\right)
\end{aligned}$$

$$\begin{aligned}
u_{2,xx}+u_{2,yy}+u_{2,zz} &= \pi^3\cos(\pi x)\exp(-s)\left(\frac{1}{2}-z\right)+2\pi\cos(\pi x)\exp(-s)\left(\frac{1}{2}-z\right)(4-2s)\\
&= \pi\cos(\pi x)\exp(-s)\left(\frac{1}{2}-z\right)\left(\pi^2+8-4s\right)
\end{aligned}$$

$$\begin{aligned}
u_{3,xx} &= \frac{\partial}{\partial x}\left(\frac{\partial}{\partial x}\left(-\pi\cos(\pi x)\exp(-s)\left(y-\frac{1}{2}\right)\right)\right) = \frac{\partial}{\partial x}\left(\pi^2\sin(\pi x)\exp(-s)\left(y-\frac{1}{2}\right)\right)\\
&= \pi^3\cos(\pi x)\exp(-s)\left(y-\frac{1}{2}\right)\\
u_{3,yy} &= \frac{\partial}{\partial y}\left(\frac{\partial}{\partial y}\left(-\pi\cos(\pi x)\exp(-s)\left(y-\frac{1}{2}\right)\right)\right) = \frac{\partial}{\partial y}\left(-\pi\cos(\pi x)\left(\exp(-s)-2\left(y-\frac{1}{2}\right)^2\exp(-s)\right)\right)\\
&= \frac{\partial}{\partial y}\left(-\pi\cos(\pi x)\exp(-s)\left(1-2\left(y-\frac{1}{2}\right)^2\right)\right)
\end{aligned}$$

$$
\begin{aligned}
&= -\pi\cos(\pi x)\left(\exp(-s)\left(-4\left(y-\frac{1}{2}\right)\right)-2\left(y-\frac{1}{2}\right)\left(1-2\left(y-\frac{1}{2}\right)^2\right)\exp(-s)\right)\\
&= 2\pi\cos(\pi x)\exp(-s)\left(y-\frac{1}{2}\right)\left(3-2\left(y-\frac{1}{2}\right)^2\right)\\
u_{3,zz} &= \frac{\partial}{\partial z}\left(\frac{\partial}{\partial z}\left(-\pi\cos(\pi x)\exp(-s)\left(y-\frac{1}{2}\right)\right)\right)=\frac{\partial}{\partial z}\left(-\pi\cos(\pi x)\left(y-\frac{1}{2}\right)\left(-2\left(z-\frac{1}{2}\right)\exp(-s)\right)\right)\\
&= \frac{\partial}{\partial z}\left(2\pi\cos(\pi x)\exp(-s)\left(y-\frac{1}{2}\right)\left(z-\frac{1}{2}\right)\right)\\
&= 2\pi\cos(\pi x)\left(y-\frac{1}{2}\right)\left(\exp(-s)-2\left(z-\frac{1}{2}\right)^2\exp(-s)\right)=2\pi\cos(\pi x)\exp(-s)\left(y-\frac{1}{2}\right)\left(1-2\left(z-\frac{1}{2}\right)^2\right)
\end{aligned}
$$

$$
\begin{aligned}
u_{3,xx}+u_{3,yy}+u_{3,zz} &= \pi^3\cos(\pi x)\exp(-s)\left(y-\frac{1}{2}\right)+2\pi\cos(\pi x)\exp(-s)\left(y-\frac{1}{2}\right)(4-2s)\\
&= \pi\cos(\pi x)\exp(-s)\left(y-\frac{1}{2}\right)\left(\pi^2+8-4s\right)
\end{aligned}
$$

$$
\Delta\mathbf{u} = \begin{bmatrix}\nabla\cdot\nabla u_1\\ \nabla\cdot\nabla u_2\\ \nabla\cdot\nabla u_3\end{bmatrix}=\begin{bmatrix}u_{1,xx}+u_{1,yy}+u_{1,zz}\\ u_{2,xx}+u_{2,yy}+u_{2,zz}\\ u_{3,xx}+u_{3,yy}+u_{3,zz}\end{bmatrix}=\begin{bmatrix}0\\ \pi\cos(\pi x)\exp(-s)\left(\frac{1}{2}-z\right)\left(\pi^2+8-4s\right)\\ \pi\cos(\pi x)\exp(-s)\left(y-\frac{1}{2}\right)\left(\pi^2+8-4s\right)\end{bmatrix}
$$

the inertial term

$$
\begin{aligned}
\mathbf{u}\cdot\nabla\mathbf{u} &= \begin{bmatrix}\mathbf{u}\cdot\nabla u_1\\ \mathbf{u}\cdot\nabla u_2\\ \mathbf{u}\cdot\nabla u_3\end{bmatrix}=\begin{bmatrix}u_1\frac{\partial u_1}{\partial x}+u_2\frac{\partial u_1}{\partial y}+u_3\frac{\partial u_1}{\partial z}\\ u_1\frac{\partial u_2}{\partial x}+u_2\frac{\partial u_2}{\partial y}+u_3\frac{\partial u_2}{\partial z}\\ u_1\frac{\partial u_3}{\partial x}+u_2\frac{\partial u_3}{\partial y}+u_3\frac{\partial u_3}{\partial z}\end{bmatrix}\\
&= \begin{bmatrix}0\\ (u_2)\left(2\pi\cos(\pi x)\exp(-s)\left(\frac{1}{2}-z\right)\left(y-\frac{1}{2}\right)\right)+(u_3)\left(-\pi\cos(\pi x)\exp(-s)\left(-1+2\left(\frac{1}{2}-z\right)^2\right)\right)\\ (u_2)\left(-\pi\cos(\pi x)\exp(-s)\left(1-2\left(y-\frac{1}{2}\right)^2\right)\right)+(u_3)\left(2\pi\cos(\pi x)\exp(-s)\left(z-\frac{1}{2}\right)\left(y-\frac{1}{2}\right)\right)\end{bmatrix}\\
&= \begin{bmatrix}0\\ -2\pi^2\cos^2(\pi x)\exp(-2s)\left(\frac{1}{2}-z\right)^2\left(y-\frac{1}{2}\right)+\pi^2\cos^2(\pi x)\exp(-2s)\left(y-\frac{1}{2}\right)\left(-1+2\left(\frac{1}{2}-z\right)^2\right)\\ \pi^2\cos^2(\pi x)\exp(-2s)\left(\frac{1}{2}-z\right)\left(1-2\left(y-\frac{1}{2}\right)^2\right)-2\pi^2\cos(\pi x)\exp(-2s)\left(y-\frac{1}{2}\right)^2\left(z-\frac{1}{2}\right)\end{bmatrix}
\end{aligned}
$$

$$= \begin{bmatrix} 0 \\ -\pi^2 \cos^2(\pi x) \exp(-2s) \left(y - \frac{1}{2}\right) \\ -\pi^2 \cos^2(\pi x) \exp(-2s) \left(z - \frac{1}{2}\right) \end{bmatrix}$$

the gradient of the pressure

$$\begin{aligned} \nabla p &= \begin{bmatrix} p_x \\ p_y \\ p_z \end{bmatrix} = \begin{bmatrix} -\frac{1}{2}\frac{\partial}{\partial x} \sin^2(\pi x) s \exp(-2s) \\ -\frac{1}{2}\frac{\partial}{\partial y} \sin^2(\pi x) s \exp(-2s) \\ -\frac{1}{2}\frac{\partial}{\partial z} \sin^2(\pi x) s \exp(-2s) \end{bmatrix} \\ &= \begin{bmatrix} -\pi \sin(\pi x) \cos(\pi x) s \exp(-2s) \\ -\frac{1}{2} \sin^2(\pi x) \left(s \exp(-2s) \left(-4 \left(y - \frac{1}{2}\right)\right) + \exp(-2s) \left(2 \left(y - \frac{1}{2}\right)\right)\right) \\ -\frac{1}{2} \sin^2(\pi x) \left(s \exp(-2s) \left(-4 \left(z - \frac{1}{2}\right)\right) + \exp(-2s) \left(2 \left(z - \frac{1}{2}\right)\right)\right) \end{bmatrix} \\ &= \begin{bmatrix} -\pi s \sin(\pi x) \cos(\pi x) \exp(-2s) \\ \sin^2(\pi x) \exp(-2s) \left(y - \frac{1}{2}\right) (2s - 1) \\ \sin^2(\pi x) \exp(-2s) \left(z - \frac{1}{2}\right) (2s - 1) \end{bmatrix} \end{aligned}$$

the cross-product of the current density with the magnetic field

$$\begin{aligned} \mathbf{J} \times \mathbf{B} &= \begin{bmatrix} J_2 B_3 - J_3 B_2 \\ J_3 B_1 - J_1 B_3 \\ J_1 B_2 - J_2 B_1 \end{bmatrix} = \begin{bmatrix} -\pi \sin(\pi x) \cos(\pi x) \exp(-2s) \left(y - \frac{1}{2}\right)^2 - \pi \sin(\pi x) \cos(\pi x) \exp(-2s) \left(z - \frac{1}{2}\right)^2 \\ -\pi \cos(\pi x) \exp(-s) \left(z - \frac{1}{2}\right) - 2(1 - s) \sin^2(\pi x) \exp(-2s) \left(y - \frac{1}{2}\right) \\ 2(1 - s) \sin^2(\pi x) \exp(-2s) \left(\frac{1}{2} - z\right) + \pi \cos(\pi x) \exp(-s) \left(z - \frac{1}{2}\right) \end{bmatrix} \\ &= \begin{bmatrix} -\pi s \sin(\pi x) \cos(\pi x) \exp(-2s) \\ -\pi \cos(\pi x) \exp(-s) \left(z - \frac{1}{2}\right) - 2(1 - s) \sin^2(\pi x) \exp(-2s) \left(y - \frac{1}{2}\right) \\ 2(1 - s) \sin^2(\pi x) \exp(-2s) \left(\frac{1}{2} - z\right) + \pi \cos(\pi x) \exp(-s) \left(y - \frac{1}{2}\right) \end{bmatrix} \end{aligned}$$

the gradient of the electric potential

$$\nabla\phi \;=\; \begin{bmatrix}\phi_x\\ \phi_y\\ \phi_z\end{bmatrix} = \begin{bmatrix}-2\sin(\pi x)\\ 0\\ 0\end{bmatrix}$$

and the cross-product of the velocity with the magnetic field

$$\begin{aligned}
\mathbf{u}\times\mathbf{B} &= \begin{bmatrix}u_2B_3 - u_3B_2\\ u_3B_1 - u_1B_3\\ u_1B_2 - u_2B_1\end{bmatrix}\\
&= \begin{bmatrix}
-\pi\cos(\pi x)\exp(-s)\left(\frac{1}{2}-z\right)\sin(\pi x)\exp(-s)\left(y-\frac{1}{2}\right)\\
\qquad +\pi\cos(\pi x)\exp(-s)\left(y-\frac{1}{2}\right)\sin(\pi x)\exp(-s)\left(\frac{1}{2}-z\right)\\
-\pi\cos(\pi x)\exp(-s)\left(y-\frac{1}{2}\right) - 0\\
0 + \pi\cos(\pi x)\exp(-s)\left(\frac{1}{2}-z\right)
\end{bmatrix}\\
&= \begin{bmatrix}
0\\
-\pi\cos(\pi x)\exp(-s)\left(y-\frac{1}{2}\right)\\
\pi\cos(\pi x)\exp(-s)\left(\frac{1}{2}-z\right)
\end{bmatrix}
\end{aligned}$$

The equations were checked for correctness against output from the symbolic package maxima (wxMaxima).

Bibliography

[1] M. Ainsworth. Essential boundary conditions and multi-point constraints in finite element analysis. *Computer Methods in Applied Mechanics and Engineering*, 190(48):6323–6339, 2001.

[2] G. Alekseev. Solvability of control problems for stationary equations of magnetohydrodynamics of a viscous fluid. *Siberian Mathematical Journal*, 45(2):197–213, 2004.

[3] D. Anderson, W. Cooper, R. Gruber, S. Merazzi, and U. Schwenn. Methods for the efficient calculation of the (mhd) magnetohydrodynamic stability properties of magnetically confined fusion plasmas. *International Journal of High Performance Computing Applications*, 4(3):34–47, 1990.

[4] D. Arnold. Differential complexes and numerical stability. *arXiv preprint math/0212391*, 2002.

[5] D. Arnold, R. Falk, and R. Winther. Differential complexes and stability of finite element methods i. the de rham complex. In *Compatible spatial discretizations*, pages 23–46. Springer, 2006.

[6] D. Arnold, R. Falk, and R. Winther. Finite element exterior calculus, homological techniques, and applications. *Acta numerica*, 15:1–155, 2006.

[7] S. Balay, J. Brown, K. Buschelman, V. Eijkhout, W. Gropp, D. Kaushik, M. Knepley, L. Curfman McInnes, B. Smith, and H. Zhang. Petsc users manual revision 3.4. 2013.

[8] W. Bangerth. Assembling matrices in deal. ii. Technical report, Technical report, ETH Zürich, 2002.

[9] W. Bangerth, C. Burstedde, T. Heister, and M. Kronbichler. Algorithms and data structures for massively parallel generic adaptive finite element codes. *ACM Transactions on Mathematical Software (TOMS)*, 38(2):14, 2011.

[10] W. Bangerth, R. Hartmann, and G. Kanschat. deal. ii—a general-purpose object-oriented finite element library. *ACM Transactions on Mathematical Software (TOMS)*, 33(4):24, 2007.

[11] W. Bangerth and G. Kanschat. *Concepts for Object Oriented Finite Element Software: The Dea1. II Library*. IWR, 1999.

[12] W. Bangerth and O. Kayser-Herold. Data structures and requirements for hp finite element software. *ACM Transactions on Mathematical Software (TOMS)*, 36(1):28, 2009.

[13] R. Beatson and L. Greengard. A short course on fast multipole methods. *Wavelets, multilevel methods and elliptic PDEs*, 1:1–37, 1997.

[14] R. Bensow and M. Larson. Discontinuous least-squares finite element method for the div-curl problem. *Numerische Mathematik*, 101(4):601–617, 2005.

[15] M. Benzi. Preconditioning techniques for large linear systems: a survey. *Journal of Computational Physics*, 182(2):418–477, 2002.

[16] M. Benzi and A. Wathen. Some preconditioning techniques for saddle point problems. In *Model order reduction: theory, research aspects and applications*, pages 195–211. Springer, 2008.

[17] M. Bergot and P. Lacoste. Generation of higher-order polynomial basis of nédélec h (curl) finite elements for maxwell's equations. *Journal of Computational and Applied Mathematics*, 234(6):1937–1944, 2010.

[18] O. Besson, J. Bourgeois, P. Chevalier, J. Rappaz, and R. Touzani. Numerical modelling of electromagnetic casting processes. *Journal of computational physics*, 92(2):482–507, 1991.

[19] P. Bochev and M. Gunzburger. *Least-Squares Finite Element Methods: Finite Element Methods*, volume 166. Springer, 2009.

[20] C. Burstedde, L. Wilcox, and O. Ghattas. p4est: Scalable algorithms for parallel adaptive mesh refinement on forests of octrees. *SIAM Journal on Scientific Computing*, 33(3):1103–1133, 2011.

[21] M. Charina-Kehrein. *A MHD free boundary value problem.* PhD thesis, Auburn University, Auburn, Alabama, 2002.

[22] H. Childs. Visit: An end-user tool for visualizing and analyzing very large data. 2013.

[23] H. Childs, D. Pugmire, S. Ahern, B. Whitlock, M. Howison, M. Prabhat, G. Weber, and W. Bethel. Extreme scaling of production visualization software on diverse architectures. 2010.

[24] R. Coifman, V. Rokhlin, and S. Wandzura. The fast multipole method for the wave equation: A pedestrian prescription. *Antennas and Propagation Magazine, IEEE*, 35(3):7–12, 1993.

[25] B. Collins-Sussman, B. Fitzpatrick, and M. Pilato. *Version control with subversion.* O'Reilly Media, Inc., 2004.

[26] M. Costabel and M. Dauge. Singularities of electromagnetic fields in polyhedral domains. *Archive for Rational Mechanics and Analysis*, 151(3):221–276, 2000.

[27] M. Costabel and M. Dauge. Weighted regularization of maxwell equations in polyhedral domains. *Numerische Mathematik*, 93(2):239–277, 2002.

[28] M. Costabel, M. Dauge, and C. Schwab. Exponential convergence of hp-fem for maxwell equations with weighted regularization in polygonal domains. *Mathematical Models and Methods in Applied Sciences*, 15(04):575–622, 2005.

[29] P. Davidson. *An Introduction to Magnetohydrodynamics*. Cambridge University Press, Cambridge, UK, 2001.

[30] J. Dongarra, J. Hittinger, J. Bell, L. Chacon, R. Falgout, M. Heroux, P. Hovland, E. Ng, C. Webster, S. Wild, et al. Applied mathematics research for exascale computing, 2014.

[31] J. Dongarra, D. Reed, R. Bajcsy, M. Fernandez, J. Griffiths, R. Mott, C. Johnson, A. Inouye, W. Miner, M. Matzke, et al. Computational science: Ensuring america's competitiveness, 2005.

[32] P. Dreyfuss and J. Rappaz. Numerical modelling of induction heating for two dimensional geometries. *Preprint EPFL*, 2001.

[33] H. Elman, V. Howle, J. Shadid, D. Silvester, and R. Tuminaro. Least squares preconditioners for stabilized discretizations of the navier-stokes equations. *SIAM Journal on Scientific Computing*, 30(1):290–311, 2007.

[34] H. Elman, D. Silvester, and A. Wathen. Iterative methods for problems in computational fluid dynamics. 1998.

[35] H. Elman, D. Silvester, and A. Wathen. Block preconditioners for the discrete incompressible navier–stokes equations. *International journal for numerical methods in fluids*, 40(3-4):333–344, 2002.

[36] H. Elman, D. Silvester, and A. Wathen. Performance and analysis of saddle point preconditioners for the discrete steady-state navier-stokes equations. *Numerische Mathematik*, 90(4):665–688, 2002.

[37] H. Elman, D. Silvester, and A. Wathen. *Finite Elements and Fast Iterative Solvers: with Applications in Incompressible Fluid Dynamics*. Oxford University Press, Oxford, UK, 2006.

[38] D. Fleisch. *A Student's guide to Maxwell's equations*. Cambridge University Press, 2008.

[39] G. Fleming and M. Ratner. Grand challenges in basic energy sciences. *Physics Today*, 28, 2008.

[40] T. Geenen, C. Vuik, G. Segal, S. MacLachlan, et al. On iterative methods for the incompressible stokes problem. *International Journal for Numerical methods in fluids*, 65(10):1180–1200, 2011.

[41] J. Gerbeau. A stabilized finite element method for the incompressible magnetohydrodynamic equations. *Numerische Mathematik*, 87(1):83–111, 2000.

[42] J. Gerbeau, C. Le Bris, et al. Existence of solution for a density-dependent magnetohydrodynamic equation. *Advances in Differential Equations*, 2(3):427–452, 1997.

[43] C. Geuzaine and J. Remacle. Gmsh: A 3-d finite element mesh generator with built-in pre-and post-processing facilities. *International Journal for Numerical Methods in Engineering*, 79(11):1309–1331, 2009.

[44] G. Golub and C. Van Loan. *Matrix computations*, volume 3. JHU Press, 1996.

[45] N. Gould, J. Scott, and Y. Hu. A numerical evaluation of sparse direct solvers for the solution of large sparse symmetric linear systems of equations. *ACM Transactions on Mathematical Software (TOMS)*, 33(2):10, 2007.

[46] L. Greengard. *The rapid evaluation of potential fields in particle systems*. MIT press, 1988.

[47] L. Greengard and V. Rokhlin. A fast algorithm for particle simulations. *Journal of computational physics*, 73(2):325–348, 1987.

[48] C. Greif and D. Schötzau. Preconditioners for the discretized time-harmonic maxwell equations in mixed form. *Numerical Linear Algebra with Applications*, 14(4):281–297, 2007.

[49] R. Griesse and K. Kunisch. Optimal control for a stationary mhd system in velocity-current formulation. *SIAM Journal on Control and Optimization*, 45(5):1822–1845, 2006.

[50] R. Griesse and A. Meir. Modelling of a magnetohydrodynamics free surface problem arising in czochralski crystal growth. *Mathematical and Computer Modelling of Dynamical Systems*, 15(2):163–175, 2009.

[51] D. Griffiths. *Introduction to electrodynamics*, volume 3. prentice Hall Upper Saddle River, NJ, 1999.

[52] R. Gruber and J. Rappaz. Finite element methods in linear ideal magnetohydrodynamics. *Berlin and New York, Springer-Verlag, 1985, 189 p.*, 1, 1985.

[53] M. Gunzburger. *Finite element methods for viscous incompressible flows: a guide to theory, practice, and algorithms*. Academic Press, Computer Science and Scientific Computing, Boston, MA, 1989.

[54] M. Gunzburger, A. Meir, and J. Peterson. On the existence, uniqueness, and finite element approximation of solutions of the equations of stationary, incompressible magnetohydrodynamics. *Mathematics of Computation*, 56(194):523–563, 1991.

[55] M. Gunzburger, E. Ozugurlu, J. Turner, and H. Zhang. Magnetic control of transport phenomena in cz crystal growth processes. *ASME-PUBLICATIONS-HTD*, 369:123–130, 2001.

[56] M. Gunzburger, E. Ozugurlu, J. Turner, and H. Zhang. Controlling transport phenomena in the czochralski crystal growth process. *Journal of Crystal Growth*, 234(1):47–62, 2002.

[57] M. Gunzburger and C. Trenchea. Analysis and discretization of an optimal control problem for the time-periodic mhd equations. *Journal of mathematical analysis and applications*, 308(2):440–466, 2005.

[58] J. Hemminger, G. Fleming, and M. Ratner. Directing matter and energy: Five challenges for science and the imagination, 2007.

[59] M. Heroux, R. Bartlett, V. Howle, R. Hoekstra, J. Hu, T. Kolda, R. Lehoucq, K. Long, R. Pawlowski, E. Phipps, et al. An overview of the trilinos project. *ACM Transactions on Mathematical Software (TOMS)*, 31(3):397–423, 2005.

[60] M. Heroux and J. Willenbring. *Trilinos users guide*. United States. Department of Energy, 2003.

[61] R. Hiptmair. Finite elements in computational electromagnetism. *Acta Numerica*, 11:237–339, 2002.

[62] L. Hou and A. Meir. Boundary optimal control of mhd flows. *Applied Mathematics and Optimization*, 32(2):143–162, 1995.

[63] P. Houston, I. Perugia, and D. Schotzau. Mixed discontinuous galerkin approximation of the maxwell operator. *SIAM Journal on Numerical Analysis*, 42(1):434–459, 2004.

[64] A. Ihler. An overview of fast multipole methods. *Area Exam, April*, 2004.

[65] T. Isaac, C. Burstedde, and O. Ghattas. Low-cost parallel algorithms for 2: 1 octree balance. In *Parallel & Distributed Processing Symposium (IPDPS), 2012 IEEE 26th International*, pages 426–437. IEEE, 2012.

[66] S. Jardin. Review of implicit methods for the magnetohydrodynamic description of magnetically confined plasmas. *Journal of Computational Physics*, 231(3):822–838, 2012.

[67] B. Jiang. *The least-squares finite element method: theory and applications in computational fluid dynamics and electromagnetics*. Springer, 1998.

[68] M. Kronbichler, T. Heister, and W. Bangerth. High accuracy mantle convection simulation through modern numerical methods. *Geophysical Journal International*, 191(1):12–29, 2012.

[69] L. Landau. *Fluid mechanics: volume 6 (course of theoretical physics) Author: LD Landau, EM Lifshitz, Publisher: Bu*. Butterworth-Heinemann, 1987.

[70] C. Le Bris, T. Lelièvre, et al. *Mathematical methods for the magnetohydrodynamics of liquid metals*. Oxford University Press, 2006.

[71] A. Meir. Thermally coupled magnetohydrodynamics flow. *Applied mathematics and computation*, 65(1):79–94, 1994.

[72] A. Meir. Thermally coupled, stationary, incompressible mhd flow; existence, uniqueness, and finite element approximation. *Numerical Methods for Partial Differential Equations*, 11(4):311–337, 1995.

[73] A. Meir, S. Bakhtiyarov, R. Overfelt, and P. Schmidt. Numerical simulation of steady liquid-metal flow in the presence of a static magnetic field. *Journal of applied mechanics*, 71(6):786–795, 2004.

[74] A. Meir and P. Schmidt. A velocity current formulation for stationary mhd flow. *Applied Mathematics and Computation*, 65(1–3):95–109, 1994.

[75] A. Meir and P. Schmidt. Variational methods for stationary mhd flow under natural interface conditions. *Nonlinear Analysis: Theory, Methods & Applications*, 26(4):659–689, 1996.

[76] A. Meir and P. Schmidt. Analysis and finite element simulation of mhd flows, with an application to seawater drag reduction. In *Proceedings of an International Symposium on Seawater Drag Reduction*, pages 401–406. Citeseer, 1998.

[77] A. Meir and P. Schmidt. Analysis and finite element simulation of mhd flows, with an application to liquid metal processing. In *Fluid Flow Phenomena in Metals Processing, Proceedings, 1999 TMS Annual Meeting*, pages 561–569, 1999.

[78] A. Meir and P. Schmidt. Analysis and numerical approximation of a stationary mhd flow problem with nonideal boundary. *SIAM Journal on Numerical Analysis*, 36(4):1304–1332, 1999.

[79] A. Meir, P. Schmidt, S. Bakhtiyarov, and R. Overfelt. Velocity, potential, and temperature distributions in molten metals during electromagnetic stirring: Part ii-numerical simulations. *ASME-PUBLICATIONS-FED*, 249:87–96, 1999.

[80] W. Nagel. *Subversion Version Control: Using the Subversion Version Control System in Development Projects*. Prentice Hall PTR, 2005.

[81] J. Nédélec. Mixed finite elements in r3. *Numerische Mathematik*, 35(3):315–341, 1980.

[82] W. Perry, A. Broers, F. El-Baz, W. Harris, B. Healy, W. Hillis, et al. Grand challenges for engineering. *National Academy of Engineering, Washington, DC*, 2008.

[83] J. Rappaz and R. Touzani. On a two-dimensional magnetohydrodynamic problem. i. modelling and analysis. *ESAIM: Mathematical Modelling and Numerical Analysis-Modélisation Mathématique et Analyse Numérique*, 26(2):347–364, 1992.

[84] J. Rappaz and R. Touzani. On a two-dimensional magnetohydrodynamic problem. ii. numerical analysis. *Modélisation mathématique et Analyse numérique*, 30(2):215–235, 1996.

[85] Y. Saad. *Iterative Methods for Sparse Linear Systems*. Society of Industrial and Applied Mathematics, Philadelphi, PA, 2003.

[86] M. Sala, M. Heroux, and D. Day. Trilinos tutorial. *Sandia National Laboratories, Tech. Rep. SAND2004-2189*, 2004.

[87] M. Schäfer, S. Turek, F. Durst, E. Krause, and R. Rannacher. *Benchmark computations of laminar flow around a cylinder*. Springer, 1996.

[88] P. Schmidt. On a magnetohydrodynamic problem of euler type. *Journal of differential equations*, 74(2):318–335, 1988.

[89] P. Schmidt. A galerkin method for time-dependent mhd flow with nonideal boundaries. *Communications in Applied Analysis*, 3(3):383–398, 1999.

[90] D. Schötzau. Mixed finite element methods for stationary incompressible magneto–hydrodynamics. *Numerische Mathematik*, 96(4):771–800, 2004.

[91] D. Silvester, H. Elman, D. Kay, and A. Wathen. Efficient preconditioning of the linearized navier–stokes equations for incompressible flow. *Journal of Computational and Applied Mathematics*, 128(1):261–279, 2001.

[92] P. Solin, K. Segeth, and I. Dolezel. *Higher-order finite element methods*. CRC Press, 2004.

[93] J. Strickland and R. Baty. An overview of fast multipole methods. Technical report, Sandia National Labs., Albuquerque, NM (United States), 1995.

[94] E. Strohmaier, S. Williams, A. Kaiser, K. Madduri, K. Ibrahim, D. Bailey, J. Demmel, T. Simos, G. Psihoyios, and C. Tsitouras. A kernel testbed for parallel architecture, language, and performance research. In *AIP Conference Proceedings*, volume 1281, page 1297, 2010.

[95] L. Trefethen and D. Bau III. *Numerical Linear Algebra*. Society of Industrial and Applied Mathematics, Philadelphi, PA, 1997.

[96] E. Tyrtyshnikov and R. Chan. Spectral equivalence and proper clusters for matrices from the boundary element method. *International Journal for Numerical Methods in Engineering*, 49(9):1211–1224, 2000.

[97] H. Van der Vorst. *Iterative Krylov methods for large linear systems*, volume 13. Cambridge University Press, 2003.

[98] C. Vuik, G. Segal, et al. A comparison of preconditioners for incompressible navier–stokes solvers. *International Journal for Numerical methods in fluids*, 57(12):1731–1751, 2008.

[99] J. Wetzl. The landscape of parallel computing research. 2012.

[100] B. Whitlock, J. Favre, and J. Meredith. Parallel in situ coupling of simulation with a fully featured visualization system. In *Proceedings of the 11th Eurographics conference on Parallel Graphics and Visualization*, pages 101–109. Eurographics Association, 2011.

[101] P. Wriggers. *Nonlinear finite element methods*, volume 4. Springer, 2008.

[102] S. Wu, T. Huang, and C. Li. Modified block preconditioners for the discretized time-harmonic maxwell equations in mixed form. *Journal of Computational and Applied Mathematics*, 237(1):419–431, 2013.